FREEZE-THAW TESTING OF CONCRETE

-

INPUT TO REVISION OF CEN TEST METHODS

WORKSHOP PROCEEDING

FROM A

NORDIC MINISEMINAR

VEDBÆK – DENMARK

4. – 5. MARCH 2010

PREFACE

This publication contains 7 papers presented at a Workshop (Nordic Mini Seminar) concerning freeze-thaw testing of concrete, with the aim to submit information to the working groups concerned with the revision of the European test methods. Many of the participants are also active in several standardisation committees, both nationally and within CEN. Hence the information and knowledge gained during this workshop can have a direct impact on the revision.

The workshop was organised by Dirch H. Bager, DHB-Consult, with kind economic support from the Danish Concrete Association, the Norwegian Concrete Association, Norcem, The Swedish Concrete Association and Cementa.

In order to stimulate discussions between the participants, the Workshop was arranged as a two-day residential course, located in Vedbæk, north of Copenhagen, March 4 – 5, 2010.

Nordic Mini Seminars are workshops arranged solely for researchers from the Nordic Countries in order to strengthen the inter-Nordic co-operation. A few foreign specialists can however be invited. To further stimulate discussions, only participants actively contributing are invited. 73 such Mini Seminars have been held since 1975.

11 researchers from Denmark, Iceland, Norway, Sweden and Germany participated in the workshop.

The present publication is Number 9 in a special series of Workshop-Proceedings of the Nordic Concrete Research.

Nordic Concrete Research (NCR) is a bi-annual publication of The Nordic Concrete Federation, presenting research and practical experience in the field of concrete technology, both from structural and material perspective. Every third year one of the publications is devoted to abstracts from the Nordic Concrete Research Meeting. (Nordic Concrete Research – Research Projects 20XX).

Papers published in NCR are normally thoroughly reviewed by three reviewers. The papers in the present proceeding have however not been reviewed in this way. Instead the authors revised their papers after the workshop, based on comments and information obtained there.

Vodskov, May 2010

Dirch H. Bager
Editor

CONTENTS:

LIST OF PARTICIPANTS:

Dirch H. Bager	DHB-Consult	Denmark
Marianne Tange Hasholt	COWI A/S	Denmark
Stefan Jacobsen	NTNU	Norway
Peter Laugesen	Pelcon Aps	Denmark
Sture Lindmark	Lund University	Sweden
Tang Luping	CBI & Chalmers University of Technology	Sweden
Christoph Müller	Verein Deutscher Zementwerke	Germany
Roar Myrdal	SINTEF	Norway
Terje F. Rønning	Norcem A/S	Norway
Sveinbjörn Sveinbjörnsson	Mannvit hf	Iceland
Peter Utgenannt	CBI	Sweden

Qualitative description of the micro ice body freeze-thaw damage mechanism in concrete

Dirch H. Bager
M.Sc., Ph.D
DHB-Consult
Lavendelparken 5, DK 9310 Vodskov
E-mail: dirch.bager@webspeed.dk

ABSTRACT

The paper argues for formation of micro ice bodies as the main reason for freeze-thaw damage in concrete.

A conceptual model for the damage mechanism due to the formation of micro ice bodies is presented. The model widens the classical critical degree of saturation model in order to be able to distinguish between expansion of paste [α-saturation] and the successive crack formation [β-saturation]

Key-words: micro micro ice bodies, freeze-thaw damage, scaling, internal damage

INTRODUCTION

In the period from 1996 to 2001 several research projects regarding freeze-thaw mechanisms in concrete have been carried out within the framework of NORDTEST by six laboratories: The Norwegian Building Research Institute (NBI), The Swedish Research and Testing Institute (SP), Technical Research Centre of Finland (VTT), Lund Institute of Technology/Division of Building Materials (LTH), The Icelandic Building Research Institute (IBRI) and the Cement and Concrete Laboratory / Aalborg Portland (CBL). The NORDTEST projects, which concern simultaneous measurement of scaling, internal damage and water-uptake on the same samples and during the same test, have been reported in /1, 2, 3, 4 & 5/

Besides documenting the ability of the Swedish test method, SS137244, the Slab Test, for freeze-thaw testing, these projects have also increased the general understanding of the mechanism, leading to the model described in following /6/.

It is well known, that drying of cement-paste and concrete alters the pore structure. Drying leads to an increase in the continuous system of larger capillary pores which increase the ice formation above -20^{o}C /7/. In order to make the test procedure as realistic as possible, the preconditioning of the specimens includes a drying in a relative humidity of 65 +/- 5 %, followed by a re-saturation with water, before the freeze/thaw cycles are initiated. Thus, the preconditioning of the sample, the uni-directional temperature gradient and the one-cycle-a-day temperature cycle, makes the test conditions in the slab test close to reality.

Water-uptake during the freeze-thaw cycles is essential for the destructive mechanism. Therefore comprehensive experimental investigations on water-uptake have been carried out during spring in year 2000 /4/. In 2001 a study on the influence of freezing media on freeze-thaw deterioration took place /5/ and in 2003 a study of water distribution inside the specimen was carried out at Aalborg Portland /8/. These studies were planned in such a manner, that the results either could support or reject the model.

1 FREEZE-THAW DAMAGE MECHANISMS

The two most accepted mechanisms for freeze-thaw damage in concrete are described:

i) The hydraulic pressure mechanism
ii) The microscopic ice body growth

1.1 The hydraulic pressure theory

Regarding the hydraulic pressure mechanism, the mechanism is caused by the 9 vol. percent increase in volume when water transforms to ice. In a saturated pore system, this will lead to an increase in the pressure in the water which might be greater than the tensile strength of the concrete.

The mechanism implies, that increasing water/cement ratio increase the freeze able amount of water and hence the internal pressure. On the other hand, an increasing water/cement ratio also results in a decrease in tensile strength. Thus, the higher the water/cement ratio, the more vulnerable the concrete are for freeze-thaw action – and vice versa.

Furthermore, the mechanism also implies that the internal pressure, and the corresponding volume change, should be directly proportional with the ice formation. For pure cement paste specimens this have been found, see figure 1

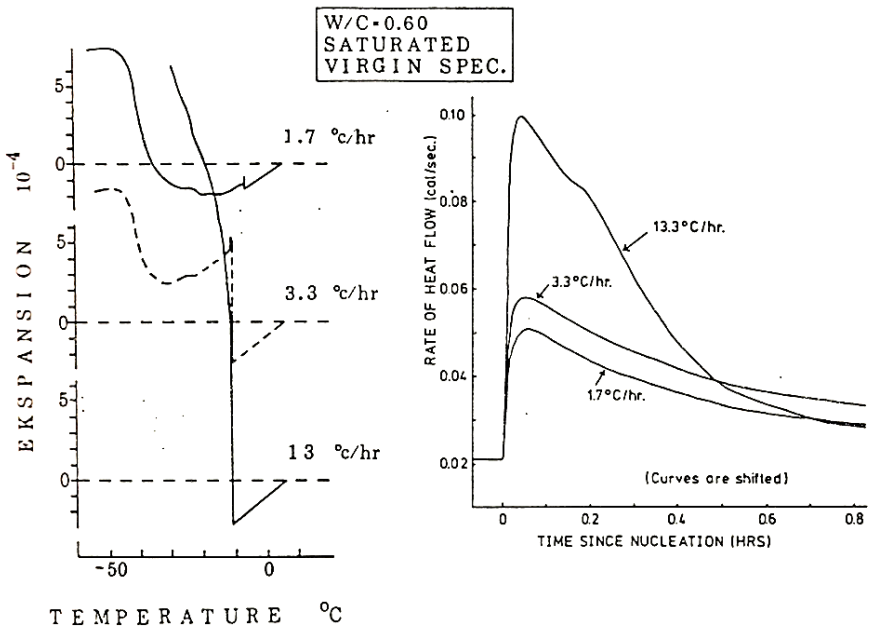

Figure 1 *Expansion of saturated cement paste as function of cooling rate / ice formation. Left: Length change for mature cement paste specimens at different cooling rates. Each curve is for a separate virgin specimen. Right: Rate of heat flow – ice formation – during cooling at three different rates. Each curve is for a separate virgin specimen. From /9/*

In figure 1, left, the sudden expansion at freezing for a cooling rate of 1.7 ^{o}C/h and 3.3 ^{o}C/h is followed by an immediate contraction, suggesting creation and dissipation of pressure in the unfrozen water (Powers hydraulic pressure hypothesis). This effect has not been observed for less porous specimens.

If the pressure can be released, for example to the surface or to air filled artificial air bubbles, no pressure will be built up and no damage will occur. This idea has lead to the formulation of critical distance between the pores, the spacing factor.

Katja Fridh /10/ has studied length change as function of cooling rate for mortars with water/cement ratios of 0.60, 0.45 and 0.40. The specimens had natural air content (no admixtures) and 4, 6 & 10 percent entrained air. Cooling rate 3.6 and 7.8 ^{o}C/h. See figure 2.

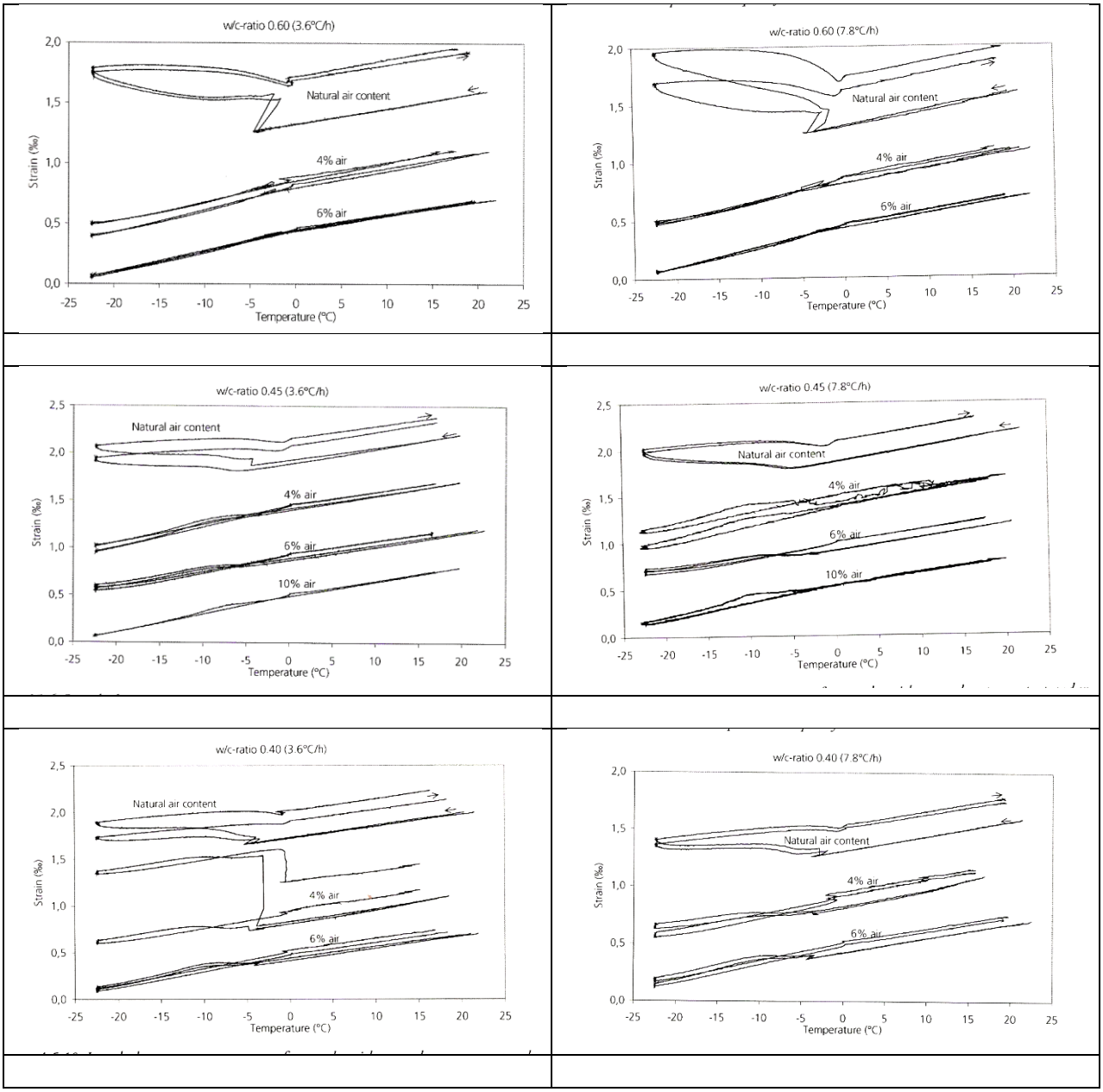

Figure 2 Length chances versus temperature (No explanation for the sudden expansion of one sample of w/c = 0.40, 3.6 ^{o}C/h. It might be caused by the measuring system, since no heat increase from ice formation is measured)

Figure 2 shows

i) Air entraining leads to contraction instead of expansion.
ii) The sudden expansions only are seen for water/cement ratio of 0.60, in agreement with /9/.
iii) For water/cement ratio of 0.60, the cooling rate does not influence the sudden expansion, as were expected according to the hydraulic pressure theory.

Thus, the hydraulic pressure theory seems not to be applicable to dense quality concrete with prober artificial air pore system. This is also in agreement with Powers, who concluded, that the hydraulic pressure Theory did not work for higher quality concrete /11/.

The hydraulic pressure theory will therefore not be dealt with any further in this paper.

1.2 Microscopic ice body formation theory

According to this theory, ice forms as micro ice bodies in the pores. Micro ice body formation has been thoroughly described by Setzer /12 & 13/. Such micro ice bodies in porous materials acts in two opposite ways:

i) They have a lower chemical potential than the "free" pore water. Therefore water will move towards the micro ice bodies which therefore will grow and exert pressure on the surrounding pore walls leading to an increase in volume of the paste.
ii) On the other hand, the driving forces for water to move towards these micro ice bodies are so strong, that water can be drawn from the gel pores, resulting in shrinkage of the paste.

It is believed, that for highly saturated concrete with high water/cement ratio this mechanism will lead to a volume increase during cooling, while for low water/cement ratio concrete shrinkage can be expected as long as the liquid uptake from the exterior is not sufficient

2 MATERIALS

Most effort have been focused on dense non-air-entrained concrete with low w/c-ratio (Type I: w/c = 0.32 & Type II: w/c = 0.48). Some tests have also been made with a Type III with w/c = 0.7. The concrete has been produced with both Swedish SRPC – CEM I 42.5 R and Norwegian OPC – CEM I 52.5 LA. Concrete strength was approximately 85 MPa, 55 MPa and 30 MPa. Granite aggregates with good frost durability were used.

3 EXPERIMENTAL SET-UP

Freeze-thaw tests were carried out according to the proposed coming European reference test for Scaling – the Slab Test, which later was published as CEN/TS 12390-9:2006. This method is almost identical with the Swedish test method SS137244 – the "Borås method" /14/. This method can be used either with demineralised water or with a 3 % sodium chloride solution as the freezing media.

In order to increase the understanding of the freeze-thaw damage mechanism, the following test procedures gave been used:

A. Freezing in wet state - without access to free water or de-icing solutions on surface during the test. Water or solution applied only at +20 ^{o}C - the "Classical" test
B. Freezing in wet state with access to water on the surface - the "Wet" test
C. Freezing in saturated surface dry condition, melting with demineralised water on surface – the "Sealed Wet" test
D. Freezing in saturated state, with access to de-icing solution on the surface - the "Salt" test
E. Freezing in saturated surface dry condition, melting with de-icing solution on surface – the "Sealed salt" test

Test procedures B and D are the standard test procedures.

During the different test series the following measurements were carried out:

- Relative change in ultrasonic pulse transmission time - UPTT
- Relative length change - dilation
- Water-uptake
- Surface scaling

For the UPTT, 54 Hz conical transducers have been used. Contact between the transducers and the concrete have been obtained through the rubber sleeve. No other contact media has been used. A special measuring equipment was built, which presses the transducers correct aligned on the opposite sides of the specimen by pneumatic pressure cylinders, see fig 3. The UPTT are calculated as changes relative to the 0-cycle value.

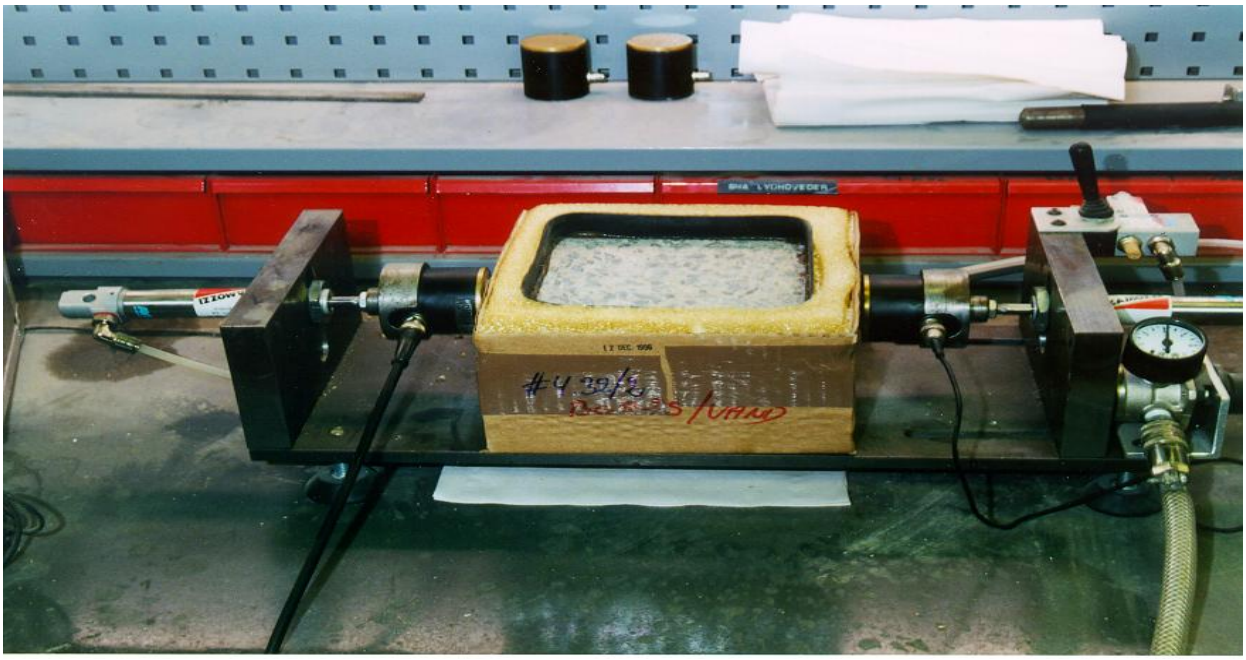

Figure 3 Measurement of UPTT

Length change was measured with an electrical digital gauge. Steel studs were glued into holes in the specimen. A special measuring stand for these measurements, which secure the same position of the sample for each measurement, were constructed, see figure 4.

Figure 4 Measurement of dilation

Water-uptake was determined by weighing the surface dry specimen after each scaling measurement. Weight of scaled material, corrected for evaporable water content, was included. The water-uptake was calculated as kg/m^2.

3.1 Study of water-uptake

For the tests carried out in year 2000, some modifications to the standard test have been used. First of all, the measuring terms have been altered. In order to establish temperature equilibrium in the specimens, measurements were carried out at two consecutive days, i.e. directly after removal from the freezing cabinet and after 24 hours storage at 20 ^{o}C, with freezing media on top surface.

The different tests are explained in the following:

- STD. WET: Standard test, with demineralised water as freezing media.
- SEALED WET: Freezing in saturated surface dry condition, melting with demineralised water on surface.
- STD. SALT: Standard test, with 3 % sodium chloride solution as freezing media.
- SEALED SALT: Freezing in saturated surface dry condition, melting with 3 % sodium chloride solution on surface.

In the sealed tests, the surface was covered with a thin polyurethane foil directly on the concrete during freezing.

Measurements have been made after 0, 2, 6, 12, 18, 24, 36 & 48 freeze-thaw cycles. The experiments have shown that the specimens were not in temperature equilibrium directly after removal from the freezing cabinet; hence only results from measurements carried out after 24 hours storage at 20 ^{o}C is reported in this paper.

All tests have been carried out using the same temperature variation in the freezing cabinet during freezing and thawing as defined in CEN/TS 12390-9:2006. Minor differences in the temperature on the sample surface must be expected due to the different conditions during the test.

Measurements carried out:

- Scaling
- Water absorption
- Dilation

3.1.1 Freezing of pore water

During cooling freezing of water will take place. However, three different situations have to be evaluated:

- "Wet": Ice formation will generally start in the water layer on top of the specimen, since during cooling this will be the coldest spot on the sample. The ice will spread into the specimen via the continuous system of larger capillary pores as an ice front. During thawing the surface will be the warmest part, hence there can be ice in the specimen and water on the surface.
- "Sealed": Without free water or salt solution on the surface, ice formation will take place as nucleation of ice crystals randomly in the pore system. The ice will spread in the concrete through the continuous system of larger capillary pores
- "Salt": Since the freezing point of the salt solution has been lowered due to the salt, then the first ice formation might be initiated as nucleation of ice crystals randomly in the pore system saturated with pure water. The ice will spread in the concrete through the continuous system of larger capillary pores as for the classical test. During thawing there can be ice in the specimen and liquid salt solution on the surface, as in the "wet" test.

3.1.2 Melting of pore water and water-uptake

- Wet: In this set-up, water-uptake can take place during melting. We assume that the pure ice on the upper surface will melt before most of the ice inside the specimen. Therefore water-uptake can take place due to two mechanisms:
    1. suction towards the micro ice bodies and
    2. suction due to the 9 vol. pct. decrease when ice melts.

  Assuming that melting in the specimen starts in the upper layer and gradually goes down towards the bottom, these mechanism results in a continuous water-uptake right down to the bottom layer. The moisture distribution will therefore be very even within the specimen.

- Sealed Wet: As in the Wet test, water can be taken up during melting. However, the +20 ^{o}C water is poured on a –20 ^{o}C frozen concrete, more or less filled with micro ice bodies. This large temperature difference and hence the large difference in chemical potential between water and ice bodies, might give rise to extensive water-uptake during the short time period from the water has been poured on the surface until it freezes. Water-uptake during the following melting is identical to the Wet test.

- Salt: When a salt solution is applied as the freezing media, the water-uptake during the test differs from the previous. During freezing micro ice bodies forms randomly within the specimen before the salt solution freeze. Therefore water-uptake can take place during the

cooling period of the freeze-thaw cycle. It must be expected that the major part of these micro ice bodies forms first in the coldest upper part of the specimen, thus leading to water movement from the lower part. Furthermore, due to the salt ions present in the freezing media, water moves from the lower part of the specimen towards the upper part caused by osmotic forces. This result in a higher saturation in the upper layer of the specimen, and expansion due to increase in volume of the micro ice bodies, while shrinkage prevails in the lower part caused by the removal of water towards the upper layer. Thus the specimen will be in an unstable internal stress situation which can be released by formation of horizontal cracks. Scaling is therefore the major destructive mechanism when salt is used as freezing media, while internal damage prevails when water is used as freezing media.

- Sealed Salt: As for the sealed Wet test, extensive water- or solution-uptake can take place immediately after the salt solution has been poured on the –20 ^{o}C frozen concrete surface.

4 RESULTS

4.1 Water-uptake and increasing damage in concrete

Water-uptake during freeze-thaw is believed controlled by the formation of micro ice bodies in the pore system during freezing. Moisture mechanics therefore plays a major role in freeze-thaw damage of concrete. Hence the experimental set-up is a major controlling parameter for the water-uptake and the further breakdown of the concrete during the succeeding freeze-thaw cycles, as described in the following.

During cooling, after formation of micro ice bodies, the chemical potential in these ice bodies is lower than the chemical potential of the un-frozen water, thus resulting in condensing of the un-frozen water on the ice bodies. Thermal contraction of the solid matrix may further strengthen this transport by squeezing water out from the gel. The ice body therefore can fill the pore and exert pressure on the pore walls.

Heating leads to expansion of both the ice body and the solid matrix. Since thermal expansion of ice is approximately 6 times larger than that of the solid matrix, an overall expansion of the concrete is seen. In the actual experimental set-up, the freezing media on the upper surface melts before the ice in the concrete melts. Thus, since the volume of ice is 9 vol. pct. larger than the corresponding water volume, melting will give rise to suction of water from the outside of the specimen. The one-dimensional temperature gradient ensures that the last ice to melt will be in the bottom of the specimen, thus resulting in suction of water all through the specimen. Therefore the water content will be almost identical in the top and in the bottom of the specimen.

This mechanism explains why it sometimes happens, that dense high strength concrete breaks into small pieces in full depth of the specimen within a few freeze/thaw cycles.

4.2 Dilation

Continuous measurement during the freeze-thaw cycle normally shows expansion during the heating part of the cycle. Thermal expansion of ice is approximately 6 times larger than the thermal expansion of concrete. Since ice have been formed at lower temperatures than it melts,

then the thermal expansion of the ice will exert pressure on the inner walls of the pores during heating, thus giving rise to expansion. Figure 5 from /2/ illustrate this phenomenon.

When the internal ice melts, the volume decrease by 9 vol. pct., and the water can be redistributed in the specimen. The specimen will then shrink. Most of the ice melts close to 0°C, even if it freezes far lower. Bager and Sellevold /15/ explain this with "ink-bottle" pores into which water first freezes when the "bottle-neck" freezes. Spontaneous nucleation of ice in some of these pores might of cause happen.

The results presented in figure 5 clearly show the influence of water/cement ratio. The higher the water/cement ratio, the larger is the expansion during both cooling and heating. Note, that after 42 freeze-thaw cycles, the specimens have reached a degree of saturation higher than the critical, thus all three types shows a permanent length increase after the freeze-thaw cycle.

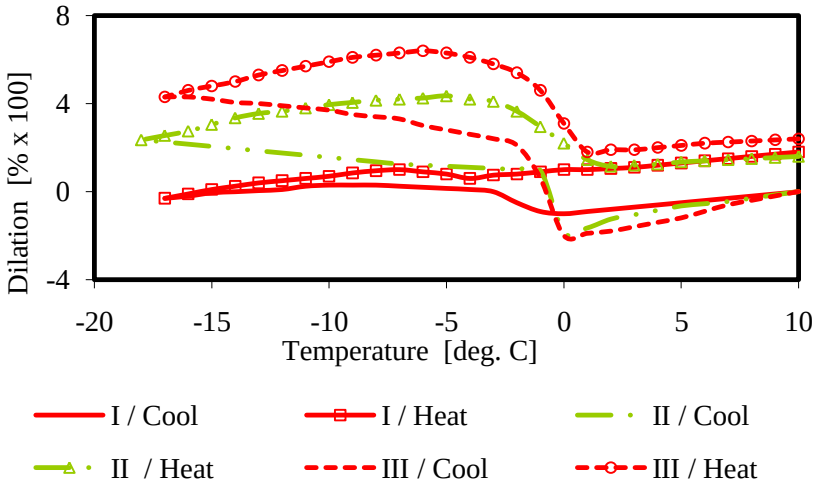

Figure 5 *Continuous dilation during the 42'd freeze-thaw cycle, measured at LTH /2/. Three types of concrete: I: w/c = 0.3; II: w/c = 0.5 & III: w/c = 0.7*

4.3 Crack formation

Andersen /16/ has measured acoustic emission during freeze/thaw cycles for two types of non-air entrained concretes, one with w/c-ratio of 0.9 and one with w/c-ratio of 0.5. His measurements demonstrated, that the major part of cracks appeared during the first freezing and only a very limited amount of cracks appeared during the melting period, see figures 6 & 7. The figures are examples for concretes with w/c-ratio of 0.5. This crack formation is not caused by thermal incompatibility between aggregate and cement paste, according to Sellevold et.al /18/.

Andersen further showed, that for weak concrete (w/c = 0.91) a linear relationship between accumulated acoustic emission and dilation exist, while for concrete with w/c-ratio of 0.5, such a linear relationship does not exist. For the latter, the accumulated acoustic emission in the first cycle is larger than the corresponding length change, see figure 7.

This can be explained by the following: For the high w/c-ratio, the cracks will be water filled almost spontaneously thus increasing the ice formation during the succeeding cycles and thereby

increasing the crack width, and the number of cracks. For w/c-ratio of 0.5, the cracks opened during the first cycle will first be water filled after some cycles. In this case, water can be drained from the finer pores into the cracks which result in a decrease in the dilation. The water uptake from outside sources of water and the internal drainage acts in opposite directions with regard to deformation of the specimen. For very dense specimens, as Type #1 with w/c-ratio of 0.32, the water uptake from outside is so slow, that the internal drainage leads to an overall shrinkage of the specimen during the first cycles, as seen in figure 8. Furthermore it is likely; that the degree of saturation in such concretes is below the critical degree of saturation which will result in no cracks appear during the first freezing. Formation of microscopic ice bodies can happen, which leads to absorption and suction of water from the outside. The critical degree of saturation will therefore be reached after several freeze/thaw cycles, and the ice formation will lead to expansion of the specimen.

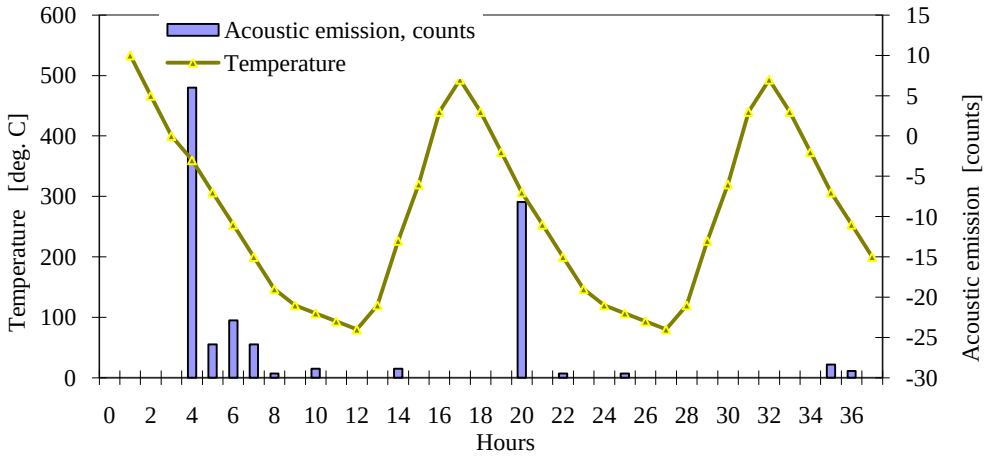

Figure 6 *Acoustic emission evolved in concrete with w/c-ratio of 0.5 during the first three cycles /16/. The test conditions were analogous but not identical to the present test conditions. The present author has redraw the curves.*

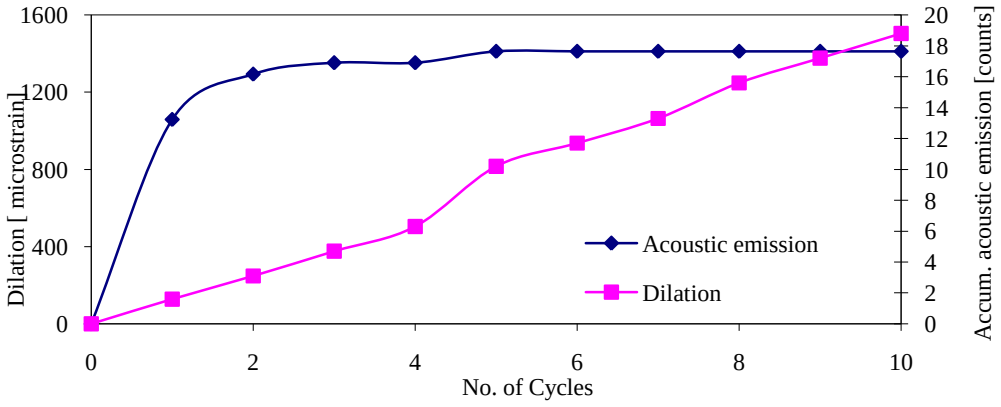

Figure 7 *Accumulated acoustic emission and dilation for concrete with w/c-ratio of 0.5, during the first 10 cycles /16/*

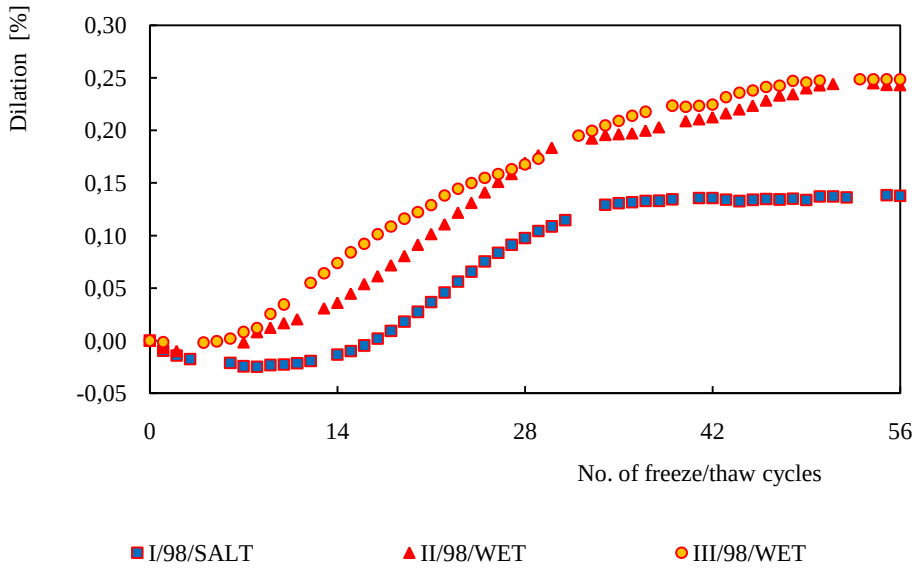

Figure 8 Accumulated dilation [%] as function of no. of freeze/thaw cycles.

4.4 Inner or outer salt solution

If the sample in the "salt" test has been saturated with salt solution before freezing is initiated, then the driving force for water-uptake is lowered, and scaling in decreased. This has clearly been demonstrated by Petersson /17/. Figure 9 shows the scaling from a non-air entrained mortar, with w/c-ratio of 0.5, tested either with pure tap water or with a 3 % NaCl-solution as the freezing media. Prior to the freeze/thaw test; the specimens had been stored for three months in NaCl-solutions of different concentrations between 0 % and 12 %, as indicated on the abscissa.

The figure shows:

- The largest scaling is obtained for the situation when the specimen is saturated with NaCl-solution below 0.5 %, and tested with 3 % NaCl-solution. This is in agreement with the normal test procedure.
- Independent of the concentration of NaCl in the pores, no scaling occurs when tested with pure tap water. (No information regarding internal damage exists).
- For freezing with 3 % NaCl-solution as the freezing media, the scaling decreases when the salt-concentration in the pores is higher than 1 %, compared to the scaling for lower concentrations. This can be explained by pore water freezing almost as pure pore-water, while the salt solution on the surface has a lower freezing point. I.e. the concentration on the surface decreases the freezing point of the solution, so that the difference in chemical potential between the salt solution on the surface and the solution in the pores is lowered compared to the "pure water inside - salt solution outside" test. The driving force for water movement to the upper layer from the bottom is therefore reduced, likewise the difference in internal stresses. As a result, scaling is reduced.

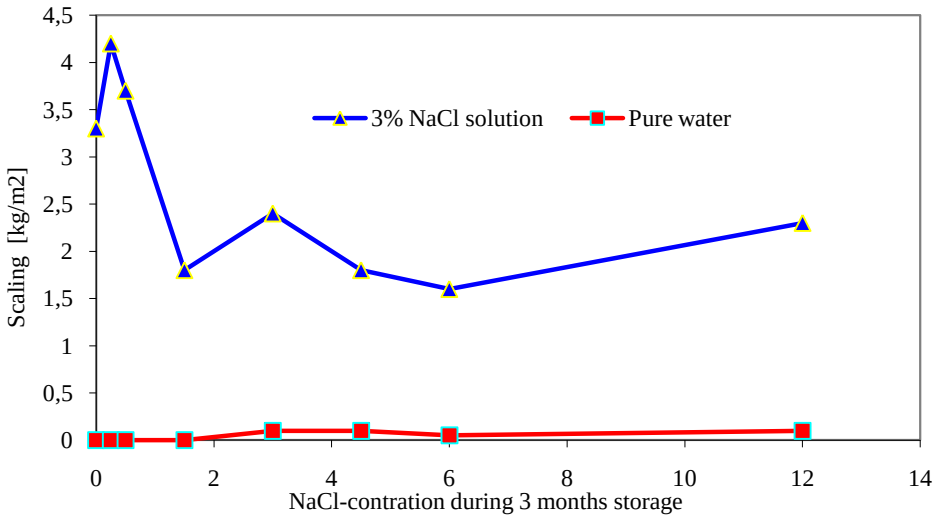

Figure 9 *Scaling from mortar bars (w/c-ratio = 0.5). Prior to the freeze/thaw test, the specimens had been stored for three months in NaCl-solutions of different concentrations between 0 % and 12 % /17/*

4.5 Measured water-uptake

Water-uptake was determined by weighing the saturated surface dry specimen after each scaling measurement. Weight of scaled material, corrected for evaporable water content, has been included.

The model predicts, that the micro ice body formation, and the affiliated moisture movements control the water-uptake.

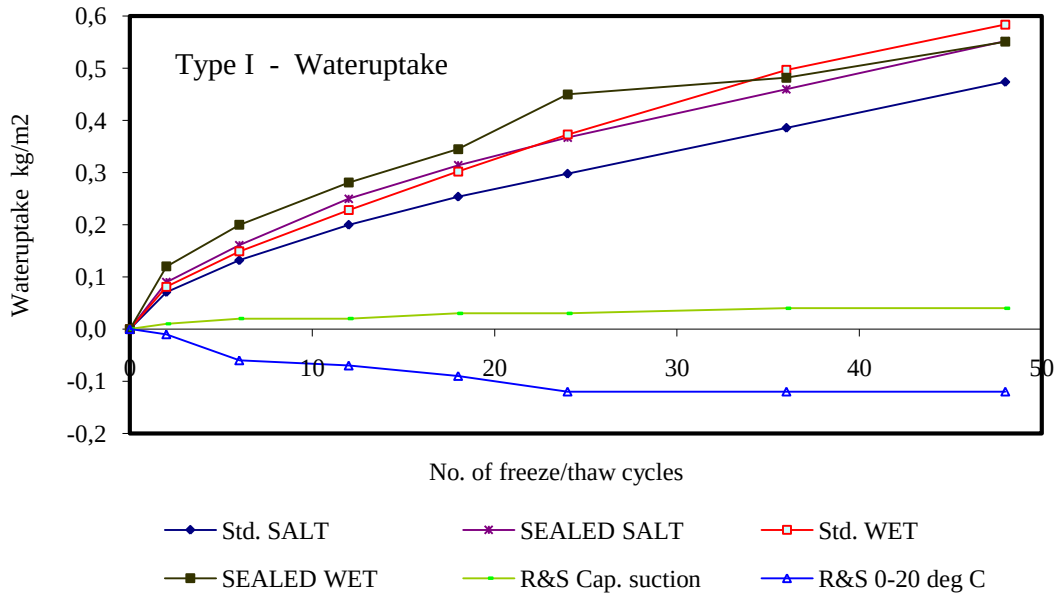

Figure 10 Water-uptake in concretes of type I

A lower water-uptake (kg/m^2) in the SALT specimen than in the WET specimen is expected according to the model if the moisture transport from the bottom to the SALT surface is sufficient. The measured water-uptake shown in figures 10 and 11 confirms this.

It is remarkable, that the water-uptake in the Sealed tests is higher than in the Std. tests. This clearly illustrates the suction forces from the micro ice bodies, when +20 ^{o}C water is poured on the specimen at -20 ^{o}C.

The water-uptake in the std. test measured by Relling & Sellevold /19/ is identical to the water-uptake in the Std. freeze-thaw test in the present investigation. For pure capillary suction, no further water-uptake takes place, and for the temperature cycle above 0 ^{o}C, a small weight loss is seen. No explanation for the latter phenomena has been found.

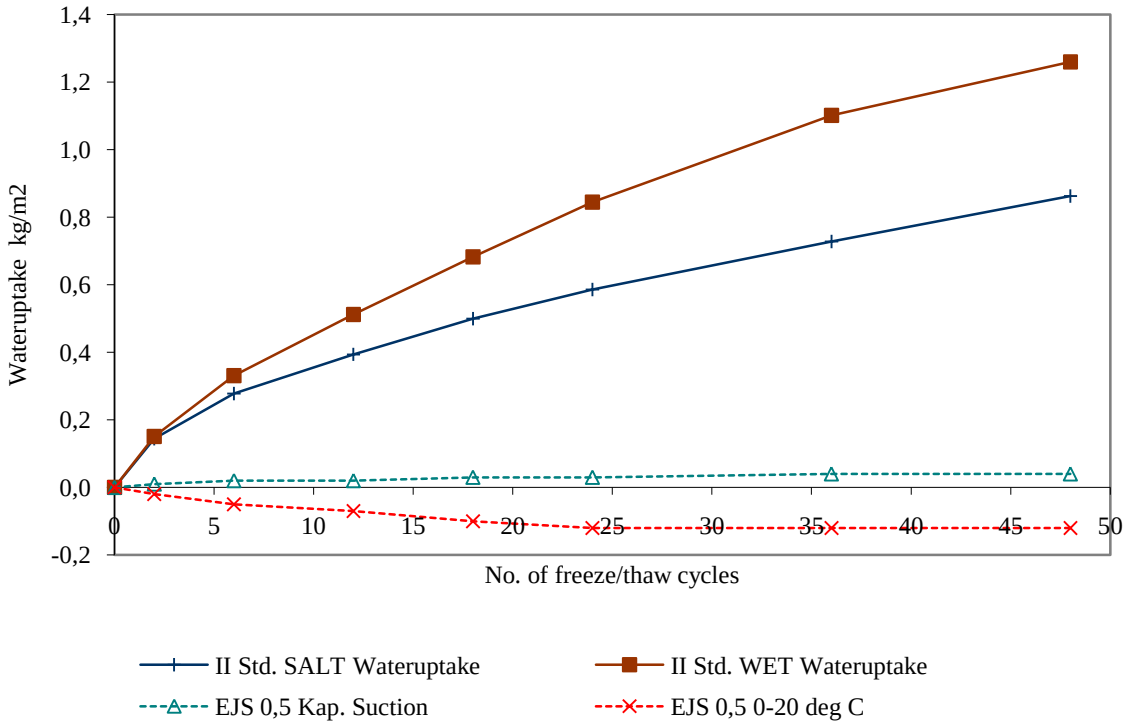

Figure 11 Water-uptake in concretes of type II

4.6 Moisture distribution

In order to verify the model regarding moisture distribution, experiments were carried out with type I concrete, tested both with the "Wet" test and the "Salt" test.

Distribution of water inside the specimens were measured by splitting the sample into two in order to measure the water content in top and bottom parts, see figure 12. To study the variation of the moisture profile during the test, half of the specimens were splitted while they were frozen (-20 ^{o}C), and half at +20 ^{o}C. These measurement were carried out both with 3 % NaCl-solution and demineralised water as freezing media

Figure 12 *Sample divided by splitting in upper and lower part for measurement of water content*

The moisture content was measured in the upper and lower parts of the specimens. The difference in moisture content given in table 1 is calculated as the difference between upper and lower parts relative to the moisture content in the lower part. Each figure represents mean values for six specimens. The absolute moisture content was about 4.2 weight percent of dry concrete, which corresponds to app. 60 grams in each part. A difference of 6 % thus equals 3.6g.

Table 1 *Difference in moisture content in the upper and lower part of the specimen. The figures indicate the higher content in the upper part compared to the lower part.*

+ 20 °C - SALT	+ 20 °C - WET
5.4 %	**0 %**
- 20 °C - SALT	- 20 °C - WET
5.1 %	**6.6 %**

The moisture distribution at +20 °C is as predicted in section 3.1.2, where a homogeneous distribution for the WET test, and higher moisture content in the upper part in the SALT test. The higher content in the upper part at –20 °C for both tests can be caused by suction towards the coldest part – the upper surface – during the cooling phase. For the WET test, the moisture is redistributed during the melting phase.

4.7 Detection of internal cracking

Internal cracks in the concrete will be associated with an increase in dimension. Furthermore, cracks will increase the UPTT. Hence measurements of dilation and UPTT have been carried out.

In the following figures the results are shown. Figure 13 shows the correlation between increase in transmission time for the ultrasonic pulse signal (UPTT) and linear expansion for Type #1 up to 112 freeze/thaw cycles.

In the former NORDTEST-project /1/, identical large increase in UPTT measured at 28 and 42 cycles was observed for the same type of concrete.

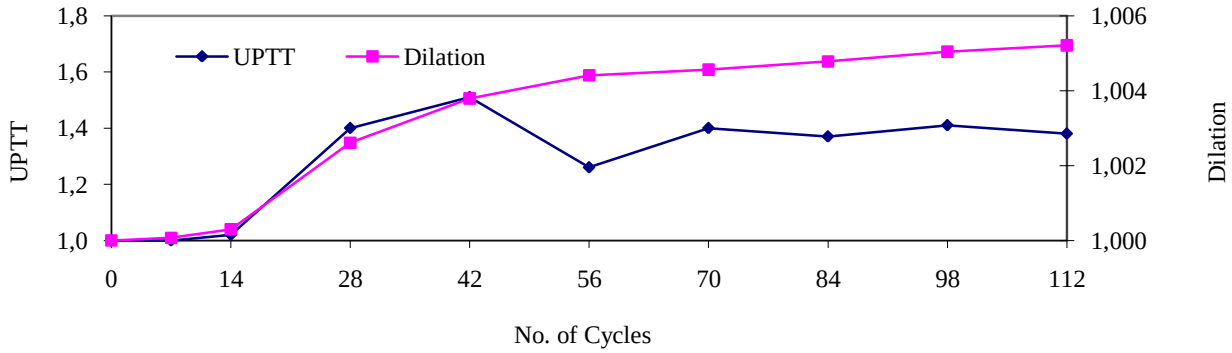

Figure 13 UPTT and dilation vs. no. of cycles for concrete Type #1 [w/c = 0.31]

In figure 14, the crack pattern in one of the four Type #1 samples can be seen. The sample has been impregnated with fluorescent epoxy in order to visualize the cracks. The width of the specimen is smaller than 150 mm, since the insulation layer has been removed by sawing the edges of the specimen.

In this specimen the majority of the cracks surround the larger aggregate particles. Such cracks are caused by volumetric expansion of the cement paste. Such empty cracks appear around the individual aggregate particles when the paste has reached a critical degree of saturation [α-saturation]. The UPTT will increase due to these air-filled cracks, and later decrease to a lower level, when the cracks after a number of freeze/thaw cycles become water-filled. When these cracks around the individual aggregate particles reach a critical degree of saturation [β-saturation], cracks between the individual particles will form.

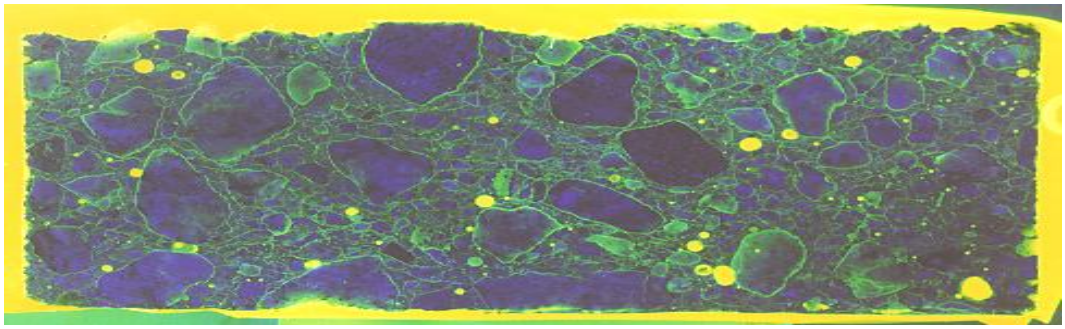

Figure 14 Crack pattern in specimen #1 after 112 cycles. Specimen width: 105 mm. The concrete has been impregnated with fluorescent epoxy in order to see the cracks.

Figure 15 shows the correlation between UPTT and length change for concrete Type #2, and figure 16 the corresponding crack pattern.

In figure 15 the same increase in UPTT between 28 and 42 cycles as seen for Type #1 can be seen, although the magnitude is smaller.

The crack pattern in Type #2, figure 16, is very much alike the crack pattern in concrete Type #1. The same mechanism for internal damage must therefore be active, irrespectively of the difference in water/cement-ratio and the freezing media.

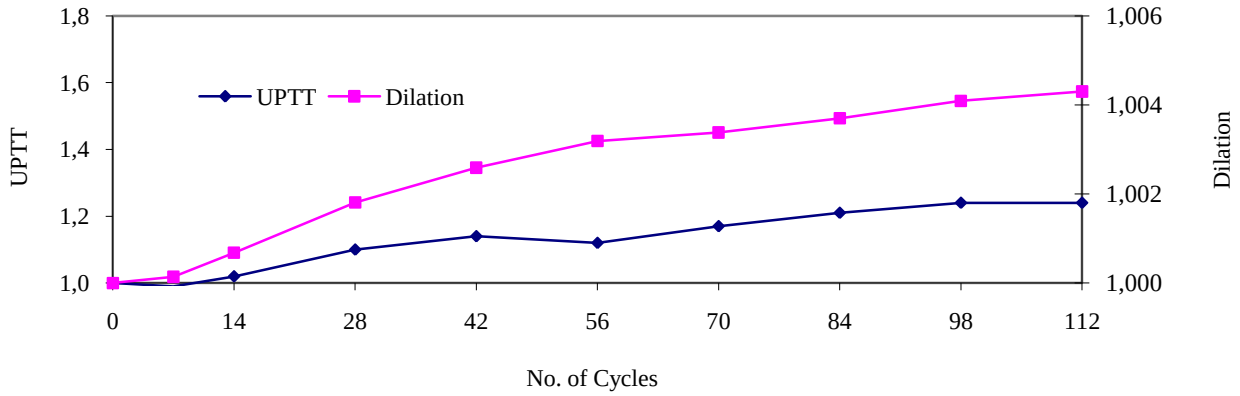

Figure 15 UPTT and dilation vs. no. of cycles for concrete Type #2 [w/c = 0.48]

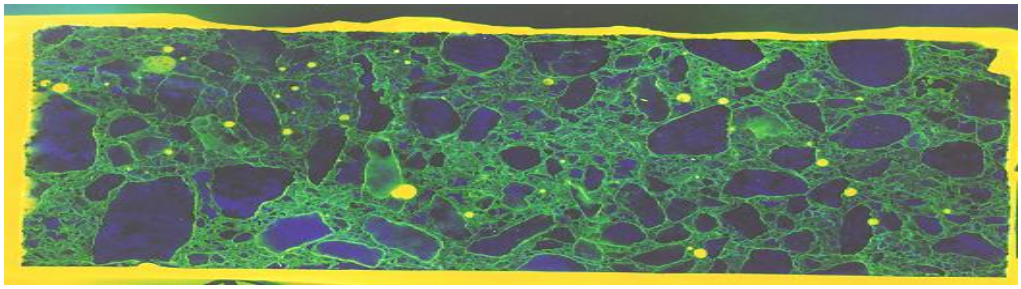

Figure 16 Crack pattern in specimen #2 after 112 cycles. Specimen width: 120 mm.

A very good correlation between UPTT and length change has been found for concrete Type #3 up to 56 freeze/thaw cycles, as shown in figure 17. Results up to 98 cycles are shown in figure 18.

In this concrete both UPTT and dilation increases with increasing freeze/thaw cycles, and there is no sign of the mechanism discussed for concrete Types #1 & #2 between 28 and 42 cycles. The high water/cement-ratio and coarse continuous capillary pore system secure a fast water-filling of internal cracks.

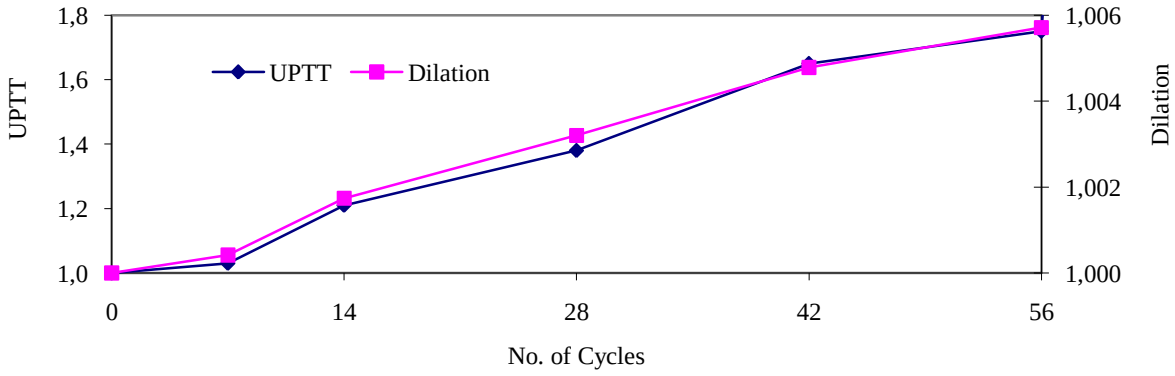

Figure 17 UPTT and dilation vs. no. of cycles for concrete Type #3 [w/c = 0.67] up to 56 cycles

It can be seen in figure 18, that UPTT for Type #3 increases to infinity between 56 and 84 cycles indicating a more or less total breakdown of the internal structure. In fact this concrete turned out to be so damaged by internal cracking that the freeze/thaw cycles had to be stopped after 98 cycles. Despite the structural break down, the scaling was rather low, only 0.235 kg/m^2 after 98 cycles. The results presented in figure 23 show how the water-uptake increases from cycle 56 and onwards, which can be explained by water filling of cracks and larger continuous pores.

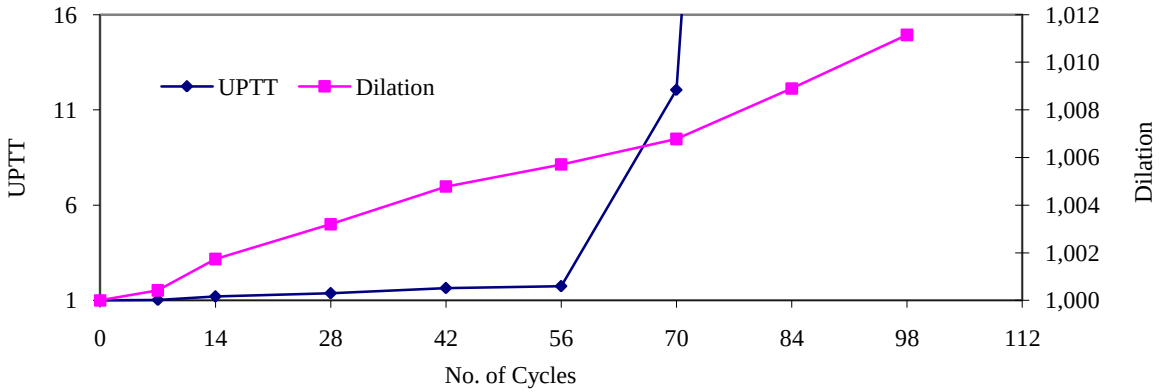

Figure 18 *UPTT and dilation vs. no. of cycles for concrete Type #3 [w/c = 0.67] up to 98 cycles {Note: The scale for the UPTT axis has been increased 5 times more than the scale on the dilation axis compared to figure 17}*

In figure 19 the crack pattern in Type #3 can be seen.

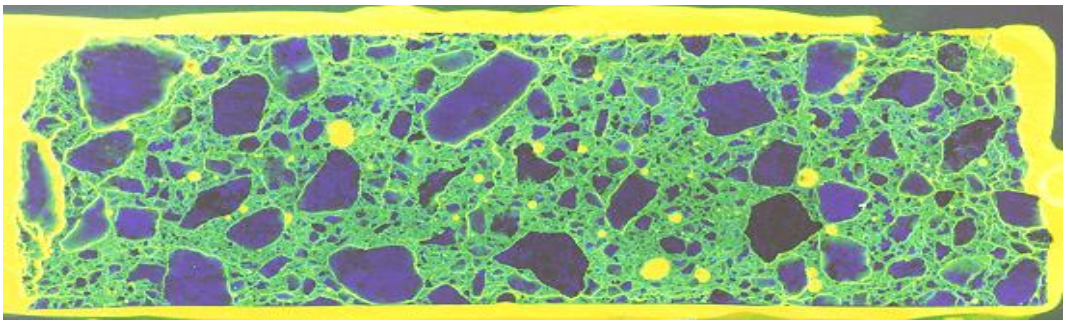

Figure 19 *Crack pattern in specimen #3 after 98 cycles. Specimen width: 150 mm.*

In figure 20 the relationship between water uptake and increase in length is illustrated. It can clearly be seen, that after internal cracking is initiated, the length increase is proportional to the amount of water uptake as further evidence that the same mechanism is active, irrespectively of the water/cement ratio and the freezing media.

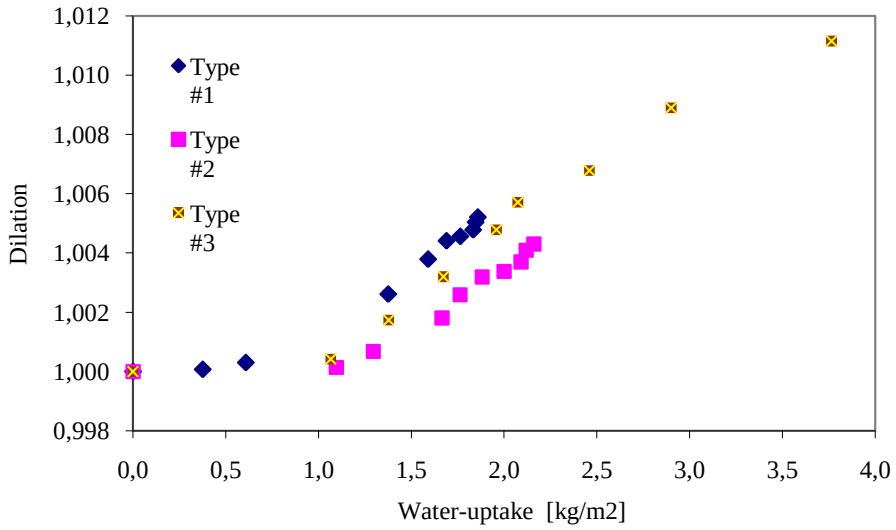

Figure 20 Dilation as function of water-uptake. Type #1: Salt, Type #2 & Type #3: Wet. /6/

4.8 Scaling

In figures 21 – 23 it can be seen, that the water-uptake almost ceases after 28 cycles for Type #1 & Type #2, whereas it increases continuously for Type #3. This agrees well with the increase in UPTT and the dilation for Types #1 & #2, indicating that nearly all crack-formation takes place just after the critical degree of saturation has been reached. Furthermore, this is in agreement with measurements of decrease in compressive strength on specimens exposed to the same freeze/thaw test, but at different stages of the test. This test showed a dramatically decrease in compressive strength between 7 and 28 cycles, followed by a slower reduction in strength., for a concrete almost identical with Type #1 /1/, see figure 24. In this case, the freeze/thaw test has been carried out according to the slab test for #1 & #3, while for #3-sf (sealed freeze/thaw), water-uptake has only taken place at constant temperature of +20 ^{o}C, the "classical" test. The cycles for #3-sf was: 7 f/t-cycles with the surface moist, but without free water, then 7 days at 20 ^{o}C with water on the surface, 7 f/t-cycles with moist surface, 7 days with water etc.

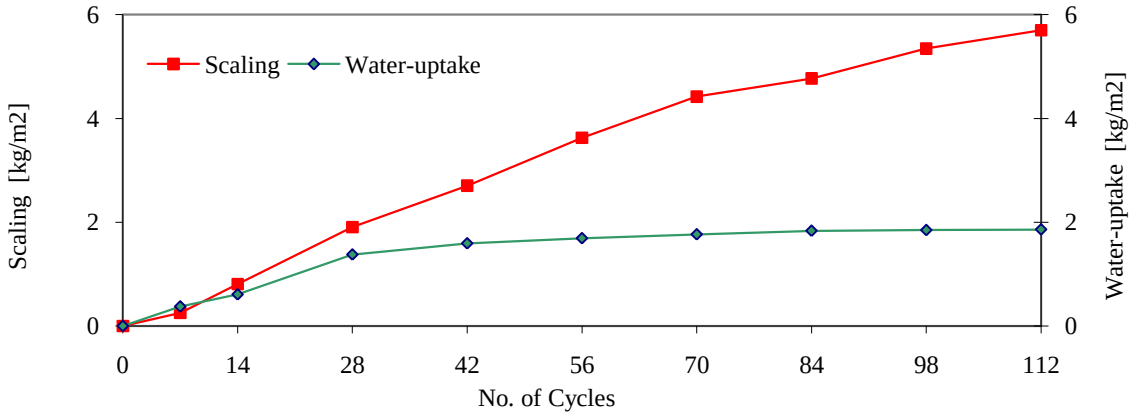

Figure 21 *Scaling and water-uptake for concrete Type #1. When this concrete has reached a certain degree of saturation after 28 cycles, the water-uptake almost ceases, while the scaling still increases. In figure 12 the large scaling can clearly be seen as an uneven surface (2.3 kg/m^2 after 112 cycles).*

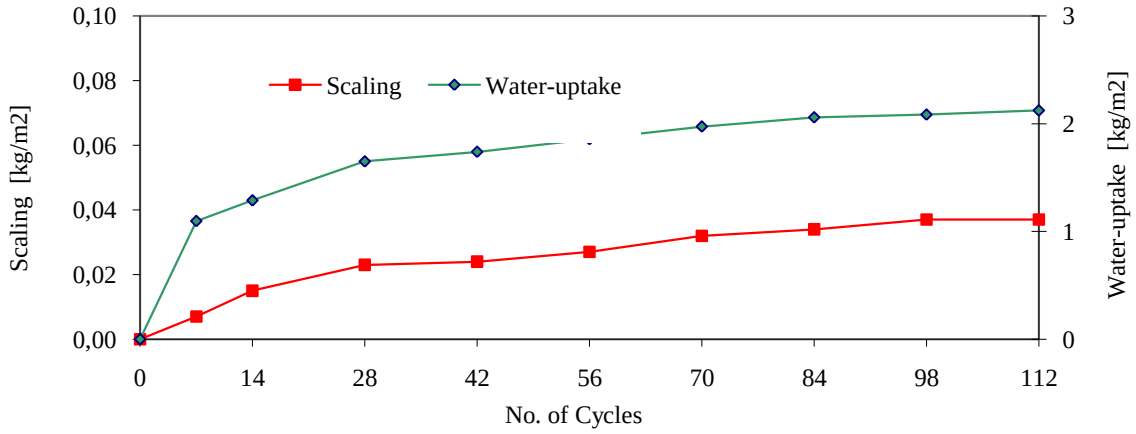

Figure 22 *Scaling and water-uptake for concrete Type #2. The water-uptake increases until app. 28 cycles, then the increase is very slow, and the scaling is very low (0.037 kg/m^2 after 112 cycles). When this concrete has reached a certain degree of saturation the water-uptake ceases. For this concrete, a clear correlation between water-uptake and scaling can be seen, supporting the theory of critical saturation.*

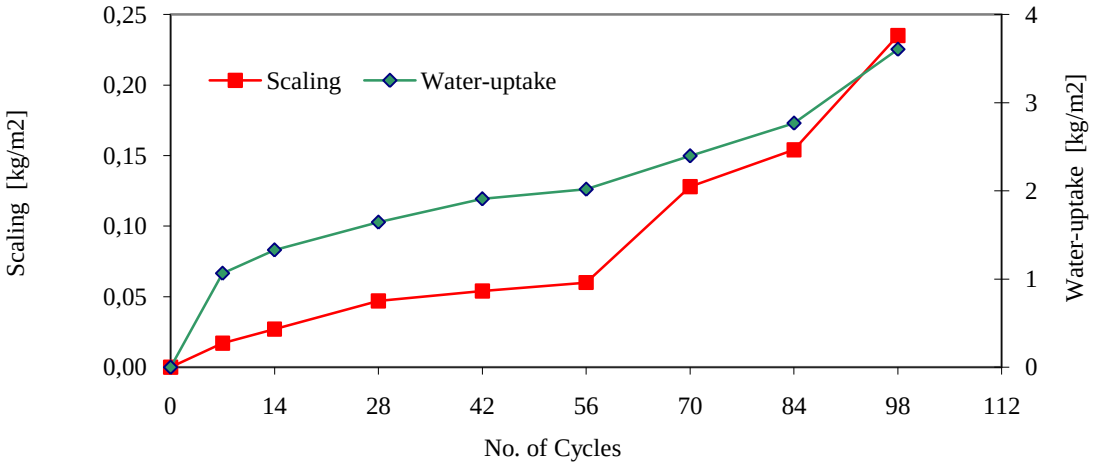

Figure 23 *Scaling and water-uptake for concrete Type #3. During the first 56 cycles, the water-uptake is almost identical with the water-uptake in Type #2. Thereafter, the water-uptake increases. The increase in water-uptake happens at the same time, as the UPTT increases to infinity, and the scaling increases.*

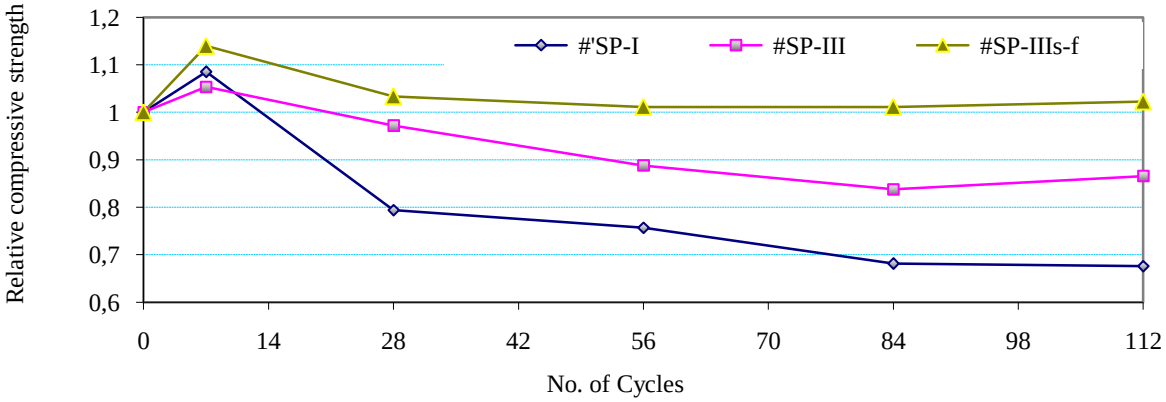

Figure 24 *Relative compressive strength. Measured at SP /3/. #I: w/c = 0.31 "salt", #III: w/c = 0.67, "wet", #IIIs-f: w/c = 0.67, "classical".*

Demineralised water as freezing media mainly results in internal damage, whereas salt solution results in surface scaling. Therefore nearly no scaling is observed for type I in Std. Wet test and Sealed Wet test, whereas fairly large scaling is observed for Std. salt and Sealed Salt test, see figure 25.

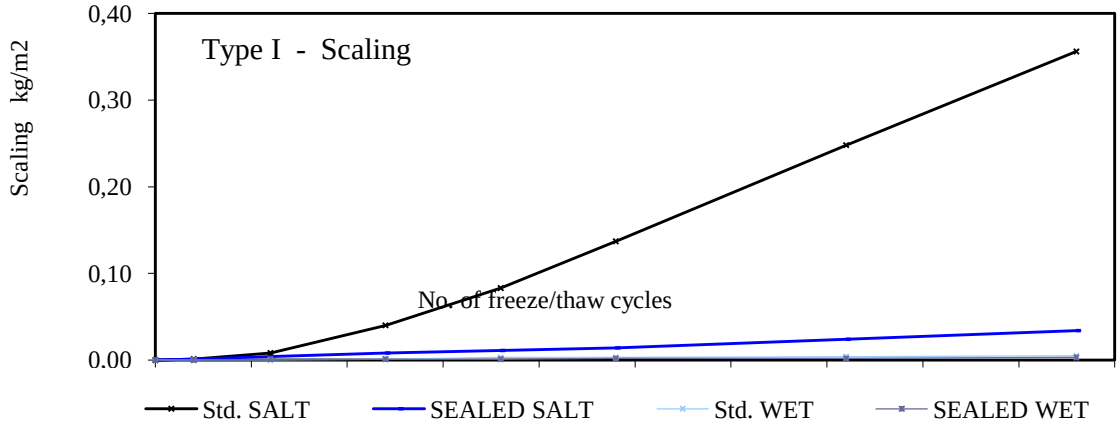

Figure 25 Scaling for type I concrete

It is remarkable, that Std. Salt test results in significant larger scaling than the Sealed Salt test, although the latter has a higher water-uptake. However, the same phenomenon is observed for other series.

The phenomenon that increased water-uptake in the sealed test lead to increased dilation and increased UPTT but reduced scaling might be explained by a different water distribution compared to the water distribution obtained during the Std. tests. As shown by the acoustic emission data, then the major amounts of cracks appear during cooling. Therefore, the extra amount of water taken up will not give rise to extra scaling in the same freeze-thaw cycle, but the successive increase in water should lead to increased damage if the water was distributed as the water sucked in during the Std. tests.

However, the extra amount of water enters the structure at the lowest temperature in the freeze-thaw cycle. The specimen is expanded due to formation of micro ice bodies in the pore system – an ice formation that has removed some water from the gel during cooling. At the lowest temperature in the freeze-thaw cycle, the system almost is in equilibrium. Therefore, since the chemical potential of the remaining un-frozen water in the gel and the micro ice bodies must be equal when the sample is at the lowest temperature, then the water might enter the gel system instead of forming more ice. Thus the gel will be saturated when the specimen is melted. This lead to an overall expansion of the specimen compared to the situation where the gel is un-saturated. If most of the extra water is used for such expansion of the solid matrix, then the capillary pore volume will increase, and it will take longer time to reach the critical degree of β-saturation. Hence, for the same number of freeze-thaw cycles, the scaling will be less in the sealed tests.

5 CONCEPTUAL MODEL FOR THE FREEZE-THAW MECHANISM

The conceptual model presented in this section has been derived on basis of a huge number of experiments, as described in the proceeding sections.

5.1 Freeze-thaw tests with pure water as freezing media

The model for freeze-thaw damage mechanism /6, 20/ predicts that frost damage in non-air entrained concrete is caused by the following sequence of events:

- During freezing microscopic ice bodies are formed in the capillary pores in the paste.
- Formation and primarily melting of these microscopic ice bodies leads to extensive water uptake from the surroundings, if free water is accessible.
- When the paste becomes critically saturated [α-saturation], formation of the microscopic ice bodies causes a volumetric expansion of the paste. This volumetric expansion of the paste results in formation of cracks surrounding the individual aggregate particles. These cracks are empty (air-filled) at the moment they appear. In the freeze-thaw test, formation of such cracks will be monitored by an increase in length or volume of the specimen.
- Further water uptake, and maybe also redistribution of water from paste towards these empty cracks due to ice formation as in artificial air-bubbles, leads to increased water content in these cracks.
- At a certain time these cracks become critically saturated [β-saturation]. Thus the "particle" of aggregate + surrounding saturated crack will expand during freezing.
- Such expanding particles will lead to cracks in the paste, connecting the individual particles. Gradually this crack formation will lead to total breakdown of the internal structure.

The model predicts that a relationship between water-uptake and damage exists.

5.2 Freeze-thaw tests with de-icing agent as freezing media

In the "salt" test, the water-uptake is a bit different, but still the basic destructive mechanism is related to microscopic ice body growth. It has to be remembered that the sample has been saturated with water before the test. The salt solution is first applied immediately before the first freezing. The water movement within the specimen will therefore be:

- During the first cooling period, the upper surface will attract water due to the lower chemical potential of the salt solution on the upper surface. This leads to a water movement from the lower part of the specimen towards the upper surface.
- When the temperature is below 0 ^{o}C, pore water in the upper saturated part of the specimen will freeze before the salt solution on the surface. Microscopic ice body formation is then governed from water both from the lower part of the specimen and from the solution on the surface.
- During melting, the salt-solution on the upper surface will melt first, and further water-uptake will take place, first caused by microscopic ice body growth until the ice into the specimen has melted, secondly by suction due to the decrease in volume when the ice melts.

Such movements of water, and formation of microscopic ice bodies, lead to a volume increase in the paste in the upper layer, and shrinkage in the lower layer. Such internal stress distribution favour scaling. The mechanism can be compared to frost heaving of soils as described by Lindmark /21/. Therefore scaling is almost always associated with a situation where the outer solution has a lower freezing point than the pore solution - the "salt" test.

This model widen the traditional model for critical degree of saturation in order to distinguish between saturation of the micro pores [α-saturation] and saturation of the cracks around the aggregate particles arising from the volumetric expansion of the pasta [β-saturation]

5.3 Influence of water/cement ratio

The higher the water/cement ratio, the faster the water-uptake and, consequently, the faster the critical degree of saturation [β-saturation] in the cracks surrounding the aggregate particles will be reached.

Concrete with a high water/cement ratio will therefore be destroyed by internal cracking far earlier than concrete having a lower water/cement ratio.

6 CONCLUSION

Results of a huge amount of experimental tests have been compiled to set up a conceptual model for freeze-thaw damage in concrete.

The model presented explains qualitatively the freeze thaw damage in concrete caused by formation of micro ice bodies. The classical model for critical degree of saturation is widened in order to distinguish between the saturation of the micro pores [α-saturation] which lead to expansion of the paste, and saturation of the cracks arisen around the aggregate particles [β-saturation] where ice formation lead to crack formation between the aggregate particles and destruction of the concrete.

The model also explains why pure water as the freezing media mainly lead to internal deterioration, while salt solutions as freezing media mainly lead to scaling.

REFERENCES

1 Tang, L., Bager, D.H., Jacobsen, S. & Kukko, H.
"Evaluation of the Ultrasonic Method for Detecting the Freeze-thaw Cracking in Concrete" NORDTEST-project No. 1321-97. Swedish National testing and research Institute - Building Technology, SP Report 1997:37, 63 p (40p. /8app.) ISBN 917848-693-3

2 Jacobsen, S., Bager, D.H., Kukko, H., Luping, T. & Nordström, K
"Measurement of internal cracking as dilation in the SS137244 frost test",
NORDTEST project 1389 - 98. Norwegian Building Research Institute Report No. 250 : 1999

3 Tang, L., Bager, D.H., Jacobsen, S., Kukko, H.
"Detecting Freeze/thaw Cracking in Concrete by Ultrasonic Pulse Velocity Methods".
Frost Resistance of Building Materials, 3rd Nordic Research Seminar on Frost Resistance of Building Materials
Report TVBM-3087, Division of Building Materials, Lund Institute of Technology.
Lund 31/8-1/9 1999

4 Tang, L., Bager, D.H., Jacobsen, S., Kukko, H., Gudmundsson, G.
"Evaluation of the modified Slab Test for Resistance of Concrete to Internal Frost Damage"
NORDTEST Project No 1485-00, SP Report 2000:34. ISBN 91-7848-835-4

5 Utgenannt, P., Ollandezos, P., Bager, D.H., Farstad, T., Gudmundsson, G., Paroll, H.:
"Influence of Freezing Media on the Frost Resistance of Concrete".
NORDTEST-project No. 1533-01. Swedish National testing and research Institute - Building Technology, SP Report 2001:38, 41 p (16p. /6app.)
ISBN 91-7848-885-0

6 Bager, D.H., Jacobsen, S.
"A Model for the Destructive Mechanism in Concrete caused by Freeze-thaw Action".
Proceedings from Minneapolis Workshop on Freeze-thaw Damage in Concrete. Minneapolis, Minnesota, USA, June 1999. RILEM Proceedings PRO 25, 2002, ISBN 2-912143-31-4

7 Bager, D.H., Sellevold, E.J
"Ice Formation in Hardened Cement Paste, Part II - Drying and Resaturation on Room Temperature Cured Pastes",
Cement and Concrete Research, Vol. 16, pp835-844, 1986

8 Bager, D.H.
"A Conceptional model for Freeze-Thaw deterioration of Concrete"
15'th IBAUSIL, Bauhaus-Universität Weimar, September 2003, ISBN 3-00-010932-3

9 Sellevold, E.J., Bager, D.H.
”Some implications of calorimetric ice formation results for frost resistance testing of cement products”
Proceedings from workshop “Beton & Frost”, Køge October 1984, Publication 22:85 1985, The Danish Concrete Association. ISBN 87-87823-44-6

10 Fridh, Katja
“Internal Frost Damage in Concrete – Experimantal studies of destruction mechanisms”
Ph.D. Thesis, Division of Building Materials, Lund Institute of Technology, Report TVBM 1023, 2005, ISBN 91-628-6558-7

11 Rønning, T.F.
“Freeze-Thaw Resistance of concrete. Effect of: Curing Conditions, Moisture Exchange and Materials”
Dr. Ing. Thesis, The Norwegian Institute of Technology, Division of Structural Engineering, Concrete Section. Trondheim 2001. ISBN 82-7984-165-2

12 Setzer, M.J. (1999)
“Micro Ice Lens Formation and Frost Damage”
Proceedings from Minneapolis Workshop on Freeze-thaw Damage in Concrete. Minneapolis, Minnesota, USA, June 1999. RILEM Proceedings PRO 25, 2002, ISBN 2-912143-31-4

13 Setzer, M.J.
“Development of the micro-ice-lens model”
RILEM Proceedings PRO 24 – ”Frost Resistance of Concrete” Essen, Germany, April 2002.
ISBN 2-912143-30-6

14 SS 13 72 44:1995, “Concrete testing – hardened concrete – Scaling at freezing”

15 Bager, D.H., Sellevold, E.J. (1986A)
“Ice formation in Hardened Cement Paste, Part I”,
Cement and Concrete Research, vol. 16, pp. 709 – 720, 1986

16 Andersen, E.Y.
“Anvendelse af akustisk emission til frostbestandighedsvurdering og konstruktionsovervågning” (In Danish). Technical University of Denmark, Department of Structural Engineering 1983

17 Petersson, P.-E.
“Inverkan av Salthaltiga Miljöer på Betongs Frostbeständighet” (In Swedish).
Proceedings from a Nordic Workshop “Beton & Frost”, Køge/Denmark 1984. Publication Nr. 22:85, The Danish Concrete Association

18 Sellevold, E.J., Jacobsen, S., Bakke, J.A
"High Strength Concrete without Air Entrainment. Effect of Rapid Temperature Cycling Above and Below 0°C",
International Workshop on the Resistance of Concrete to Scaling due to Freezing in the Presence of Deicing Salts, Centre de recherce Interuniversitaire sur le Beton, Université de Sherbrooke - Université Laval, Quebec, august 1993, RILEM Proceedings 30, 1997, ISBN 0 419 20000 2

19 Relling, R. Holen & Sellevold, E.J.
Personal information presented at the XVI Nordic Concrete Research Meeting, Espoo, Finland August 1996

20 Bager, D.H., Jacobsen, S.
"A Conceptual Model for the Freeze-Thaw Damage of Concrete".
Proceedings from the 3rd Nordic Research Seminar on Frost Resistance of Building Materials, Lund 31. August – 1. September 1999. Report TVBM-3087, Lund Institute of Technology, Division of Building Materials.

21 Lindmark, Sture
"Mechanisms of Salt Frost Scaling of Portland cement-bound Materials: Studies and Hypothesis",
Ph.D. Thesis, Lund University, Division of Building Materials, Report TVBM 1017, 1998
ISBN 91-628-3285-9

Concrete Freeze-Thaw Resistance Testing
Current testing regime & Approval: Fair basis for Performance Evaluation?

Terje F. Rønning
Ph.D
NORCEM AS / R&D Dept
P.O.Box 38
N-3991 BREVIK, Norway
E-mail: terje.ronning@norcem.no

ABSTRACT

European requests for more exposure differentiation based performance evaluation calls for a review of the adopted testing conditions. Sustainable concrete development requires a closer look on the qualifications of the basis for ranking, in particular those related to moisture exchange and degree of saturation. Also, the basis for evaluation of F-T resistance under fresh water (non saline) conditions is scarce. In summary, the moisture load during laboratory testing and under field conditions should be closer investigated.

Key words: Lab-field correlation of future concrete, differentiated requirements, non-saline environment evaluation.

1 INTRODUCTION

The testing method for determination of freeze-thaw resistance of concrete in accordance with CEN TS 12390-9 [1] is subject to review by CENT C 51 / WG 12 / TG 4. The background is a call for a testing set-up enabling expectedly more correct assessment of freeze-thaw resistance performance for "milder" exposure and requirements than under the current regime (provided in the TS).

It is also implicit that the preparation of the current testing regime mainly followed on the in-situ experience of CEM I cement (EN 197-1) containing concrete. Subjecting more slowly developing properties concrete to this regime may disfavour or even disqualify adequate binder combinations. Failing to do so, may impair our industry's ability to adopt sustainable solutions [10].

The Norwegian EN 206-1 application rules offers approval by qualification testing for cement not covered by the current application rules (e.g. CEM II/B-V (or -S)) under saline conditions only, covering all the exposure classes XF2, XF3 (high degree of water saturation, but no de-icer) and XF4 by the same procedure. (XF1 does not require qualification testing.). This is partly a result of the overall missing application guidelines, left to being established "in accordance with local conditions":

Finally, although – or because - the CEN TS provides one reference method ("Slab test") and two alternative methods ("Cube test" and "CF/CDF test"), all three with either saline or non-saline conditions, no specific statements are provided concerning linking of exposure class, selection of procedure or scaling/damage acceptance criteria. On the other hand, it is not usual to include acceptance criteria in a testing standard as done in the Swedish version (of the reference method) [2].

These concerns may be satisfied by considering changes to the testing methods (incl. pre-conditioning), their application and/or test results evaluation criteria.

2 EARLY AGE MOISTURE EXPOSURE

2.1 Pre-conditioning and moisture uptake

In figure 1, the CEN TS 12390-9 stages in the preparation procedure prior to freeze-thaw exposure are illustrated, with focus on the so-called "under-water-curing" period: From the de-molding at 24 h (+/- 2 h), the samples are stored under water until the age of seven days. During this period, the samples are subjected to capillary suction following from on-going hydration. The extent of hydration – and capillary suction volume - during this six days period may vary significantly, depending e.g. on the reactivity (mineralogy and fineness) of the cement, level of additions (clinker replacement level) and water/binder ratio.

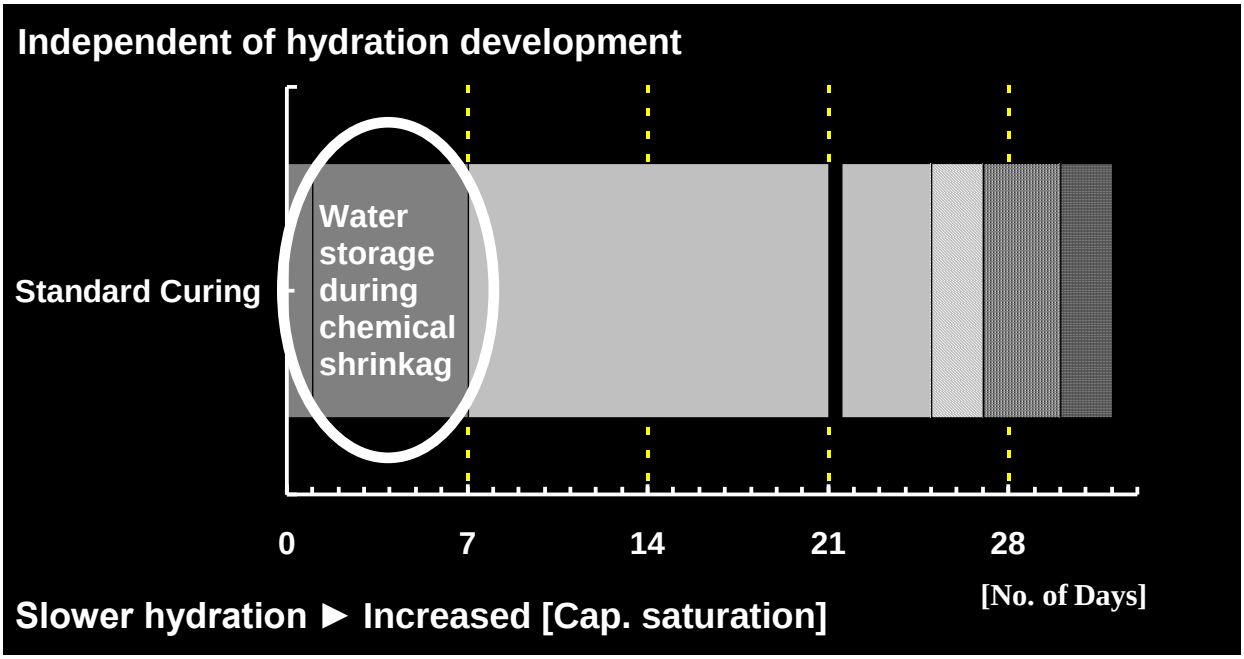

Figure 1 – Schematic illustration of the pre-storage and preparation procedure of CEN TS 12390-9 [1], i.e. independent of concrete mix design, from [3].

The implication of this various degree of suction is that the degree of saturation prior to the next stage, air climate chamber storage, may vary and induce variations to the succeeding evaporation conditions, controlled by diffusion and vapour (gradients) differences. The contribution of the water storage period to promote hydration (perception of "curing") is questionable : If a neutral "maturity" period is to be kept for allowing hydration, this could in

most cases be provided by isolated curing, i.e. only preventing loss of initially added moisture (mixing water).

An attempt to reduce the external moisture exposure at this stage ("Plastic curing") is illustrated in figure 2, and the resulting behaviour with respect to moisture uptake during the procedural re-saturation in figure 3. The latter followed almost no difference in moisture loss during "air curing" between plastic and standard curing, although the plastic stored samples had already been cut and standard cured samples lost moisture from the lateral surfaces only. Trying to isolate the effect of early age (7d) sawing lead to substantial weight loss and re-saturation uptake ("Modified standard"). Moisture uptake took place from the top surface only in all cases. The study is extracted from [3].

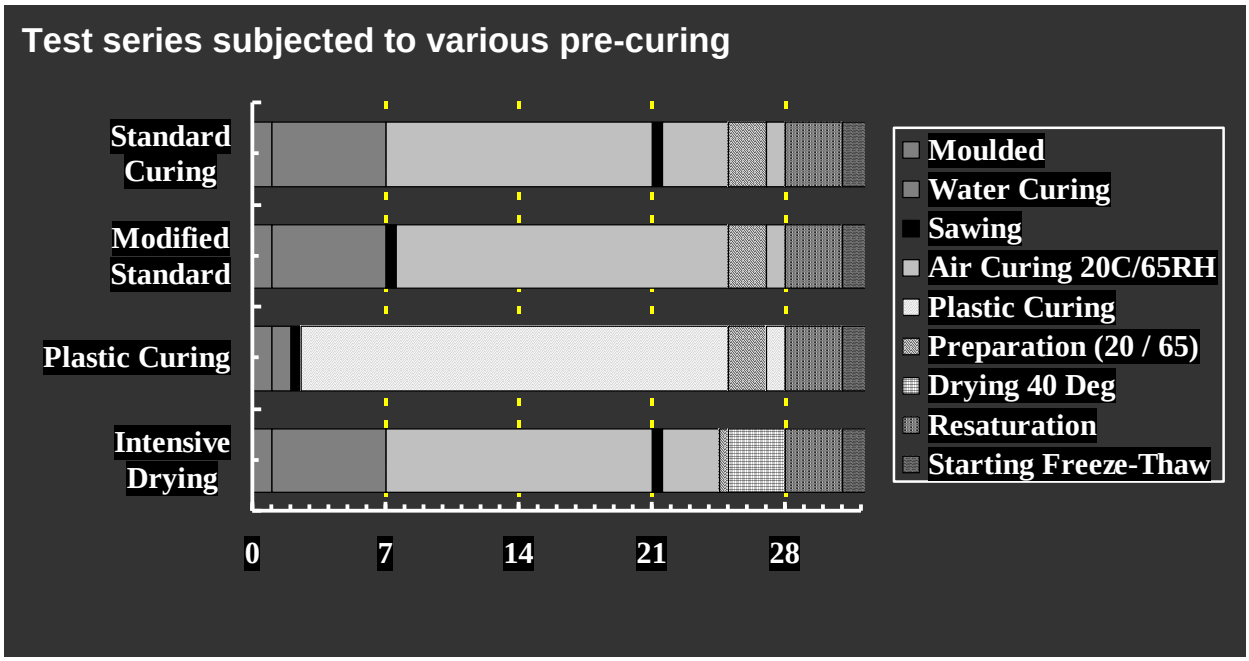

Figure 2 – Schematic illustration of investigated pre-storage conditions [3].

2.2 Pre-conditioning and scaling level

The critical issue for discussion, is to what extent differences in water uptake during the submerged storage ("curing") period, caused by different hydration (or other ;) properties are reflected in subsequent scaling level and, hence, evaluation of the material mix design.

It has been demonstrated that the moisture history of the samples significantly influences the pore structure (pore size distribution) and moisture content [4] as well as the scaling resistance [5] when the changes are temperature or even ambient conditions induced. However, few other authors have focused other causes for moisture changes than temperature in respect of potential scaling resistance influence, although it is widely accepted that wetting and drying in itself leads to closing and opening of the pores. Temperature rise is (within reason) mainly used as a means of introducing the RH changes (potential) required to trig the moisture movements. Storing samples under water during the on-going chemical shrinkage will most probably lead to water filling of pores that would not have been available to external moisture at a later stage and, hence, contribute to a different extent to the subsequent freeze-thaw caused water pumping and re-distribution effects [3].

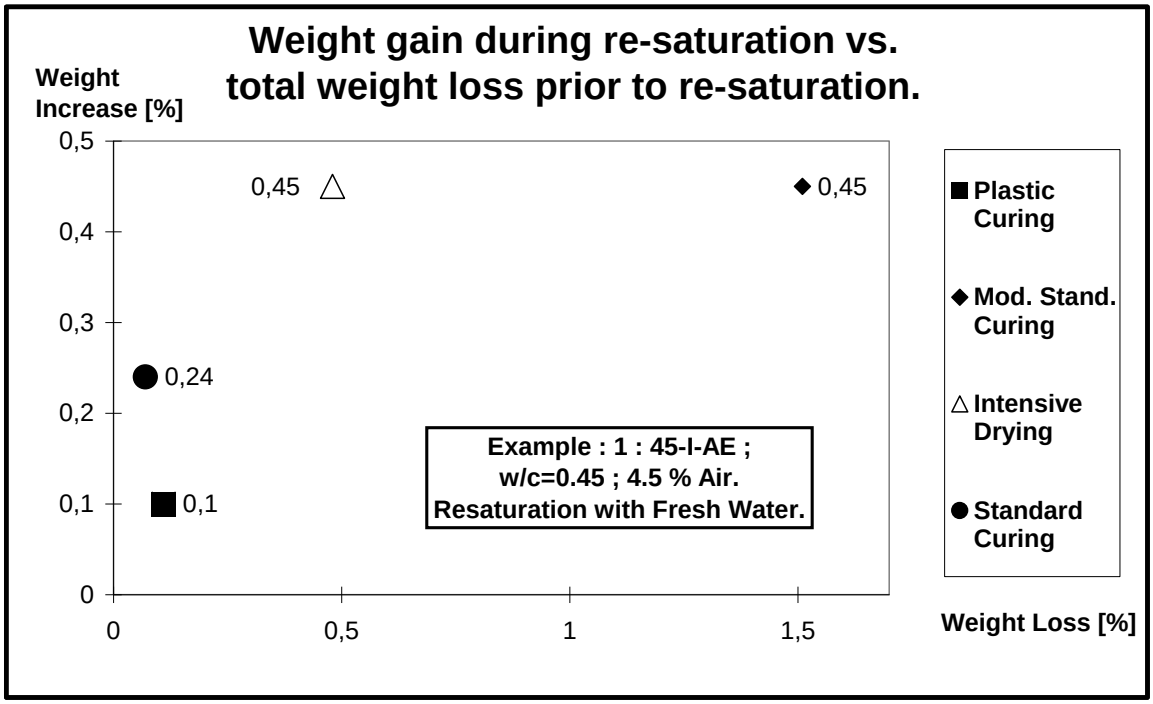

Figure 3 – Water uptake during re-saturation, depending on pre-curing procedure [3].

In addition to the higher water uptake during re-saturation, the early age moisture movements also appear to increase the water (salt solution) uptake during freeze-thaw, see figure 4.

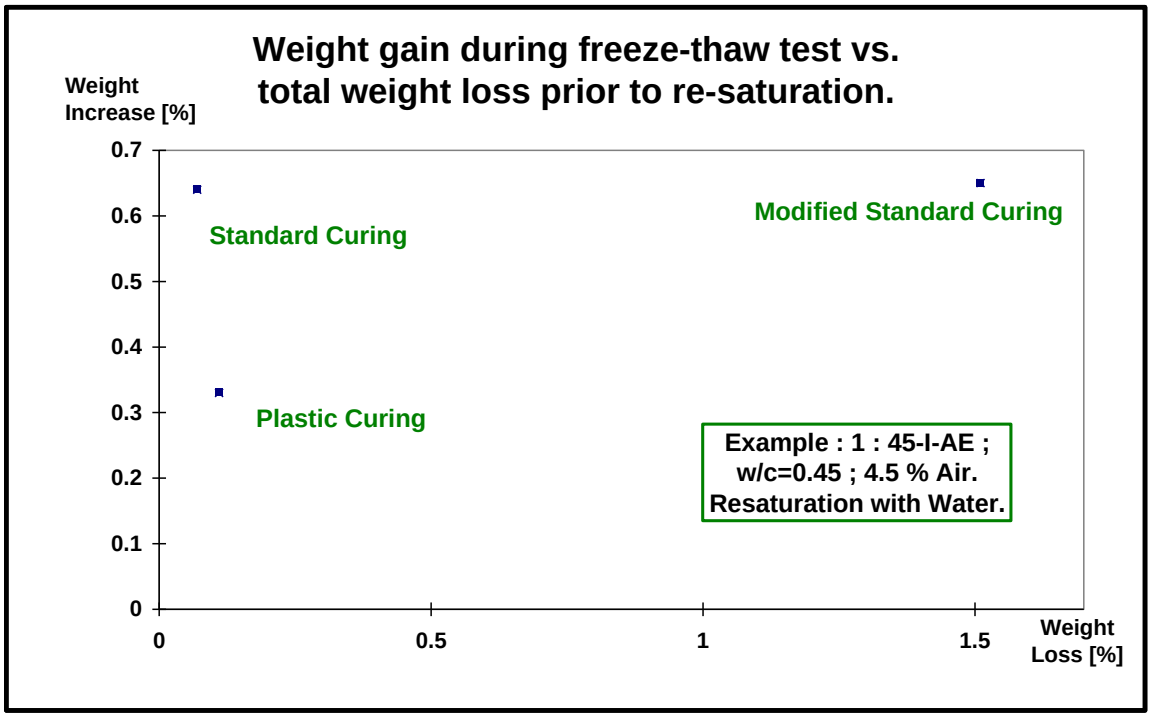

Figure 4 – Water uptake during freeze-thaw, depending on pre-curing procedure and corrected for any mass loss by scaling [3].

The accumulated moisture loss and –uptake for these three curing conditions are illustrated in figure 5, again exhibiting substantial differences.

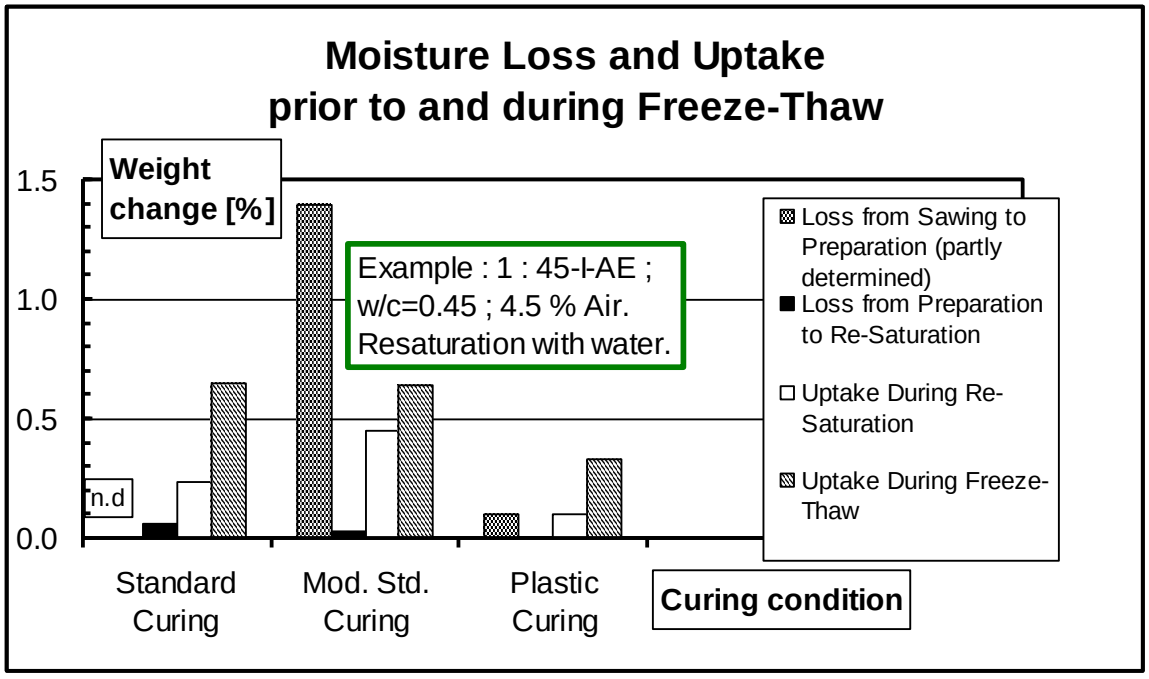

Figure 5 – Accumulated moisture uptake prior to and during freeze-thaw, depending on the pre-curing procedure and corrected for any mass loss by scaling [3].

2.3 Pre-conditioning, materials and scaling level

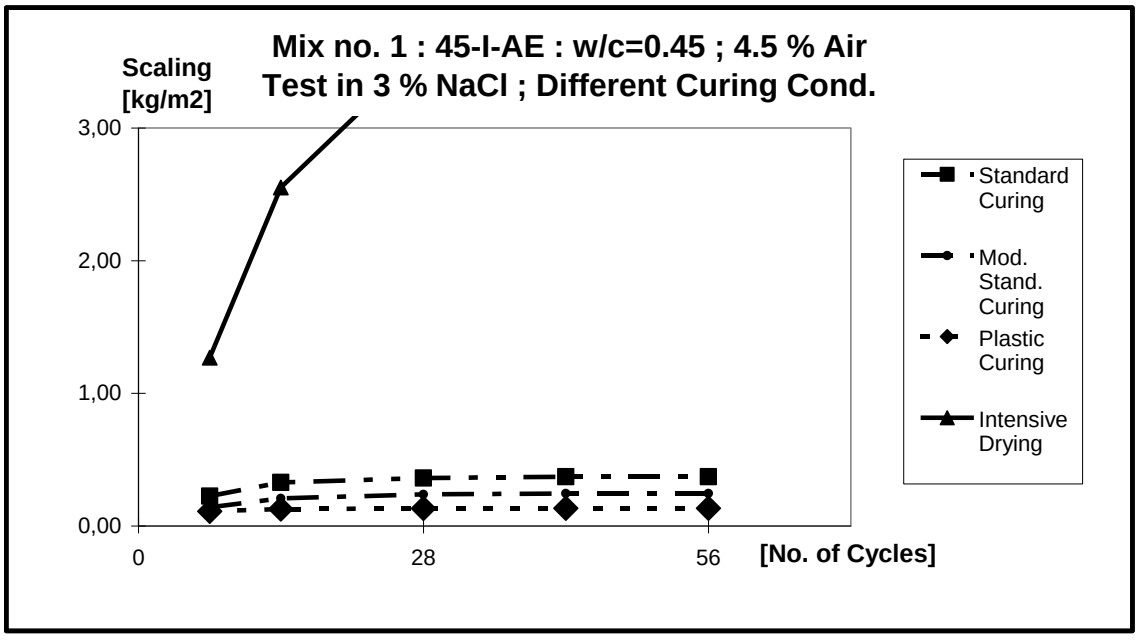

Figure 6 – Differences in scaling, depending on curing procedure, w/c = 0.45 [3].

The next step was to compare these relations for various concrete mix design. The figures 6 and 7 display scaling test results at two different w/c ratios, following four different curing regimes. In the latter, the ranking of “Standard” and “Modified Standard” shifted, but in both cases the

ranking directly relates to the level of total moisture absorption, displayed in figure 8 for the w/c 0.55 mix.

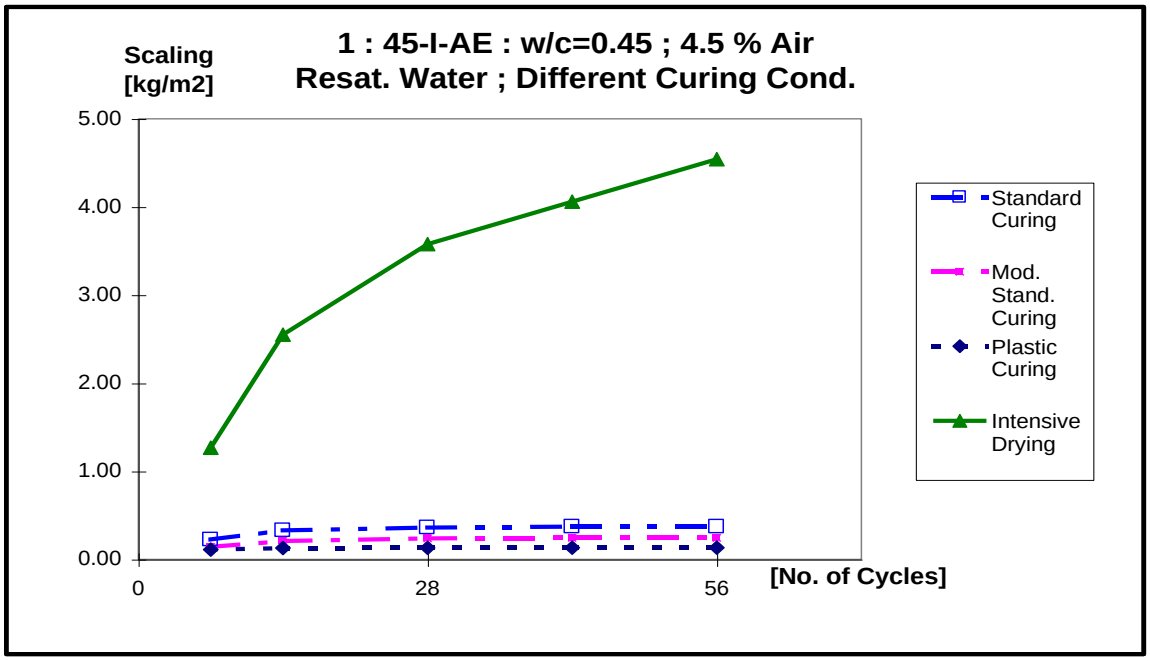

Figure 7 – Differences in scaling, depending on curing procedure, w/c = 0.55 [3].

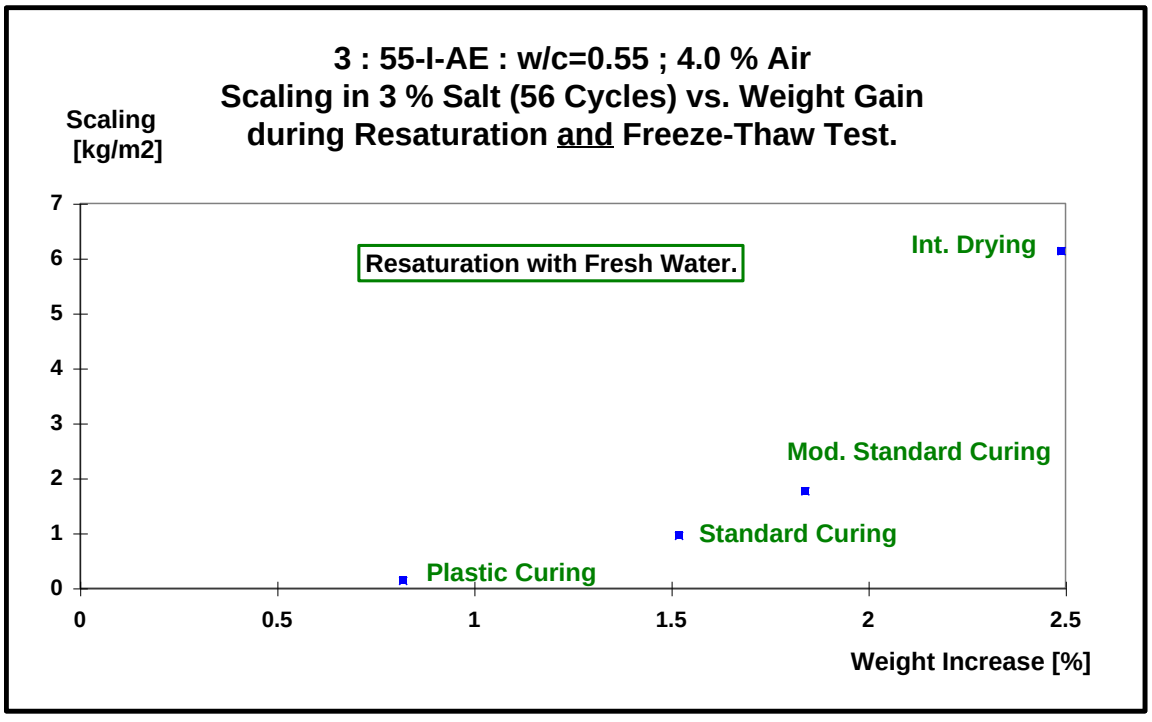

Figure 8 – Differences in scaling, depending on curing procedure and related to accumulated moisture uptake, w/c = 0.55 [3].

Although the picture was not as clear in all the cases investigated, these constitute some clear indication that the moisture history affects the scaling test results, even for CEM I cement

concrete. Figure 9 displays – for standard curing only - a comparison of moisture loss and uptake of some of the series investigated in [3]. For two w/c levels (0.45 and 0.55), a direct comparison between CEM I and CEM II/A-V is enabled : The somewhat poorer scaling results of the latter (not included in the paper) can possibly be attributed to the higher moisture loss from the stage of sample preparation to that of re-saturation.

The effect of submerged pre-storage remains speculations. A much later performed scaling test, comparing a CEM I and CEM II/A-L cement exhibited similar scaling results, but the indirect influence of the normally higher degree of clinker grinding in composite cement may very well compensate the early age hydration rate – by accelerating as well as causing a denser structure. It is, however, reasonable to believe that increasing the clinker replacement level beyond that of CEM II/A, will impair especially the early age moisture movement resistance and effects.

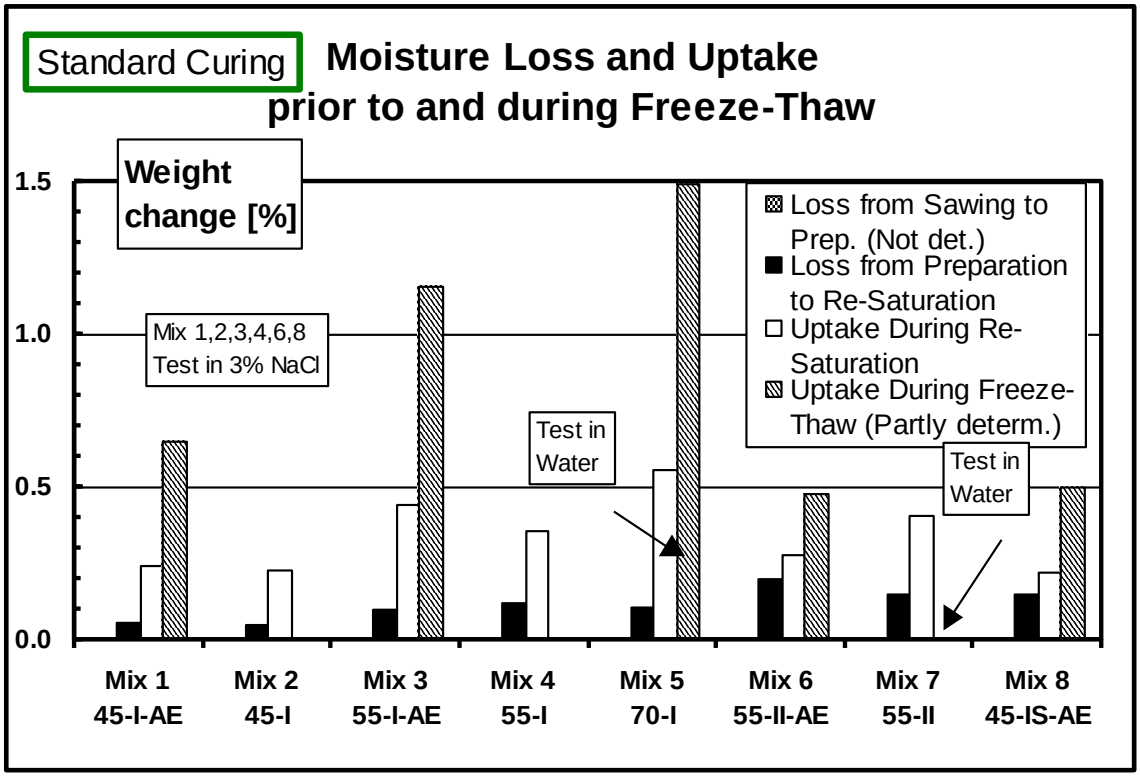

Figure 9 – Compilation of moisture loss and uptake for some concrete mix designs. (Explanations: "45" denotes w/c ratio 0.45 etc., "I" and "II" CEM I and CEM II, "AE" Air entrainment) [3].

Remark: One aspect possibly contributing to the difference between the curing versions is of course the degree of carbonation of the test surface prior to freeze-thaw. In this case (choice of constituents), reduced carbonation (e.g. plastic curing) would be expected to impair the scaling resistance and, hence, is considered irrelevant to the conclusions.

3 FROST RESISTANCE EVALUATION FOR XF1 AND XF3

For saline climate, referred to in CEN 206-1 as environmental classes XF 2 and XF 4, correlation of scaling test results and field exposure conditions has been performed for CEM I and CEM II/A cement concrete [6]. Similar correlation for non-saline environment XF1 (moderate water saturation) or XF3 (high ~) has not been much focused.

Attempting to increase the data basis for concrete designed for non-saline environment, a test series of existing and potential CEM II cement concrete mixes was submitted to testing in pure water. W/c ratio levels comprised 0.50 and 0.60, no air entrainment. Corresponding to field experience, this was expected to cover both sensitive and relatively durable qualities. The selected testing method was the reference method ("slab test") of the CEN TS 12390-9 but with pure water. Testing was initiated both at the age of (normal ;) 1 month and prolonged laboratory air climate storage (3 months).

The scaling level was in most cases limited, but ultra pulse velocity and visual inspection revealed the occurrence of substantial internal cracking, leading also to leakage of the freezing medium (water) from the test surface [7]. Consequently, it hardly makes sense to rank the test series, based on the test results. However, it is very disturbingly that cement and concrete qualities currently in use or in the pipeline are completely destroyed in the test, preventing even a ranking between these. It would be of great environmental and industrial significance to establish a frost performance testing concept enabling the correct end user value for such cement and concrete, designed e.g. for building facades.

4 LEVEL OF SATURATION – AN OPTION FOR DIFFERENTIATION?

At the start of laboratory F-T testing, the degree of capillary saturation normally is 100 %. Still, the F-T action (various mechanisms) causes additional water uptake and increasing saturation in various voids, including those being formed along the deterioration process [3]. Taking into

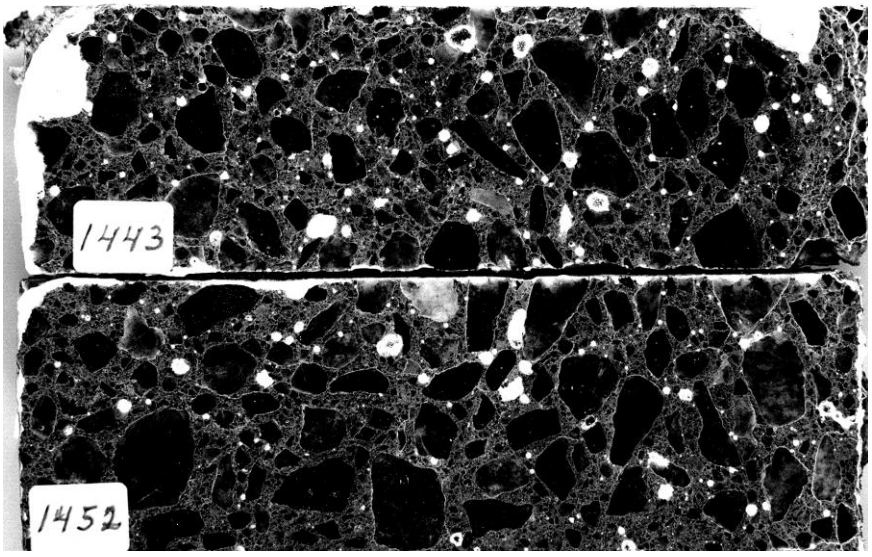

Figure 10 – Crack pattern of samples experiencing internal damage [3].

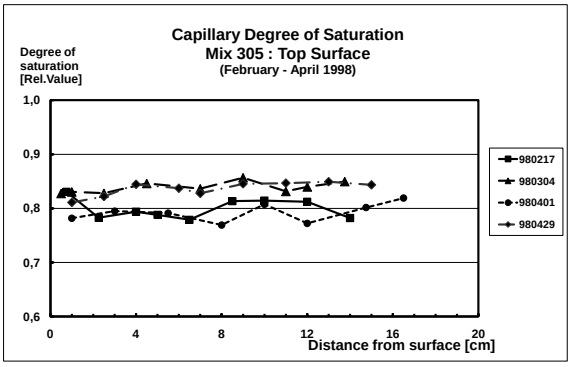

Figure 11 – In situ winter measurements of moisture content at a highway [3].

consideration the different capillary volume "available", depending on whether the samples have been pre-dried or not, the "safety level" in the sense of volume available for "pumping" may also vary. Virgin samples (never dried) stored under water during most of the clinker hydration may be particular sensitive.

The continuous uptake of moisture during F-T testing probably depends on the uninterrupted contact with moisture at the test surface. Scaling test results typically exhibit two different patterns, either 1) accumulated deterioration (acceleration) or 2) stabilizing at a low to intermediate deterioration level.

In case 1, this normally reflects a concrete quality level that would not meet the (perception of CEM I concrete …;) high performance expectations under XF 4 conditions, i.e. the relation is widely accepted. Case 2 would synthesize with the idea of local defaults being deteriorated, after which the rest of the structure appears resistant. However, in some cases and after being subjected to prolonged F-T testing exposure, the latter may very well end up accelerating. This phenomenon is sometimes attributed to "fatigue" or "non-really-sound-structure". It is true that some of these samples by micro structure examination (thin sections) may exhibit structural flaws, but is also characteristic that this often happens to high strength concrete without corresponding deteriorating behaviour in field.

Hence, it is reasonable to believe that the accelerated deterioration is an implication of the steadily increasing degree of saturation: When a critical degree of saturation has been reached (definition possibly material composition dependent and exceeding our usual definition of 100 % capillary saturation), the structure will rapidly disintegrate as suggested by Fagerlund [8]. Investigating samples subjected to F-T to an extent where freezing medium "leaking" is observed, often exhibit crack pattern as displayed in figure 10. (This crack pattern is also observed for other reasons.) Similar pattern or course of degradation is not often observed in field, except for certain combinations of exposure conditions and geometric design.

Figure 11 displays the results of in-field measurements of concrete surface and interior level of degree of capillary saturation, performed during the winter season along the RV 40 highway outside Borås, Sweden, subjected to intensive application of de-icers, at the location of a major field station for lab/field correlation studies, often referred to in articles of Nordic origin. It appears that even under such conditions, the in-field moisture "load" is far lower than the laboratory conditions. Taking the range of moisture mechanics properties of the material into consideration, it seems fair to question the current ranking of material combinations, based on laboratory performance and beyond those material combinations for which correlation is (claimed to be ;) established.

5 SUMMARY

This article is not meant for evidence of the lack of confidence to the current testing procedures provided in CEN TS 1239-9. However, it is found reasonable to question certain aspects of the testing procedures and evaluation for certain current and expected future cement and concrete qualities.

The influence of early age submerged curing and its impact on various material qualities ranking and evaluation should be investigated. It is demonstrated that different curing regimes may affect the test results substantially – and differently for different material properties. Also, the justification of long term F-T testing (moisture pumping) is questioned in view of field conditions.

Secondly, and of great significance for environmental cement and concrete product development, a "compliance evaluation system" for EN 206-1 exposure class XF 3 (1) should be established. Probably, this will require basic research on moisture mechanics under F-T both under laboratory and field conditions in order to accomplish – in double sense - a sustainable solution.

REFERENCES

1. CEN TS 12390-9 : "Testing hardened concrete – Part 9 Freeze-thaw resistance – Scaling", Ref. no. Ref. No. CENiTS 12390-9:2006: E, May 2006, 24 p.
2. SS 13 72 44 "Concrete testing – Hardened concrete – Frost resistance – (Slab test), 2005
3. Rønning, T.F.: "Freeze-Thaw Resistance of Concrete – Effect of : Curing Conditions, Moisture Exchange and Materials", Ph.D. Thesis, NTNU Trondheim – Norwegian University of Science and Technology, 2001. ISBN 82-7984-165-2, 414 p.
4. Bager, D.H.; Sellevold, E.J.: "Ice formation in hardened cement paste, Part II – Drying and re-saturation on room temperature cured pastes", *Cement & Concrete Research, Vol. 16 (1986), pp 835 – 844.*
5. Sellevold, E.J.: "Frostbestandighet : Salt-/Frostavskalling. Effekt av prøvebetingelser og betongsammensetning" (*"Frost resistance : Freeze-/Thaw scaling. Effect of testing conditions and concrete composition")*, Project report no. 27 from "Betongens funksjonsdyktighet", Sintef Report STF65 A88090, Trondheim 1988, 84 p. (In Norwegian)
6. Utgenannt, P.: "Frost resistance of concrete – Experience from three field exposure sites", Nordic Miniseminar "Nordic exposure sites", Hirtshals, Denmark, November 2008,

Workshop proceedings no. 8 from The Nordic Concrete Federation, ISBN 978-82-8208-013-2 , (www.nordicconcrete.org) pp 77 – 93.

7. Ewertson, C.: “Projekt Eco-serve : Provning av frostresistens” & “Projekt Eco-serve : Provning av ultraljud”, Test reports F504472 & F517475 (classified – in commission from the present auther) from SP Technical Research Institute of Sweden, 2005, 18 + 18 p (in Swedish).
8. Fagerlund, G.: “Kritisk vattenmättnadsgrad-metoden” *(”The method of critical degree of saturation”),* NBI/NORDTEST Symposium, Trondheim, August 1976. Reprint as CBI report 12:76, Swedish Cement and Concrete Research Institute at the Institute of Technology, Stockholm, 43 p. (in Swedish).
9. Utgenannt, P.: “The influence of ageing on the salt-frost resistance of concrete”, Ph.D. thesis at the Lund Institute of Technology, Report TVBM-1021, 2004, ISBN 91-628-6000-3, appr. 480 p.
10. Boyd, A.J.; Hooton, R.D.: ”Long-Term Scaling Performance of Concretes Containing Supplementary Cementing Materials”, *Journal of materials in civil engineering,* October 2007, pp 820-825.

On the Relation between Air void system parameters and Salt frost scaling

Sture Lindmark
M.Sc., Ph.D.
Lund University
Div Building Materials
Box 118
221 00 LUND
E-mail: sture.lindmark@byggtek.lth.se

ABSTRACT

An attempt to develop a tool based on analysis of the air void system in concrete for an early assessment of salt frost scaling resistance of concrete is presented. Relations between the air void system parameters and scaling are discussed. A new technique based on the accumulated surface area of all air voids is presented. This is a short description of the project. The full report is available from our division and also includes a) a study of the rate of water absorption at above-knick point level in capillary suction tests, b) a technique for improving the image analysis procedure with respect to edge objects and c) a comparison between different ways of analyzing the air void system.

Key words: Frost resistance, air void, image analysis.

1. INTRODUCTION

In large construction projects, the client often demands that concrete shall be resistant to saltfrost scaling. Often, this resistance is tested according to SS 13 72 44. This test method requires one month of concrete curing before testing, and then the test runs for two months (four months if the concrete contains silica fume). Thus results are obtained three (or five) months after casting. The problem is that while the test is in progress, more concrete is cast and there is an obvious risk that a large amount of concrete of insufficient quality is cast before test results are at hand. In the worst case, concrete of insufficient quality is built in so that it cannot be replaced.

This happened in a large project some years ago, when the contractor made changes in the concrete composition because the fine contents of the gravel made it possible to reduce the cement content. Then, the air void system changed in such a way that the concrete no longer would pass the salt frost scaling test.

Because this is a problem that might become expensive for the contractor, the Development Fund of the Swedish Construction Industry (SBUF) (an association for Swedish contractors) ordered a development project from Lund University, division of Building Materials in 1999. This report gives a brief description of that project.

2. AIM

The aim of the project was to develop a method with which the contractor would be able to make his own quality assessment one or two days after casting, *i.e.* he would not have to wait a long time for results from the scaling test. Because the air void system, in contrast to the capillary pore system, is fixed once the concrete hardens, it seemed reasonable that an analysis of the air void system would be a suitable tool for this assessment.

Previously, the overall air content, the Powers' spacing factor and/or the specific surface of the air voids have been used for quality assessment as regards salt frost scaling. It was assumed that none of these alone would provide the information needed with good enough accuracy. Instead, the assessment would be based on a combination of these or other parameters.

In this project, the scaling test was performed according to a slightly modified version of the SS 13 72 44 (in order to save labour and time). Thus the results from the project (the relation between scaling and combinations of air void system parameters) were not expected to hold true in a full test according to SS 13 72 44. The intention was that if the project turned out successfully, the assessment methodology would later be modified to fit results from the SS 13 72 44.

3. METHODS AND REALISATION

The main principle was to produce a large amount of concretes with different types of air void systems and then compare the outcome of salt frost scaling test with the air void system parameters.

3.1 Concrete materials

Concretes of two water cement ratios were used; 0.40 and 0.50. The air void systems were varied by adding various amounts of air entraining agent and by vibrating the moulds in four different ways, including – in some cases – vibration one hour after casting. The 0.40 concrete was produced with 10 different dosages of AEA, which, multiplied by four different ways of combining vibration and plasticizer, resulted in 40 different air void systems. For various reasons 2 of these were discarded and thus 38 air void systems of w/c 0.40 were investigated. In the same way, the 0.50 concrete was produced with 20 different systems. Thus, in total, 58 concretes were cast and tested.

The concretes were mixed in batches of 140 l. Four blocks of size 400×300×250 (mm^3) were cast of every concrete: A: heavy vibration, B: modest vibration, C: modest dosage of plasticizer, and finally one block (D) with a high dosage of plasticizer.

Cylinders were drilled from the cast blocks and then discs were sawn for saltfrost scaling test, image analysis and capillary suction tests, see fig 1.

For further details please see the original report [1].

Table 1: Basic mix compositions for concretes used in the study (no plasticizer). These mixes were varied by adding more or less air entraining agent and plasticizer.

Water cement ratio:	0.40	0.50
Cement (”Anläggning”) Dens 3200 kg/m³	512.5	410
Water	205	205
Gravel 0-8 mm (Åstorp kvartsit)	919.85	967.38
Stone 8-12 mm (Hardeberga kvartsit)	722.74	760.09

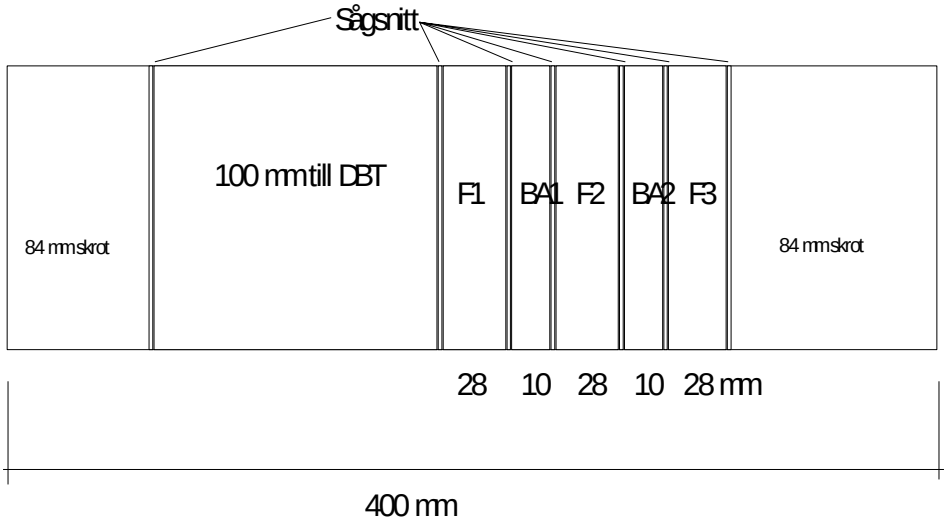

Figure 1: Distribution of samples in drilled out cores from tha cast blocks: Width of saw cuts 4 mm, total core length: 400 mm. F: Sample for scaling test, BA: Sample for image analysis. Image analysis performed on BA1.Capillary suction test performed on BA2. (“100 mm till DBT” indicates which part was sent to Dansk Beton Teknik for air void system analysis by linear traverse, ”Sågsnitt” = saw cut)

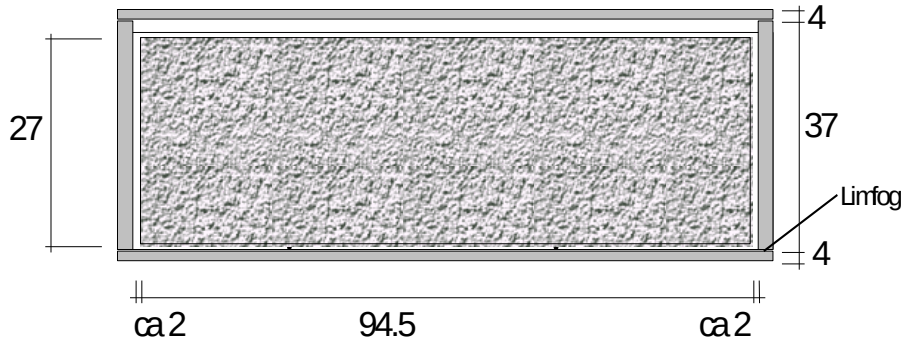

Figure 2: Set-up for the modified salt frost scaling test: Samples were placed in PVC containers, supported by 2 mm high studs. The lid, of PVC, is laid loose on top of the container. (“Limfog” = glued joint)

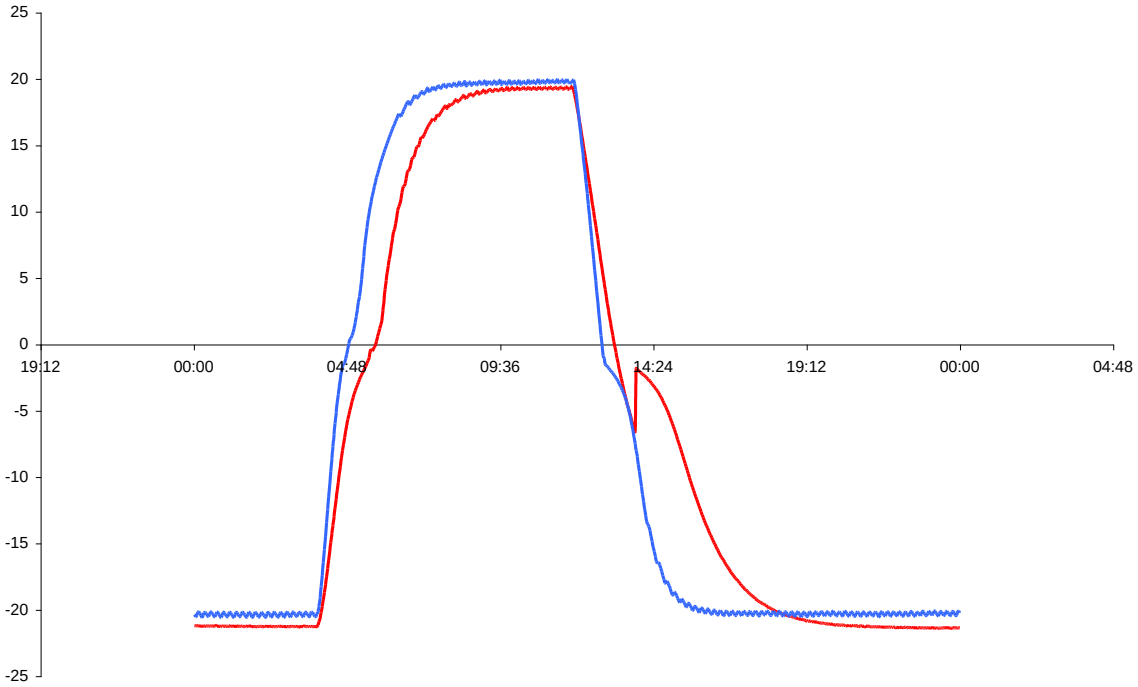

Figure 3: Temperature cycle.The two curves shown are data collected from two different samples. The difference somewhat reflects the spread in temperature cycle between different samples which is due partly to the randomly varying super cooling.

3.2 Scaling test

A complete test according to SS 13 72 44 was not possible due to lack of time. Also, the risk of leakage was estimated to be too high and thus a more reliable container had to be used. The modified setup is shown in Figure 2.

The samples were circular discs (diameter 94 mm, thickness some 27 mm). Three samples were used for every air void system. Samples were stored in lime water until one week before start of test. Then they were taken up, weighed and dried for 22±2 hours at 18°C/38%RH, weighed, imbibed in water for 5 minutes, taken up and wrapped in plastics. Then the samples were left to somewhat even out moisture gradients for four days. From 46±2 hours before start of test the samples were placed in water until start of test. Right before starting the test, the samples were once again weighed.

The temperature cycle was measured in the NaCl solution on top of some of the samples, see Figure 3.

Each frost cycle lasted 24 hours. 28 cycles were run. Scaling were collected every seven cycles.

The minimum temperature is lower than in the SS 13 72 44 (some –21°C instead of –18°). During cooling and thawing, the temperature change is more rapid than described in the standard.

After 28 cycles, so many samples were so badly damaged that a continuation was no longer meaningful. Thus the tests were interrupted.

Because the test method deviates from the standard method, the acceptance criterion of the standard cannot be used.

3.3 Air void analysis procedure

Discs of concrete were cut out from the cast blocks (Figure 1) and then ground and dyed with a blue background colour. The air voids then appear as circular, shallow cavities. These cavities are filled with a white paste to create a good contrast in black-white between background and air voids.

The prepared surface is then photographed (in black and white) in a microscope and presented on a computer screen. Each picture measures approximately 1.6×1.6 mm^2. For each concrete quality, 250 pictures were taken. The resolution is such that each pixel on the computer screen corresponds to 3.1 µm. Examples of pictures are shown below (in a different magnification).

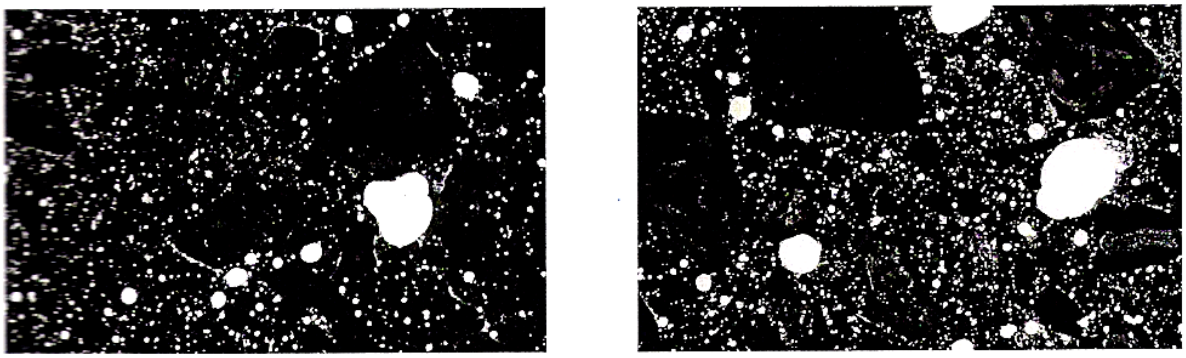

Figure 5: Example of samples for image analysis of air void systems
Left: B1, air content 1.9%, Right: B3C air content 4.6%.
Each picture shows an area of 24×36 mm².

3.4 From 2D image to 3D volume: Calculation of air void system parameters

The photographs produce 2D representations of a 3D air void system. To calculate the properties of the original 3D system, a methodology according to Underwood [2] was used (also described by Vesikari [3]). For the sake of comparison and as a quality control, the air void systems were also analysed by linear traverse (Lord and Willis [4]) by Peter Laugesen at DBT, Dansk Betonteknik, Copenhagen.

The following is a brief description of the calculation procedure:

When slicing through a unit size cube of a concrete sample, the probability of hitting a sphere of diameter D_i ($=2R_i$), is proportional to the diameter of that sphere:

$$P_{hit,i} = \frac{D_i}{l_{cube}} \qquad (1)$$

where l_{cube} is the side length of the cube.

When slicing a plane through a unit size cube through a concrete sample containing a certain air void system, each void size interval i produces a number $n_{2d,i}$ of *circles* (2D projection of the cavities) on the plane which number is calculated as

$$n_{2d,i} = n_{3d,i} \times P_{hit,i} \qquad (2)$$

The probability of cutting a sphere of radius R_i so that the diameter of the 2D circle is in the size class j ($d=2r_j$) is calculated (illustrated below):

$$P_{i,j} = \frac{\left(R_i^2 - r_j^2\right) - \left(R_i^2 - r_{j+1}^2\right)}{R_i} \qquad (3)$$

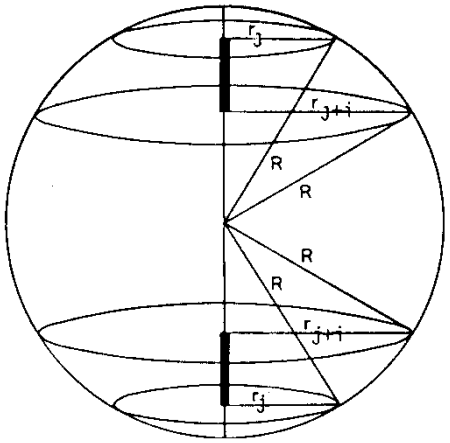

Figure 6: Illustration to calculations as given b Vesikari [3].

The number of 2D circles in circle size class j that is produced by spheres in sphere size class i thus is calculated as:

$$n_{2d,j} = P_{i,j} \times P_{hit,i} \times n_{3d,i} \qquad (4)$$

The calculation of the complete air void size distribution is done by using these formulas in a matrice form, solving for $n_{3d,i}$.

The final product of these calculations is the probable number of spheres in size class i, *i.e.* the number of spheres of diameter in the interval between two sizes. (The Underwood/Vesikari method produces somewhat different results as compared to the method of Lord and Willis).

It might turn out that the calculated number of spheres in a certain size class is negative, which of course cannot be correct. This incorrect result occurs because the statistical ground is too small (too few pictures). The calculated numbers are corrected by subtracting the absolute number of spheres in the classes where negative values are received from the number of spheres in the size class of next larger spheres.

The treatment of identified objects is further described in the original report [1].

The calculation of 3D distributions of air voids is inherently associated with several difficulties. For instance, on the 2D image, spherical air voids will appear as perfectly circular cavities. However, many air voids are not perfect spheres, and thus their 2D-representations may be more

or less oval. In the extreme end, compaction pores create cavities which are far from circular. These imperfections are handled in the automated image analysis computer program by setting a criterion on different parameters of the cavities. For example, *Roundness* is one of the parameters which may be used do differentiate cavities which are likely to have come from spheres from cavities resulting from compaction pores etc.

In Figure 10, an example of the finally calculated air void distribution is presented, described as accumulated volume of air as a function of void size. Also seen is this figure is the effect of choice of the parameter *Roundness*, which is one of the parameters which can be used as a criterion for separating circles produced by true air voids from those circles produced by irregular voids. The parameter *Roundness* has the value 1.0 for perfect circles and 1.57 for squares. The choice of limiting value for this parameter is also dependent on the absolute size of the individual object (due to the way screen pixels represent objects). In the calculations, the value of *Roundness* was finally set to R = 2.5 (a lower value would discriminate objects which, by visual inspection, most likely to stem from voids which act protectively just like air voids. Recalculations with varying values can be made quite easily.

Finally, in the microscope image there are some circles in the plane which are cut by the frame of the image. Such edge objects disturb the calculated air void size distribution. A way of handling these objects is described in the original report.

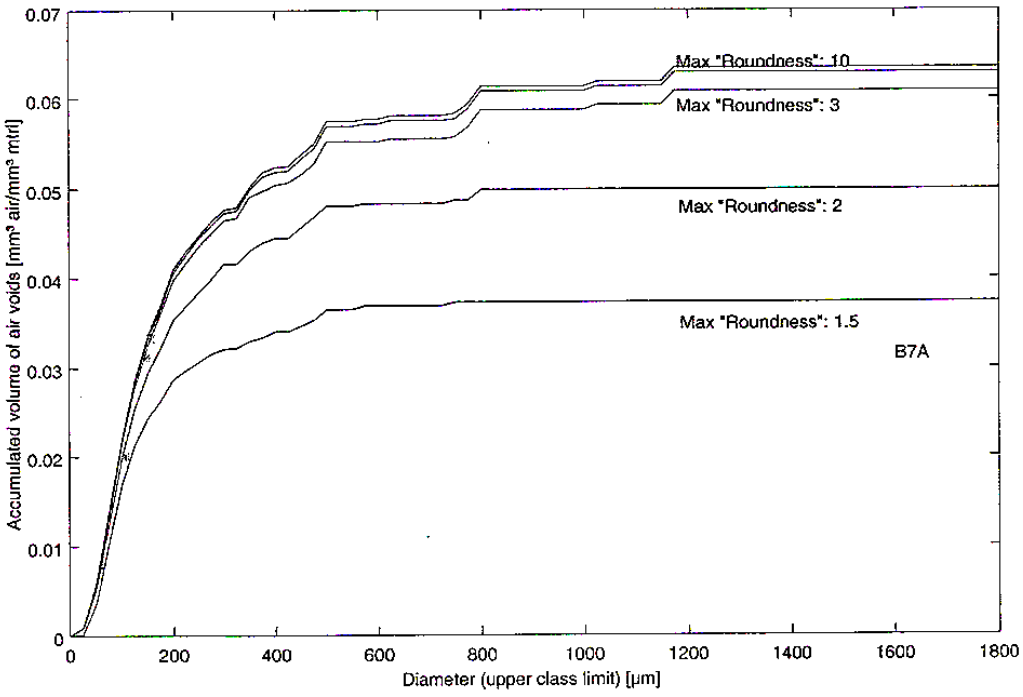

Figur 10: Effect of choice of value of parameter Roundness on calculated accumulated air content. Sample B7A (w/c 0.40), (not adjusted for edge objects).

4. RESULTS

4.1 Results from air void system analysis

The specific surface of air voids and/or air void systems may be defined in different ways. In this study, the specific surface is calculated as the total surface area of all (spherical) air voids, divided by their total volume:

$$\alpha = \frac{\sum_{d=0}^{\infty} n_d A(d)}{\sum_{d=0}^{\infty} n_d V(d)} \qquad (5)$$

This equation produces a value which is not equal to that calculated according to Powers' definition (which is calculated under presumption that all voids are of the same size).

4.2 Results from scaling tests

The amount of scaling for each concrete type after 28 cycles is given in figures 13 and 14.

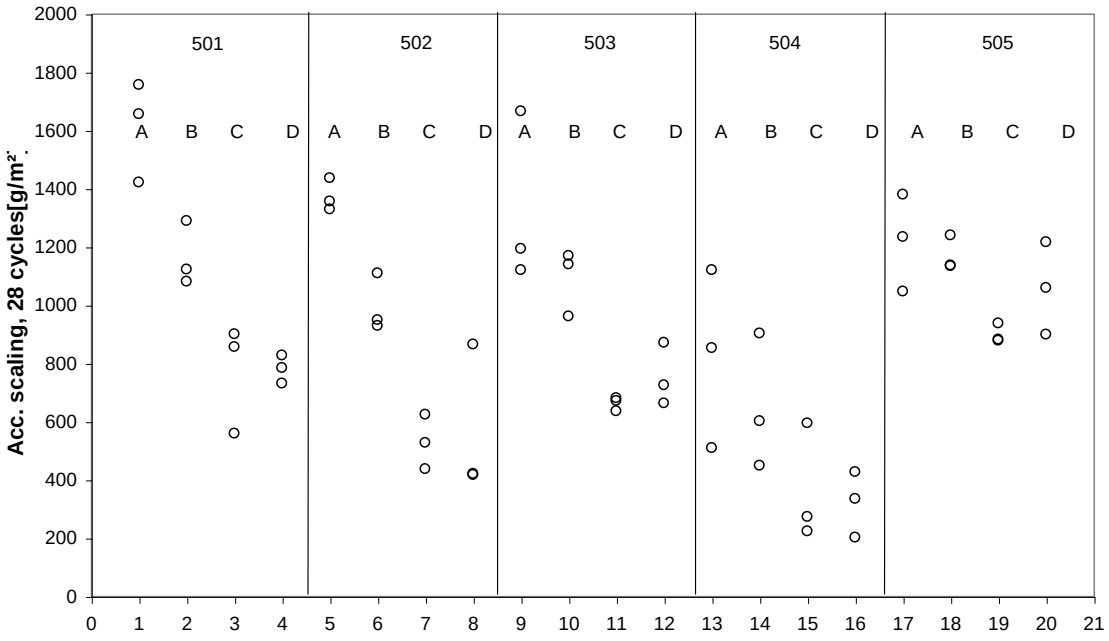

Figur 13: Spread in accumulated scaling (28 cycles) for concretes of w/c 0.50.For each concrete three samples were tested (=one ring).In cases where only two circles are visible, the third one is hidden by one of the other two.

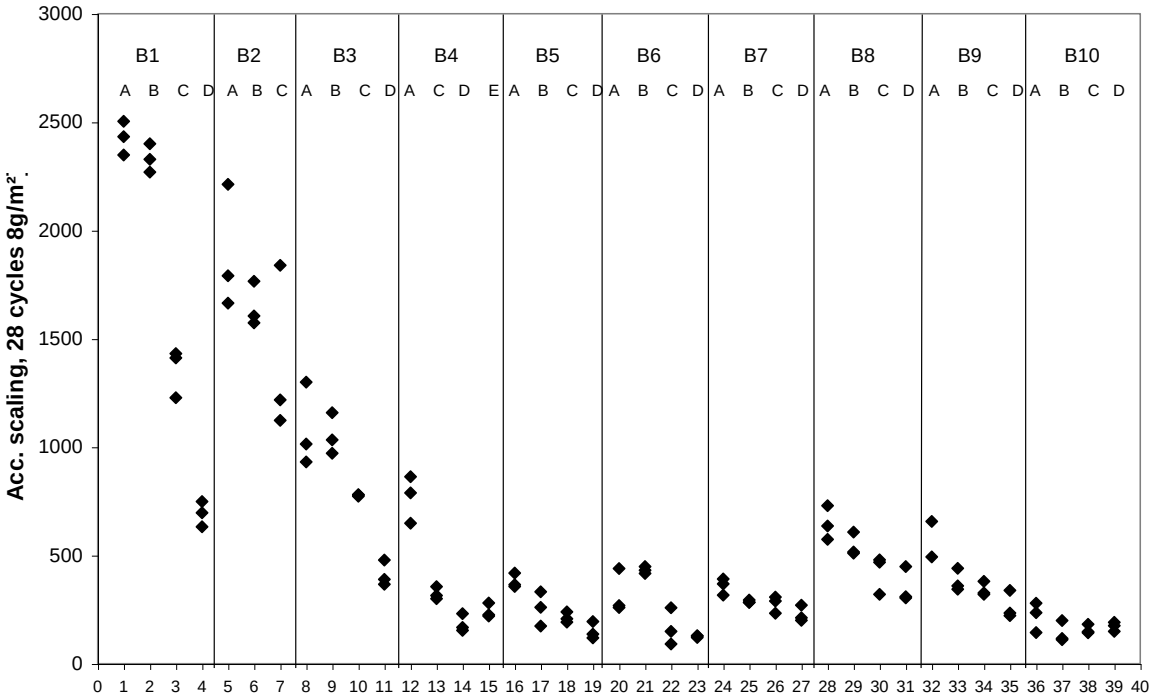

Figur 14: Spread in accumulated scaling (28 cycles) for concretes of w/c 0.40. (Concrete quality B2D was not tested.)

5. DISCUSSION

5.1 Relations between scaling and air void system parameters - ”traditional way”

Scaling in relation to single air void system parameters

The traditional ways of seeking relations between air void system parameters and frost induced deterioration (pure frost or salt frost) is by plotting scaling vs. air content, specific surface of voids or Powers’ spacing factor. Examples of such plots are given in figures 19-21. As seen in the figures, these relations are rather poor.

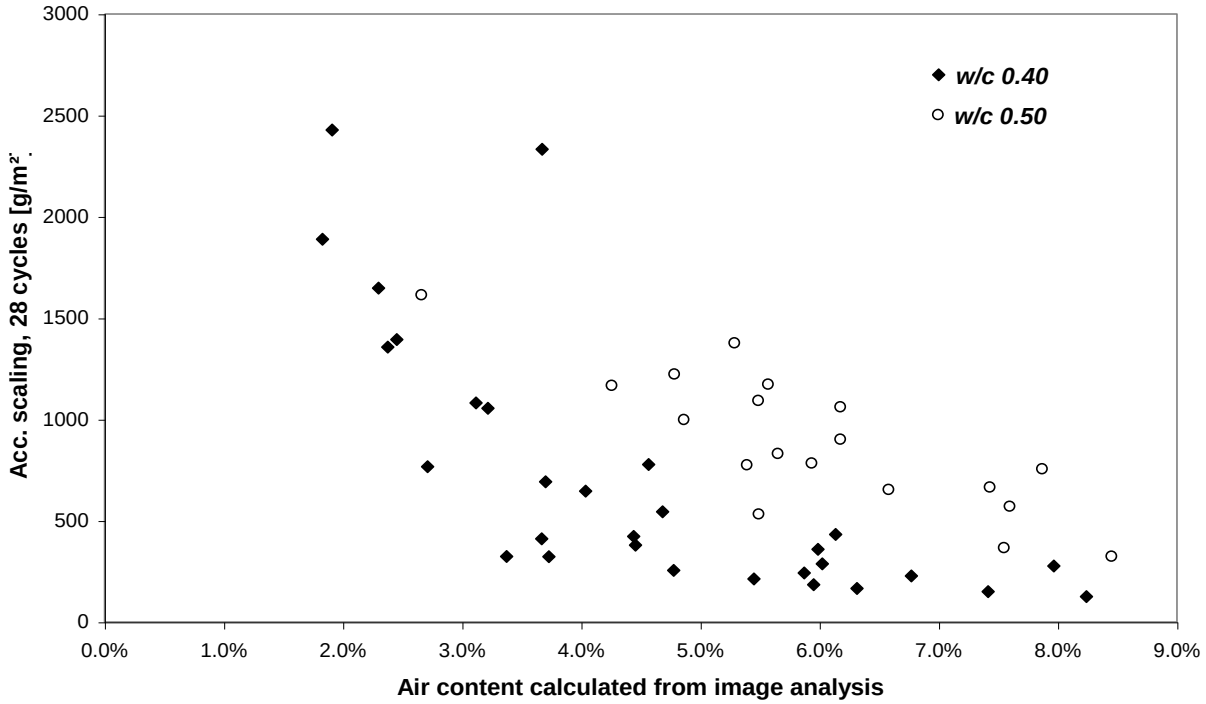

Figure 19:Accumulated scaling (mean of threesamples) vs. Total air content determined as accumulated air content in calculated air void size distribution.

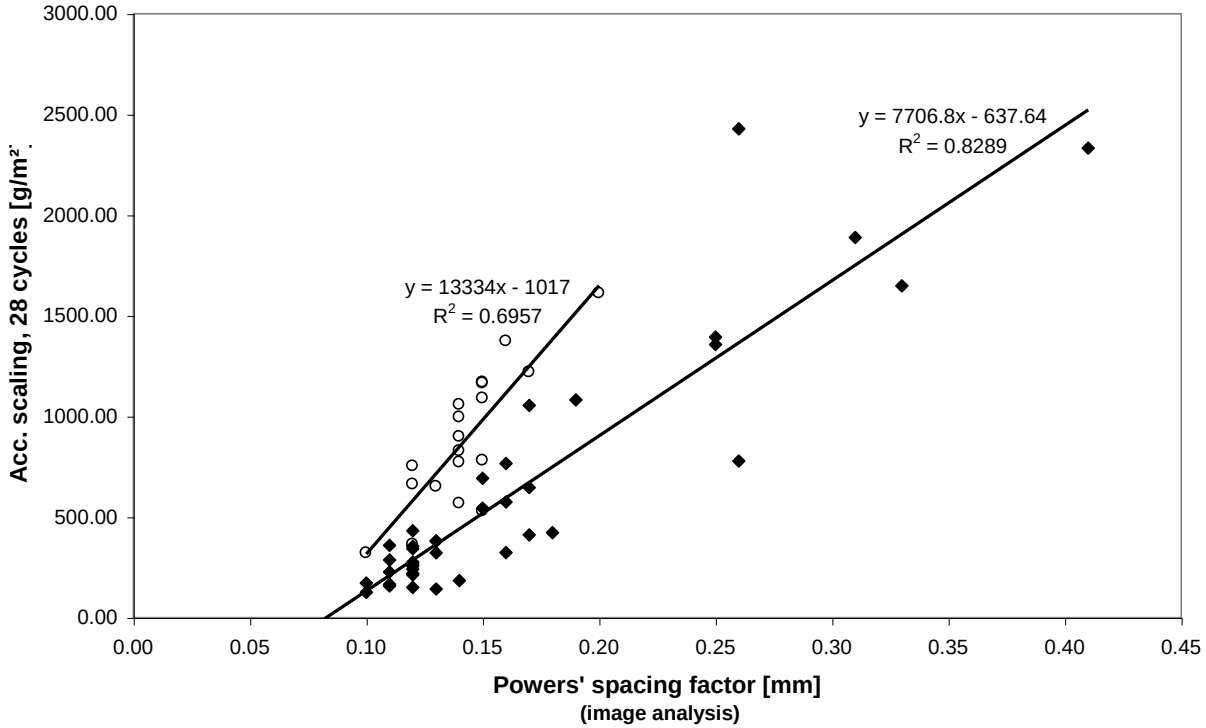

Figur 20a: Acc scaling (each dot = mean of three samples) vs. Powers spacing factor. Spacing factor determined from total calculated air content and with specific surface calculated acc. to eq 5.

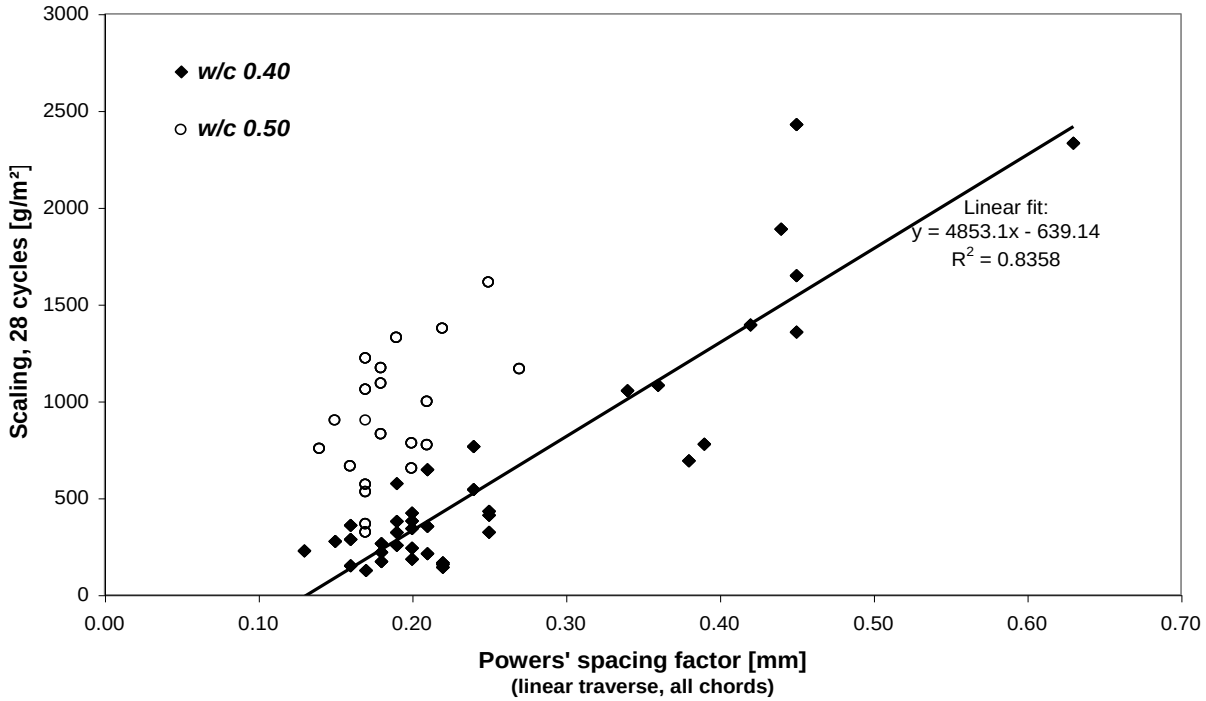

Figur 20b: Acc scaling (each dot = mean of three samples) vs. Powers spacing factor. Spacing factor determined acc. to ASTM C457 (linear traverse).

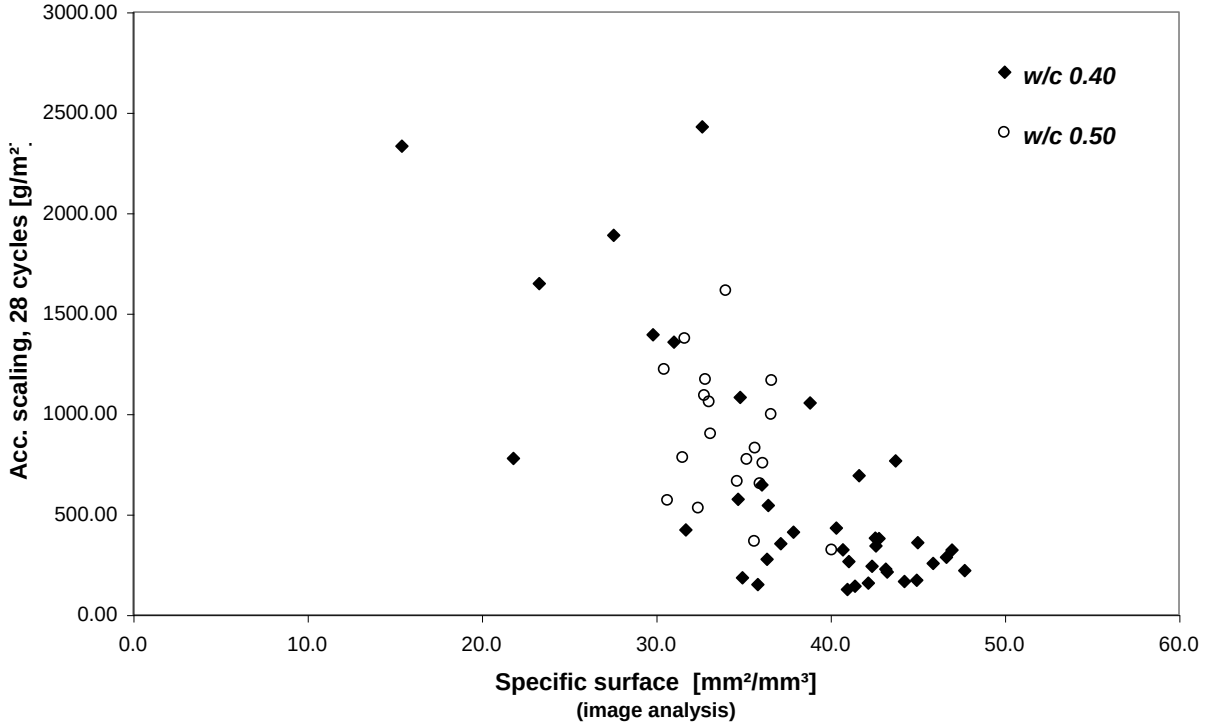

Figure 21:Accumulated scaling (mean of three samples) vs. specific surface of air void system acc. to eq 5.

According to Laugesen [5], Dansk Beton Teknik describes the quality of an air void system by determining the air content (as fraction of length of traverse crossing cavities) counting only

chords shorter than 350µm. Plotting accumulated scaling *vs*. this parameter produces the graph shown in figure 22. Apparently, there is a reasonably good correlation for the 0.40 concrete, but not for the 0.50 concrete.

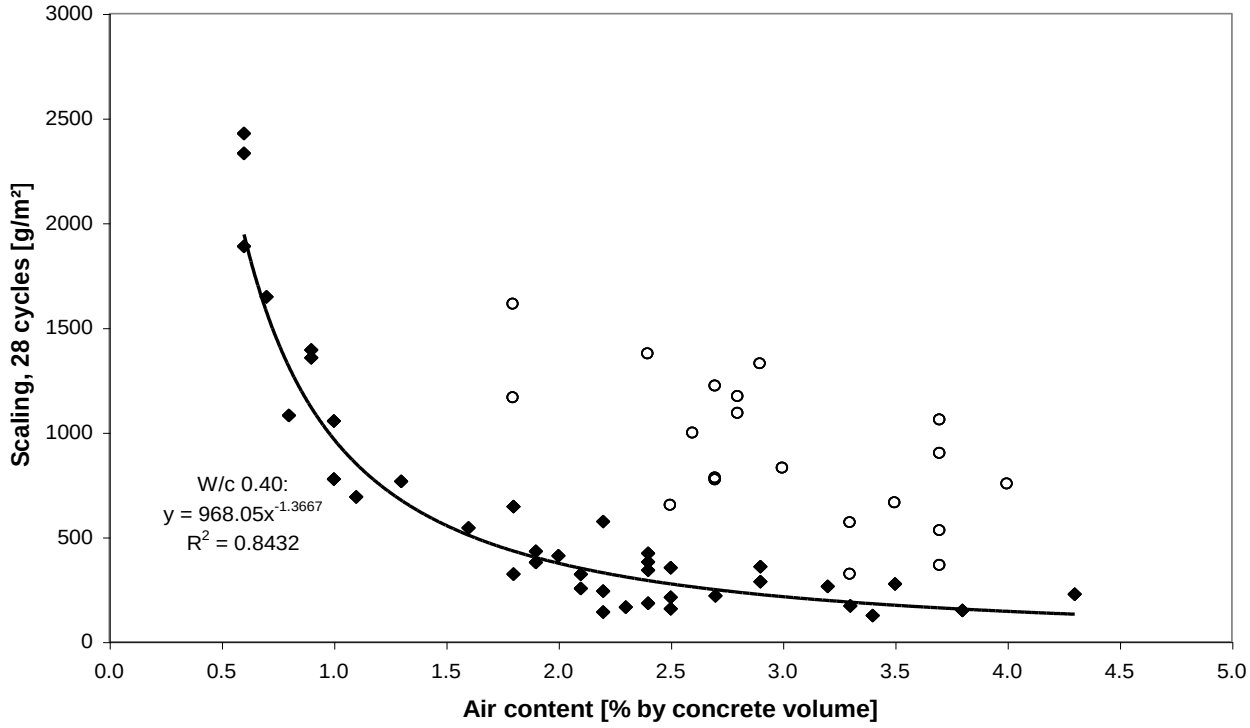

Figure 22:Accumulated scaling after 28 cycles (one dot = mean of three samples) vs air content as calculated fraction chords shorter than 350µm of total travers length.

Scaling in relation to combinations of parameters

As seen above, relating scaling to one, single air void system parameter tends to result in insufficient relations. Thus, one may try relating scaling to a combination of parameters. Different ways of doing this are shown in figures 23 and 24. In these figures, the amount of scaling is represented by the area of circles. (More examples are given in the original report.)

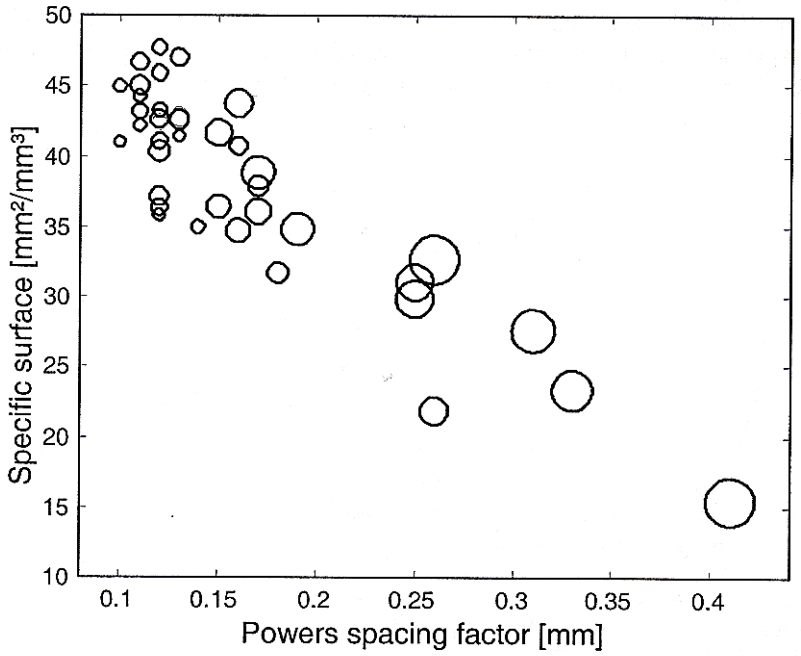

Figure 23 : Accumulated scaling ((28 cycles) for concrete of w/c 0,40 (represented relative to each other by the area of circles) in relation to specific surface (eq 5) and the Powers spacing factor.

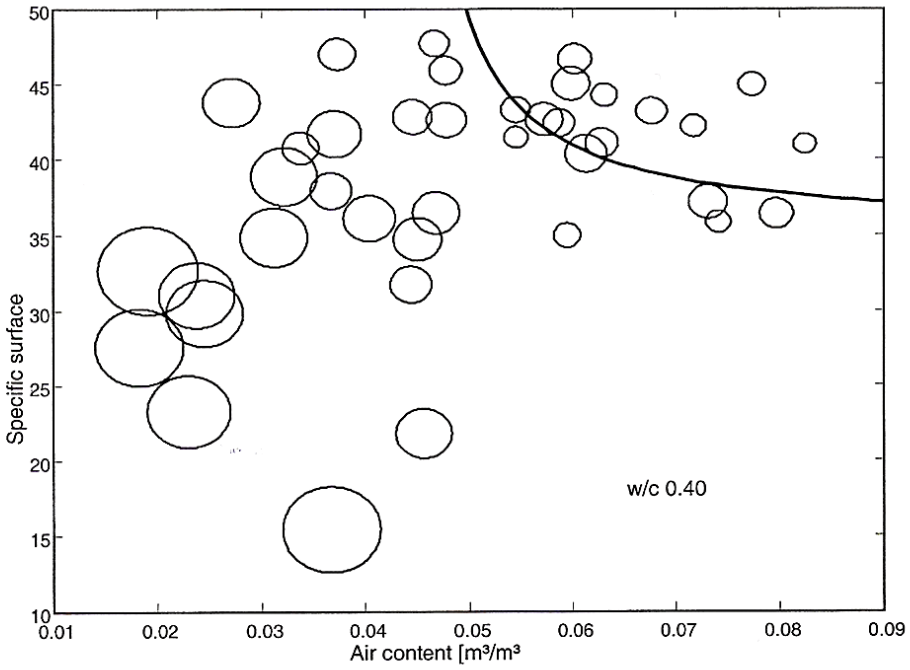

Figure 24: Amount of scaling (relative to each other, represented by area of circles) n relation to specific surface (eq 5) and total air content, w/c 0.40. Red line according to eq (6) with arbitrarily chosen parameters.

In figure 24, the amounts of scaling for different concrete qualities, expressed by the area of circles, are presented in relation to specific surface of air voids and to total air content. As seen, there is no very clear border line between different samples. However, considering the mechanisms of frost attack, one might expect that in a plot like this there should exist a lower critical value for both specific surface and for total air content. Thus an equation of the following form may be set up:

$$(\alpha - \alpha_{crit})(L - L_{crit}) > k \qquad (6)$$

in which k is some critical limit value which has to be derived from tests according to the appropriate test method (SS 13 72 44 or which other method is to be used).

In figure 24, a line has been drawn according to this equation. The parameters α_{crit}, L_{crit} and k were chosen arbitrarily to produce a line in an area that seemed reasonable. However, it is seen that the line may very well be drawn lower in the graph (*i.e.* the critical values for the respective parameters might be set lower). This kind of equation might be useful, but needs to be calibrated for the appropriate test method.

5.2 Some words about protective and non-protective voids

Which voids should be disregarded? Which voids have a protective effect with respect to frost attack? It cannot really be expected that a relation between salt frost scaling and parameters of the air void system as determined in a microscope analysis alone will be found. This is due to that some of the voids probably will become completely filled with water very quickly when the concrete is subjected to water [6], and some will become partly filled. Thus some of the air voids that are detected in the microscope do not have a protective effect. Such voids must be excluded when analyzing the relation between scaling and air void system parameters. The question of how to do this exclusion remains open. An attempt was made to study this: For concrete of w/c 0.40, scaling was plotted vs. total air content in voids of diameter D>250µm, fig 25. The relation is not very good, and for w/c 0.50 it is even worse. A continued experimenting with choice of limiting void sizes might have proven successful. However, since we know only little about the process of water filling of air voids (*e.g.* we do not know for sure whether small voids are completely filled before larger ones start filling), it is difficult to make a rational choice of limiting void size, and because there are uncertainties in the determination of air void size distributions, it is meaningless to carry this study any further in this text. (More information is found in the original report.)

Furthermore, in the automated image analysis, voids are described with various parameters, and in the subsequent calculation from 2D to 3D distributions, some cavities of a too irregular (non circular) shape are disregarded. This may not be a correct procedure; since many of the compaction pores are of the same size as air voids, they are not likely to get filled with water easily, and thus they probably do provide some protection against frost destruction. Thus they should in fact be included in the calculations. Then, on the other hand, these irregular voids cannot be treated with the mathematics described above, and thus including them in this calculation will cause an error in the calculation of different air void system parameters.

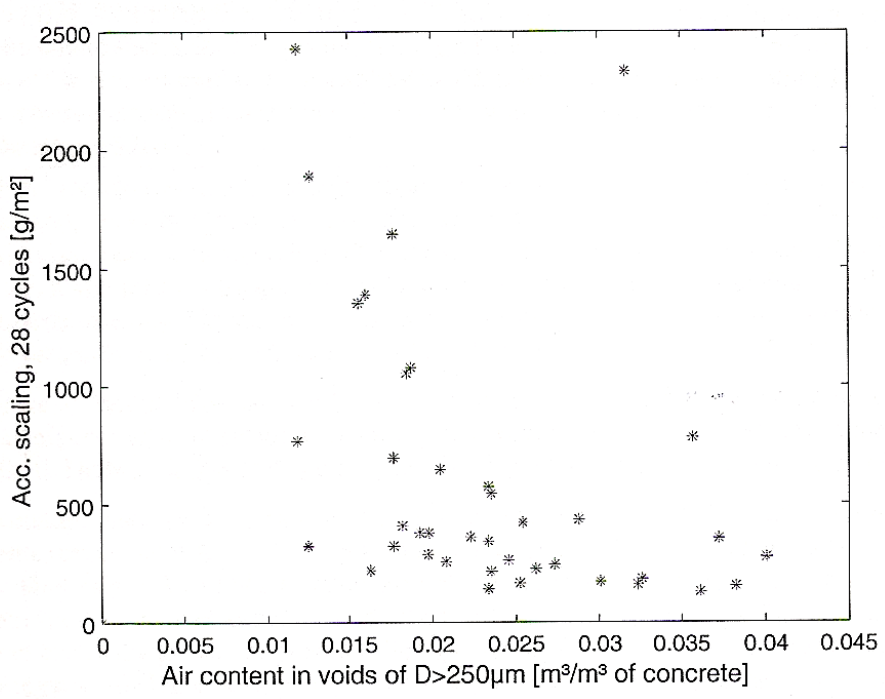

Figure 25: Scaling vs. total air content [m^3/m^3] in air voids of diameter >250µm.Concrete of w/c 0,40.

6. ALTERNATIVE TECHNIQUE FOR PREDICTING SALT FROST SCALING FROM ONE SINGLE AIR VOID SYSTEM PARAMETER

It should be clear that the demands on a high quality air void system are both that the total air volume must be large enough to provide space for ice formation (whichever way the ice formation process takes place), and that the distances between spheres must not be too large. Together, these two requirements result in an air void system in which the total sum of air void surface areas has some value: Small voids produce a large surface area per unit volume, but if there are too few of these small voids, the total air content will be too low. On the other hand, large voids will produce a volume large enough to allow ice formation without any stresses in the matrix, but then again, if there are too few of these large voids, the flow distance between them may become too large.

From this reasoning, it was hypothesized that for reasonably normal air void systems, the accumulated surface area of all air voids might be useful for assessing the quality of an air void system; Provided that the accumulated surface area is large enough, the total volume of air will be large enough and at the same time the flow distances will be kept short enough. This should hold true at least as long as ordinary air entraining agents are used. Minor shortcomings in flow distance might be counterbalanced by increased air content and vice versa.

In figure 26 the accumulated scaling of all concretes tested in this project are plotted *vs.* the accumulated surface area of their respective air void systems. The results seem to be fairly well gathered together, with concretes of w/c 0.50 consistently showing larger amounts of scaling (as might be expected). At least, there is a more obvious relation between this parameter and scaling than for any of those relations presented above (air content, specific surface or Powers spacing factor, etc.).

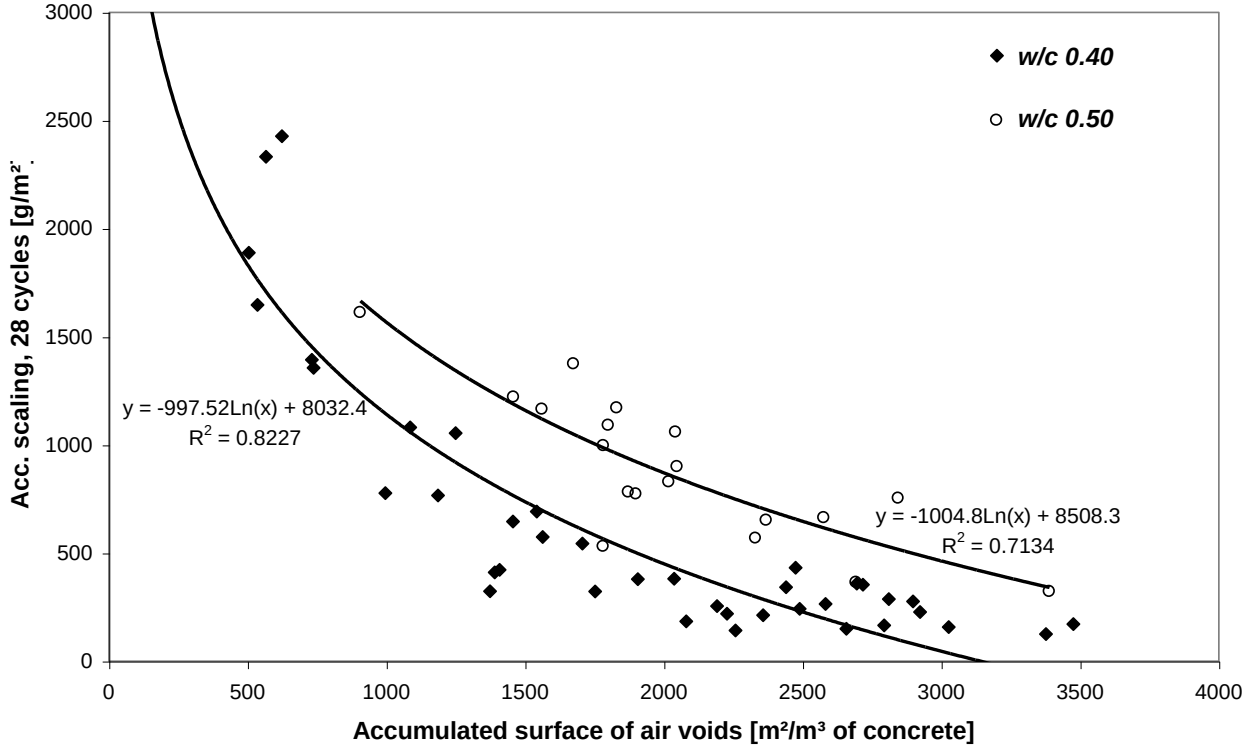

Figure 26: Scalings after 28 cykler plotted vs. the accumulated surface area of the entire air void system. In the calculatin of surface area, it is assumed that all voids are empty (non of them are filled with water).

Lines/equations have been fitted to the plots. As seen (especially for w/c 0.40) the dots actually show more clearly that scaling increases substantially as the total surface area is reduced below some 1500 m^2/m^3 of concrete than the equation reveals. (A reduction of surface area below this value leads to an increase in scaling, while an increase in surface area has little ability to reduce the scaling.) Of course, the required surface area needs to be calibrated in a full scale test with the appropriate test method (SS137244 etc.)

The logical background as to why this parameter might be useful may be visualized as follows: When ice forms in concrete, destruction may be caused either by hydraulic pressures or by microscopic ice lens growth (or a combination). In either case, there has to be empty space enough to accommodate the excess volume that appears, and also, the flow distance for water must not be too long. It is known that for many brittle, porous materials, there exists a critical thickness below which a thin flake will not be destroyed by frost even if it is frozen in a 100% complete saturation [7,8]. This is believed to be so because the flow distance for water to the surface is short enough. For concrete this critical thickness is in the order of 1 mm. Thus, if a 1 m^3 cube of concrete were sliced into 1 mm thick discs (figure 27), the flow distances would be short enough and the discs would not be destroyed. The drainage area created in such a cube by this slicing is 2000 m^2 (1000 slices with two surfaces), *i.e.* 2000 m^2/m^3. This drainage area is of the same order of size as indicated in figure 26. Although the geometries are very different, the correct order of size indicates that the proposed evaluation technique may be relevant.

Of course, the remarks made under subheading 5.2 apply also for this way of evaluating the air void system. And, again, there also has to be a minimum requirement on the total air content to accommodate the excess volume created by the ice formation.

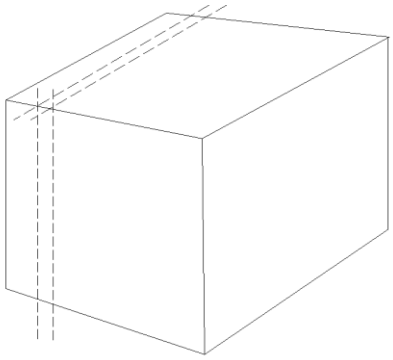

Slice in discs $D = D_{crit}$ = appr 1 mm

Total surface are of all discs = 2000 m^2/m^3 concrete

Figure 27:Illustration to the slicing of a concrete cube into thin slices of thickness D_{crit}.

7. CONCLUSIONS

Despite the use of different ways to change the air void system, the size distribution of the air void systems were very similar; More or less only the total number of bubbles increased, and thus the total air content. For a truly meaningful analysis of the relation between air void system parameters and salt frost scaling, it is necessary to produce concretes of radically different air void size distributions.

Using accumulated surface area of all voids in the air void system may be an effective tool for assessing the salt frost resistance of a concrete. The exact need for surface area is probably related to water cement ratio and to volume of paste. And of course, a certain total empty air volume too is required. The surface area required for acceptable salt frost resistance in laboratory tests needs to be determined from scaling tests according to standardized methods.

The methodology for air void system analysis needs to be improved in order to improve its repeatability.

The tool that was the aim of this project may prove successful on a relative scale rather than an absolute scale: In the pre-testing of concrete for a project, the air void system of concrete that is approved for use in the project may be analyzed and then, when the construction work starts, the cast concrete can be analyzed and compared to the concrete that was approved in pre-testing. In this way, changes in the air void structure may be discovered at an early stage, and subsequent problems with insufficient salt frost resistance may be avoided.

A continued analysis of the results in the original report might reveal better assessment techniques than those studied hitherto. An attempt will be made to finance such a study.

8. ACKNOWLEDGMENTS

My sincere thanks are due to professor Göran Fagerlund who initiated this study and who also made it possible through cooperation with SBUF. Dr. Kyösti Tuutti of Skanska acted as project leader (within SBUF), thereby contributing greatly to making the project possible. I am also greatly indebted to Peter Laugesen of Dansk Beton Teknik, Copenhagen, for truly invaluable help on the techniques of preparing samples for image analysis. Mr Bengt Nilsson carried out all

the practical work on the air void system analyses with accuracy and great patience. Thank you all for making this study possible!

9. REFERENCES

1. Lindmark, S: Studier av samband mellan betongs luftporsystem och dess saltfrostbeständighet, Lund University, Lund Institute of Technology, Report TVBM-3089, 2000
2. Underwood, E.E: ”Quantitative Stereology”, Addison-Wesley Publishing Company, Reading, Massachusetts, 1970
3. Vesikari, E: ”Image analysis in determining pore size distributions of concrete”, Technical Research Centre of Finland, Report 437, Espoo 1985
4. Lord,G.W, Willis, T.F: ”Calculation of Air Bubble Size Distribution from Results of a Rosiwal Traverse of Aerated Concrete”, ASTM Bulletin, Oct. 1951, pp 56-61
5. P. Laugesen, personal communication, 1999
6. Fagerlund, G: “Predicting the service life of concrete exposed to frost action througha modeling of water absorption process in the air-pore system”, RILEM/NATO Workshop “The modeling of microstructur and its potential for studying transport properties and durability”, St. Rémy-les-Chevreuse, July 10-13, 1994
7. Fagerlund, G: “Significance of critical degrees of saturation at freezing of porous and brittle materials”, Report 40, Lund Institute of Technology, Div. Building Technology, 1973
8. Fagerlund, G: “The critical spacing factor”, Report TVBM-7058, Lund Institute of Technology, Div Building Materials, 1993

Some Questions in Modelling of Service Life of Concrete Structures with Regard to Frost Attack

Tang Luping
Ph.D., Docent
Chalmers University of Technology
Division of Building Technology
S-412 96, Gothenburg
E-mail: tang.luping@chalmers.se

also for
CBI Swedish Cement and Concrete Research Institute
c/o SP
Box 857
S-501 15 Borås
E-mail: tang.luping@cbi.se

ABSTRACT

In this paper, the previous work in the study of mechanisms of water uptake and modelling of service life is reviewed and some questions in the modelling of service life are taken out for discussions. The results from a preliminary study of test procedures for determination of the critical degree of saturation and other necessary parameters for modelling of service life are presented. Based on the experience from the preliminary study the practical test procedures are suggested. With these test procedures, all test results can be obtained in a reasonably short period.

Key words: Concrete, durability, frost, modelling, service life and water uptake.

1. INTRODUCTION

It is well known that there are two types of damage in concrete under the frost attack, namely scaling and internal cracking. In despite of different patterns of damage, the common character is that the damage occurs when concrete becomes sufficiently saturated. Therefore, degree of saturation and its critical level are the key parameters for the modelling of service life of concrete structures with regard to frost attack. To quantify these two parameters, practical applicable test methods are needed. In addition, the effects of various influencing factors on these two parameters should also be understood in order to make a safe prediction of service life. For instance, the water uptake under the freeze-thaw action is an important factor related to the gradual increase in degree of saturation. In this paper, the previous work in the study of mechanisms of water uptake and modelling of service life will be reviewed and the results from a preliminary study of test procedures for determination of the critical degree of saturation and other necessary parameters for modelling of service life will be presented.

2. WATER UPTAKE

The phenomenon of water uptake due to the freeze-thaw action has been observed from the laboratory frost tests where the test surface of a concrete specimen is in contact with water. Many researchers reported the phenomenon of water uptake, so called "pumping effect", under the freeze-thaw action [1-5]. Tang and Petersson [5] found that the freeze-thaw action causes significant water uptake not only in the non-air-entrained concrete but also in the air-entrained concrete and that the amount of water taken up by the freeze-thaw action is significantly larger than that due to natural capillary suction, as shown in Figure 1.

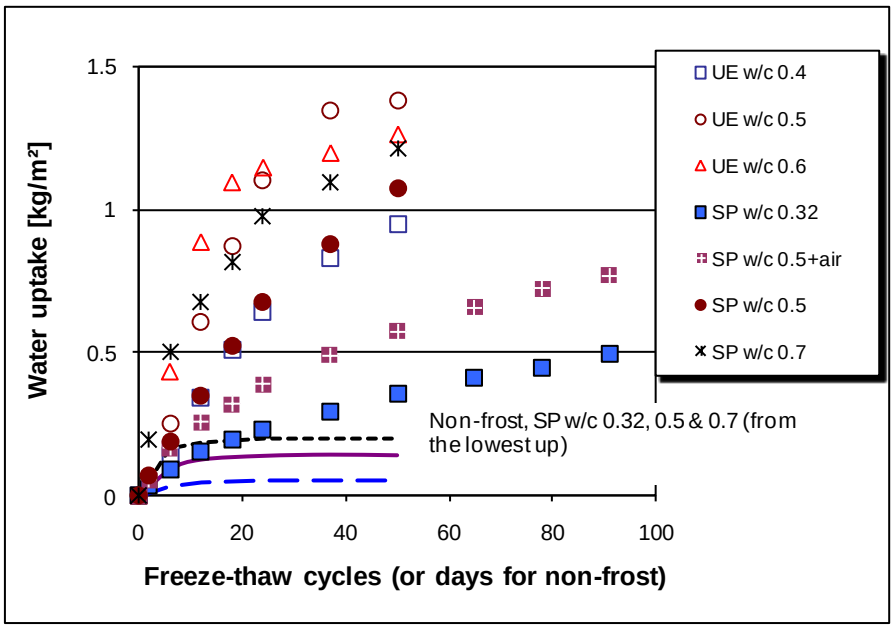

Figure 1 – Example of water uptake under the freeze-thaw action. Concrete specimens used for the Swedish slab test SS 13 72 44. "UE" denotes the concrete manufactured at University of Essen, Germany, and "SP" denotes the concrete manufactured at SP, Sweden.

The mechanism behind the water uptake is not fully clarified, although there are various possible explanations and hypothesises [6]. Although the micro-ice-lens model was proposed already in 1930 [7] for explanation of frost heaving in the earth, Setzer through his over 30-year research work developed it [8-10] on the basis of a triple-point shift and non-equilibrium thermodynamics. In Setzer's model he described the pumping effect as "the pressure differences generated following the triple-point shift act as a piston compressing the gel during cooling and expanding it during heating", while "the micro-ice-lenses act as a valve trapping the water during cooling and hindering the flow back during heating" [9]. According to Setzer's model of micro-ice-lens and Power's model of hydraulic pressure as well, the water uptake under a freeze-thaw cycle can be illustrated in Figure 2.

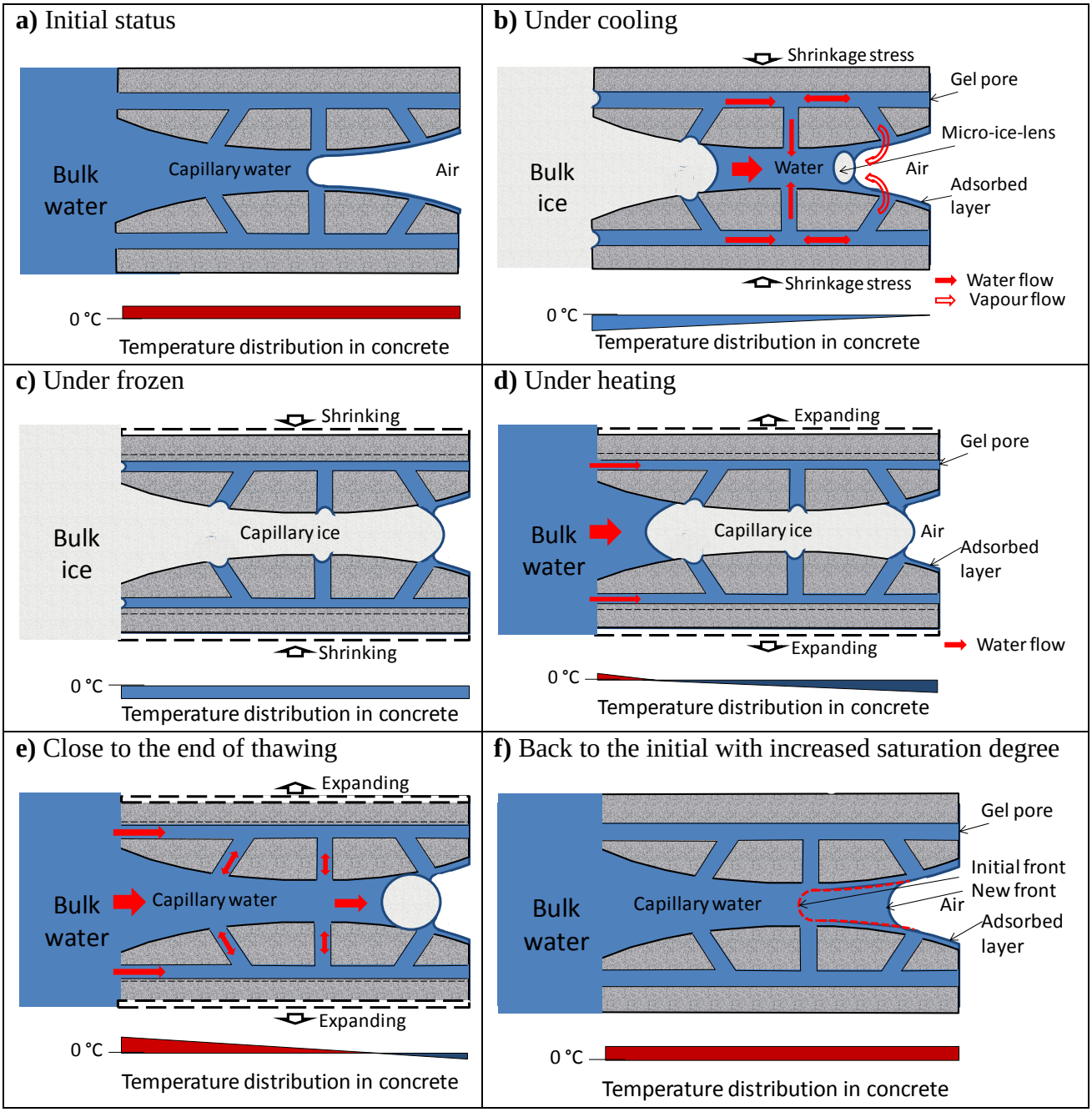

Figure 2 – Illustration of water uptake under a freeze-thaw cycle.

Under the intrusion of the bulk ice into a large capillary pore (due to the difference in surface tension between ice and water) hydraulically presses the unfrozen capillary water towards the empty space (Figure 2 b). Due to the depression of freezing point, the micro-ice-lens (after the heterogeneous nucleation) will be formed in the capillary pore at a temperature below the bulk freezing point, i.e. 0 °C. This implies a shift of triple-point where three phases coexist, generating a pressure difference between solid ice and liquid phases. Setzer [8] quantitatively calculated this pressure difference and found that a negative pressure of about 1.22 MPa for every degree Kelvin temperature below 0 °C will be generated in the unfrozen water. This negative pressure is balanced by the stress of concrete matrix, resulting in shrinkage and expression of unfrozen water in the gel pores through the unfrozen water channels towards both

the micro- ice-lens and macro-ice-lens. In addition, the gel pore water can also be transferred through the vapour phase towards the micro-ice-lens by condensation. As consequences of the unfrozen water transfer and the growth of ice crystals, the ice front moves towards the empty pores and occupies the unsaturated space (Figure 2 c).

Under the heating process, the bulk ice and the ice in the large capillary pores melt first. The increased temperature makes the concrete matrix expansion, pumping the bulk water, if available, into the gel pores to compensate the part transferred to the capillary pores under the cooling process. The micro-ice-lens in this case acts as a vacuum valve blocking the capillary channel and resulting in a one-way flow the melt water towards the ice-lens under the vacuum created by the reduction of volume when ice is melting (Figure 2 d and e). As a consequence, the additional water is uptaken and the degree of saturation in concrete increases after the cycle of freeze-thaw (Figure 2 f).

3. MODELLING OF SERVICE LIFE

3.1 Basic principle of modelling

It is known from the above section that the degree of saturation increases under the action of freeze-thaw cycles. Once the degree of saturation in concrete transgresses the critical level, damage will occur. This is the basic principle for modelling of service life of concrete structures with regard to frost attack. Fagerlund [11] summarised his over 25-year research work and established a service life model for internal frost damage in concrete. In his model, Fagerlund [11] used both the deterministic and stochastic approaches. In the deterministic approach, the basic criterion for frost damage is

$$S_{act} \geq S_{cr} \tag{1}$$

where S_{act} is the actual degree of saturation and S_{cr} is the critical degree of saturation. In the stochastic approach, the probability of the risk of frost damage is

$$P\{\text{frost damage}\} = P\{S_{act} > S_{cr}\} = \int_0^\infty F(S_{cr}) \cdot f(S_{act}) dS \tag{2}$$

where P is the probability, F and f are the distribution function and frequency function, respectively. Principally, both S_{act} and S_{cr} are time-dependent. When the time-dependent functions of S_{act} and S_{cr} as well as their standard deviations are known, the probability of risk of frost damage can be estimated, as an example shown in Figure 3.

Petersson [12] at the same time also proposed a probabilistic model as shown in Figure 4. Under the service life the probability of frost load T exceeding resistance T_R, i.e. $P(T > T_R)$, shall be less than the required one, P_{req}. Let resistance $T_R = S_{cr}(T_{min})$ and load $T = S_{act}(T_{min})$, where T_{min} is the minimum temperature for frost damage, then Petersson's model becomes similar to Fagerlund's model taking into account of temperature effects.

So far it is not clear in which way the frost load and resistance can been determined. According to Petersson [12], the frost load may involve minimum of temperature, number of freeze-thaw cycles, duration of freezing, rate of cooling, availability of water and salt, etc., while the frost

resistance may involve material properties and effect of ageing. Obviously, further research is needed in order to develop the probabilistic model to a practically applicable one.

Nevertheless, in both the models proposed by Fagerlund and Petersson, S_{cr} and S_{act} are two key parameters for estimation of frost damage.

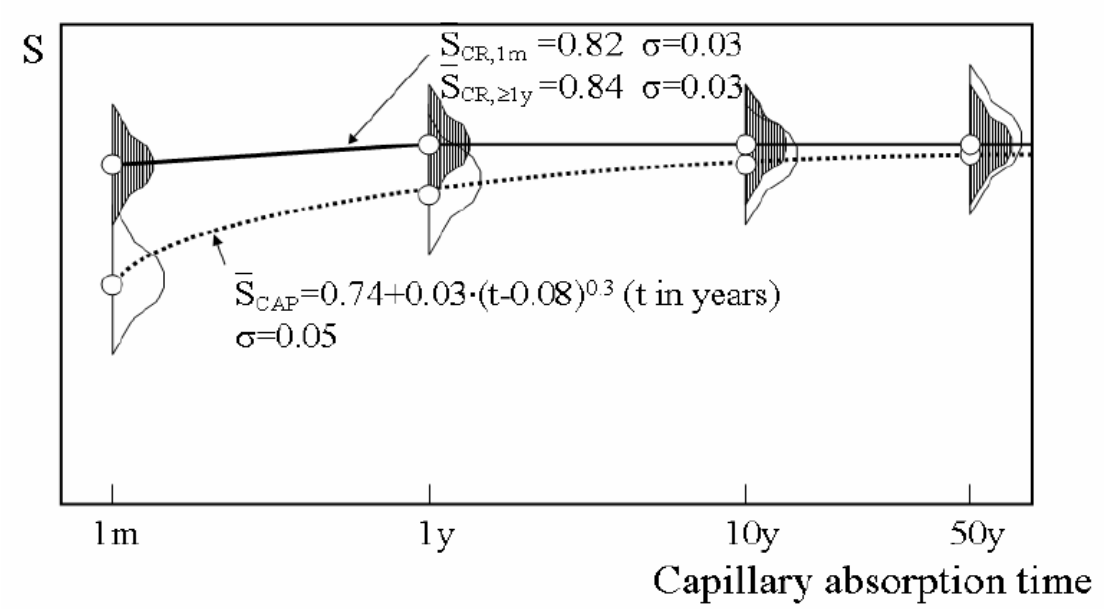

Figure 3 – Example of a stochastic service life calculation based on capillary absorption experiments [11].

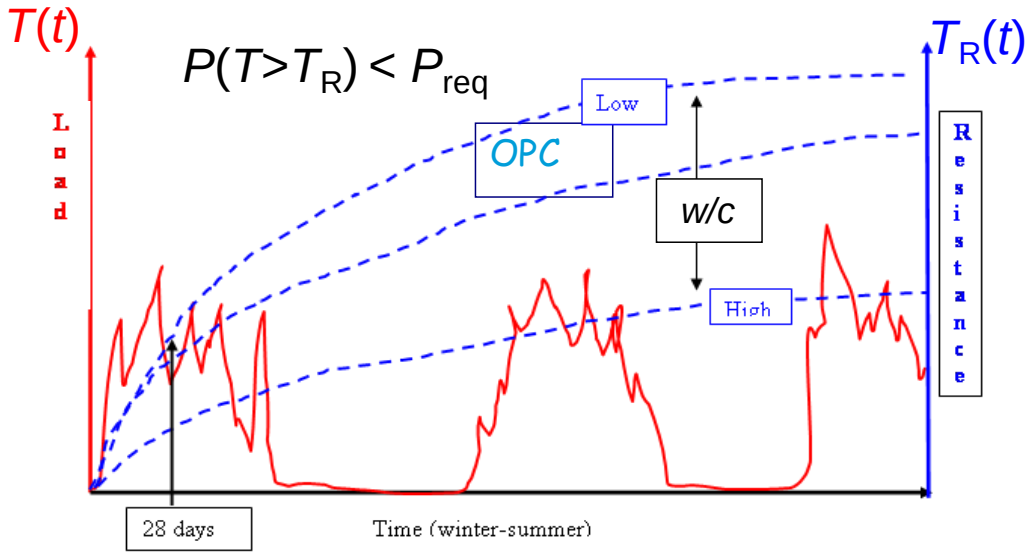

Figure 4 – Example of a probabilistic service life model based on frost load and resistance of concrete [12].

3.2 Critical degree of saturation

Theoretically, the critical degree of saturation for a closed container is 0.917. In concrete, however, the value of S_{cr} varies very much depending on the pore structures and quality of concrete. Fagerlund in Appendix A of his report [11] proposed an equation to express the critical degree of saturation in concrete, that is,

$$S_{cr,min} \le S_{cr} = 1 - a_{cr} / \varepsilon_t \le S_{cr,max} \tag{3}$$

where $S_{cr,min}$ and $S_{cr,max}$ are the lower and upper limit, respectively, a_{cr} is the critical air content, and ε_t is the total porosity. The lower and upper limits are expressed as [13]

$$S_{cr,min} = S_b - 0.09 w_f / \varepsilon_t = 0.917 S_b + 0.083 w_{nf} / \varepsilon_t \tag{4}$$

and

$$S_{cr,max} = 1 - 0.09 w_f / \varepsilon_t = 0.917 + 0.083 w_{nf} / \varepsilon_t \tag{5}$$

where S_b is the breaking point, so called "knick point" or "nick point", in the water absorption test, which will be discussed later, and w_f and w_{nf} are the freezable and non-freezable water, respectively. Assuming that the gel water is non-freezable,

$$w_{nf} = 0.20 \alpha_h \cdot C \cdot 10^{-3} \tag{6}$$

Fagerlund [13] also suggested a theoretical way to estimate the breaking point S_b using the following equation:

$$S_b = (w/c - 0.19\alpha_h) / [(w/c - 0.19\alpha_h) + 1000a \cdot C] \tag{7}$$

where *w/c* is the water-cement ratio, and *a* is the air porosity in m^3/m^3.

Since the critical air content a_{cr} is dependent on the air-pore system in concrete including air quantity, size and spacing factor of the air-pores, the value of S_{cr} in equation (3) cannot be simply solved, but give a range of possible values of S_{cr}.

3.3 Actual degree of saturation

Due to the complicated moisture conditions under the variation of the real climate, it is hardly possible to predict the actual degree of saturation in concrete in the reality. The case of free water available on the concrete surface under the freeze-thaw period represents, nevertheless, the severest exposure condition. Since the capillary suction is a very quick process when compared with the water absorption after the breaking point, the degree of saturation based on the long-term capillary absorption is adopted in Fagerlund's model [11], noted as S_{cap}, expressed as

$$S_{cap} = S_b + \frac{c \cdot t^d}{w_{sat}} \quad (8)$$

where c and d are the material dependent coefficients, and w_{sat} is the water content at complete saturation. The coefficient c is mainly dependent on the diffusivity of dissolved air, while the exponent d is dependent on the air-pore size distribution. Both the coefficients can be determined by the long-term water absorption test.

Obviously, in this test the pumping effect under the freeze-thaw action is not taken into account. Therefore, the degree of saturation based on equation (8) may not represent the severest exposure condition.

3.4 Some questions in modelling of service life

Although a complete system has been established by Fagerlund [11, 13] for calculation of service life of concrete with regard to the frost attack, the knowledge of both the critical and actual degrees of saturation as functions of various influencing factors is still very limited. Considering possible influencing factors, we can express the critical degree of saturation by the following function

$$S_{cr} = f(\varepsilon_t, a_a, \alpha_a, D_a, T_{min}, t_f, ...) \quad (9)$$

where a_a, α_a and D_a are the actual air content, actual specific surface and actual spacing factor, respectively, and t_f is the freezing duration. The first four factors have been quantitatively considered in Fagerlund's model, but the factors T_{min} and t_f do not. Since the amount of unfrozen water in concrete can vary with T_{min} and t_f, the value of S_{cr} may also be dependent on these two factors. Petersson [14] found that the effect of T_{min} on scaling is significant when the T_{min} is in the range of –10 °C and –20 °C in the slab test. This could be an indication of different critical degrees of saturation at different T_{min}. Under a certain cycle of freeze-thaw, there may exist a relationship between T_{min} and t_f, If we exclude the effect of freezing duration, the first question becomes how to find $f(T_{min})$ for S_{cr}.

On the other hand, the degree of saturation based on equation (8) does not include the water uptake by the pumping effect, as mentioned previously. Then the second question is how to estimate constants c and d in equation (8) under specific frost conditions

4. A PRELIMINARY TRIAL FOR ANSWERING THE QUESTIONS

4.1 Method for critical degree of saturation

A test method for critical degree of saturation was recommended by RILEM [15] over 30 years ago. In this method about 10 specimens of cross-sectional size larger than 3 times maximum size of aggregate and length larger than 2-3 times cross-sectional size are used. The specimens are pre-conditioned (first vacuum saturation and afterwards drying) to different degrees of saturation and then subjected to the freeze-thaw cycles. The fundamental frequencies of a specimen are measured before and after the freeze-thaw cycles. The relative dynamic modulus (*RDM*) of concrete can be estimated by the following equation:

$$RDM = \frac{E_n}{E_0} = \left(\frac{f_n}{f_0} \right)^2 \quad (10)$$

where E_0 and E_n are the dynamic modulus, and f_0 and f_n the fundamental frequency before and after the n-th freeze-thaw cycles. The critical degree of saturation is reached when the *RDM* reduces to 0.9, that is, the dynamic modulus is reduced by some 10%, indicating a notable internal damage in concrete.

This is a time-consuming and laborious test method. Some difficulties and problems in this method have been listed in [16]. It is difficult to use this time-consuming and laborious method for investigating various influencing factors. Fagerlund [16] suggested use thin slice specimens instead of large and thick ones for the S_{cr} test. Following his suggestion, thin slice specimens of about 10 mm cut from concrete cubes were used in a preliminary experimental study.

4.2 Preliminary experimental study

Two types of concrete, one without entrained air and another with 4.3% air, were used in the study. The mixture proportions of concrete are listed in Table 1. In both types of concrete, Swedish structural cement (CEM I 42.5N BV/SR/LA) was used.

Table 1 – Mixture proportions of concrete used in the study

		Cement	Aggregate, kg/m^3		SP	AEA	Air %
Concrete	*w/c*	kg/m^3	0-8 mm	8-16 mm	Glenium 51	L-14	
Mix I	0.46	475	1600	-	0.2%	-	≈ 3*
Mix II	0.45	420	510	650	-	0.026%	4.3

* not measured but estimated from previous experience in use of superplasticiser Glenium 51.

The specimens of size 150×50×10 mm (Mix I) and 100×50×10 mm (Mix II) were cut from 150 mm cubes and stored in a CO_2 free chamber at 20 °C and 33% RH (with saturated $MgCl_2 \cdot 6H_2O$ and CO_2 adsorbent) for 6 months (Mix I) and 1 month (Mix II) before testing for water absorption. After the water absorption test, the specimens were dried at 105 °C to constant weight and then vacuum saturated (dry vacuum for 3 h at 5-10 mbar, fill the container with cool boiled water when vacuum was running, continue vacuum for 1 h before release air in the container, and then keep the specimen in the water for at least 24 h) before weighing in air and in water, respectively. From these weights the degree of saturation and total porosity can easily be calculated. The results are shown in Figures 5 and 6. It can be seen that both types of concrete reveal clear breaking point at degree of saturation about 0.75, although Mix I shows a very low initial value due to long-term (6 months) drying. The repeatability of the water absorption test seems very good. Three samples revealed almost the same absorption curve (Figure 6).

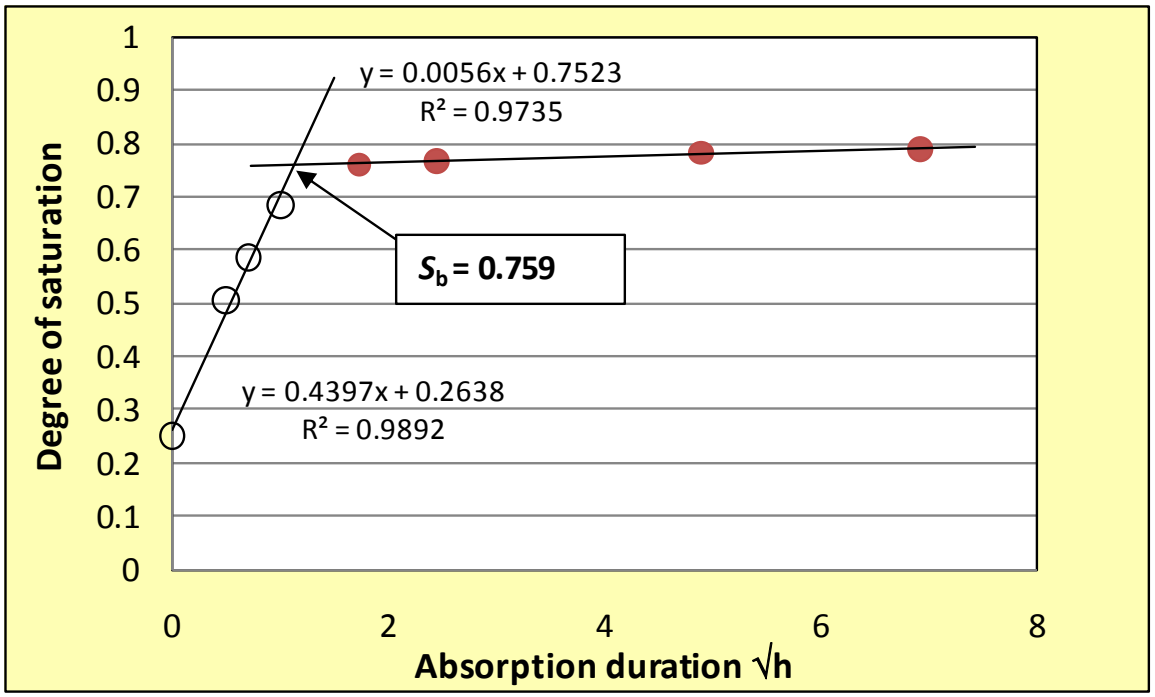

Figure 5 – Result of water absorption test for concrete Mix I.

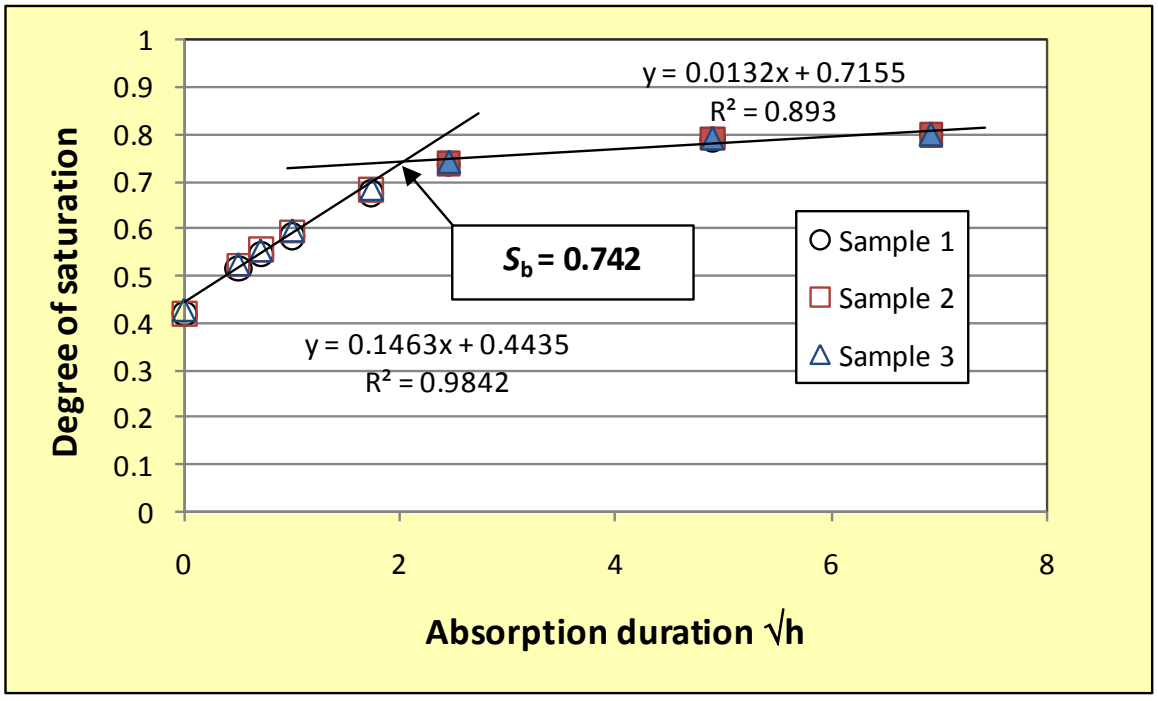

Figure 6 – Result of water absorption test for concrete Mix II.

For the S_{cr} test, vacuum saturation was used to increase the degree of saturation in the specimens. Dry specimens were vacuum treated (at a residual air pressure of 5-10 mbar) for 1-3 hours before the container was filled with cool boiled water. After the water filling, the specimens were stored in the water for different periods (from 0 hour to 5 days). The vacuum

treatment was carried out on different days or times in order to make all the treated specimens subject to the freeze-thaw test on the same day. Under the freeze-thaw test one large surface of each specimen was supported on two 2-3 mm strips in a container which was filled with demineralised water to cover another large surface of the specimen with a layer of 2-3 mm free water. The fundamental frequency was measured before and after the freeze-thaw test. The values of RDM can be calculated using equation (10). The results from the freeze-thaw test with one single cycle are shown in Figures 7 to 8.

Figure 7 shows that the S_{cr} of Mix I (non-air entrained) is about 0.95, larger than the theoretical value 0.917. This is partly because of unfreezable water in the gel pores [16] and partly because of the vacuum saturation which may not 100% saturate the specimen.

Figure 8 shows that the S_{cr} of Mix II (air-entrained) is about 0.90, close to the theoretical value 0.917. It seems that the effect of T_{min} on the S_{cr} value is not significant. However, due to the limited data of degree of saturation in the range of 0.9 and 1, no strong conclusion can be drawn.

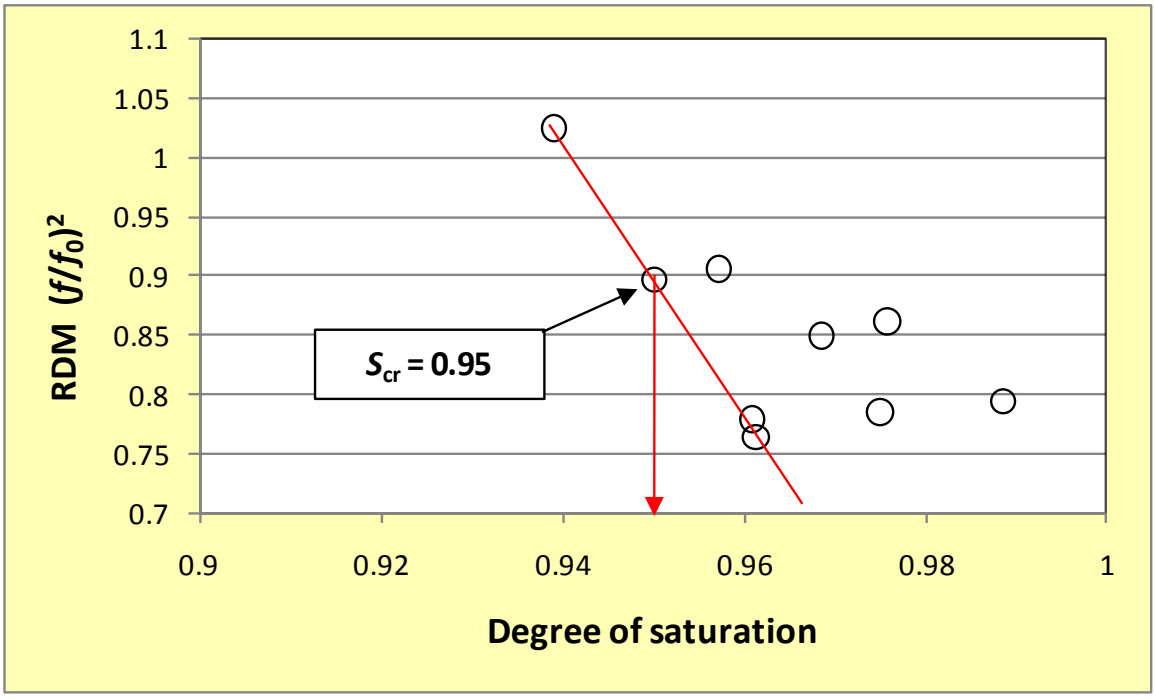

Figure 7 – Results for concrete Mix I after one freeze-thaw cycle at T_{min} = - 25 °C.

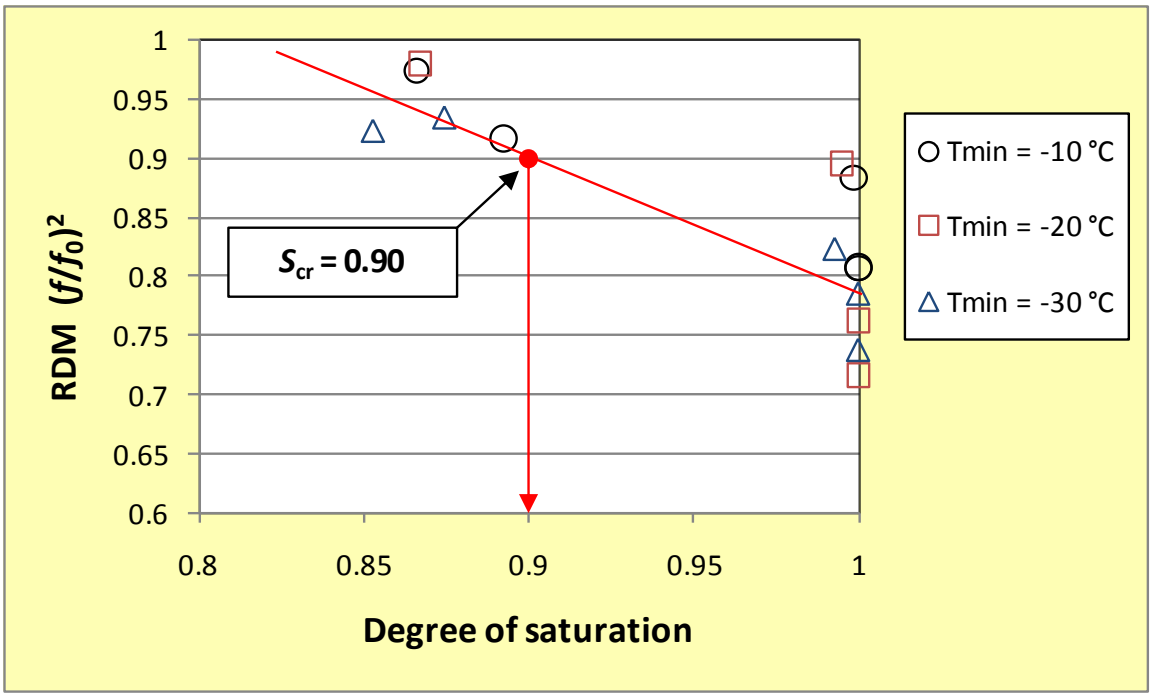

Figure 8 –Results for concrete Mix II after one freeze-thaw cycle at different minimum freezing temperatures.

.

The results from the freeze-thaw test with a number of cycles are shown in Figure 9. It can be seen that the degree of damage (reduction of RDM) is an exponent function of freeze-thaw cycles, if the specimens are pre-saturated over the S_{cr} value (e.g. 5-day storage in water after vacuum saturation). In this case the temperature effect is significant, that is, the lower the minimum freezing temperature, the quicker the damage development. Using these regression functions, we can obtain the iso-damage (equal RDM) curves relating the number of freeze-thaw cycles to different T_{min}, as shown in Figure 10. It shows that, under the equal degree of damage, the number of freeze-thaw cycles is proportional to the T_{min}. Its slope is dependent on the degree of damage. The severer the damage is (e.g. RDM = 0.6, implying a destructive structure), the more significant the effect of the T_{min}. More freezable water under the lower T_{min} could be an explanation. This increased amount of freezable water increase the degree of damage under a certain number of freeze-thaw cycles. The relationships between degree of damage, number of freeze-thaw cycles and the minimum freezing temperature can be used in the probabilistic modelling, e.g. as proposed by Petersson [12].

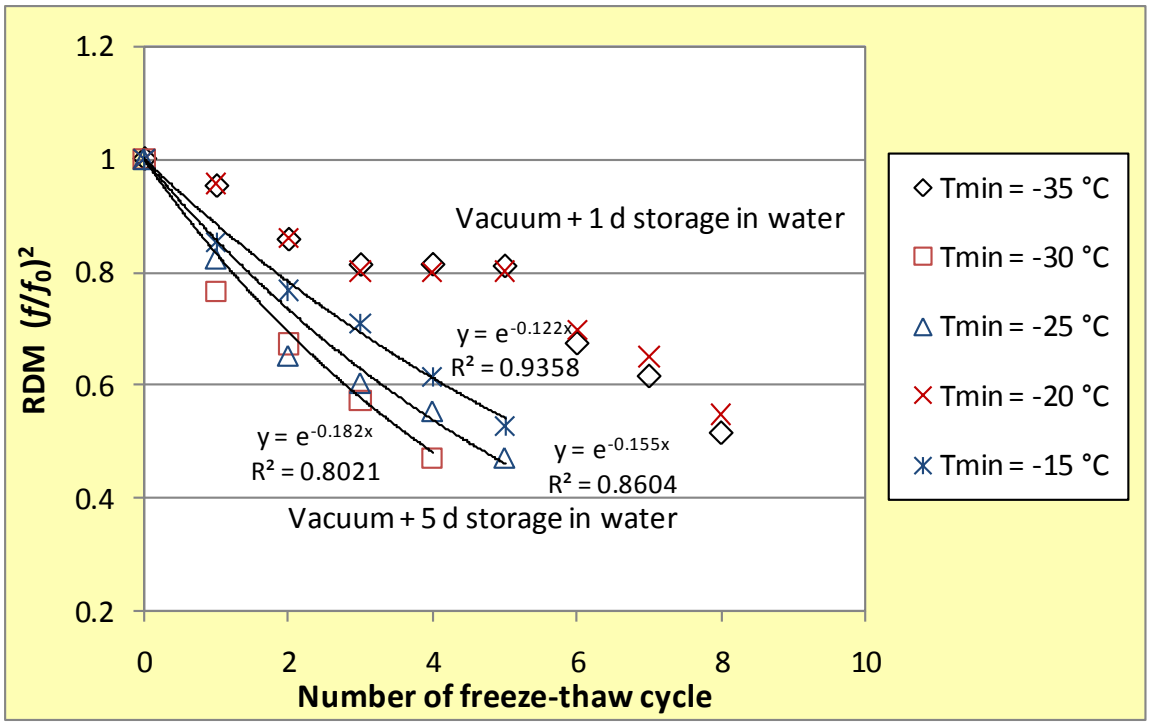

Figure 9 – Results for concrete Mix I after different freeze-thaw cycles at different minimum freezing temperatures.

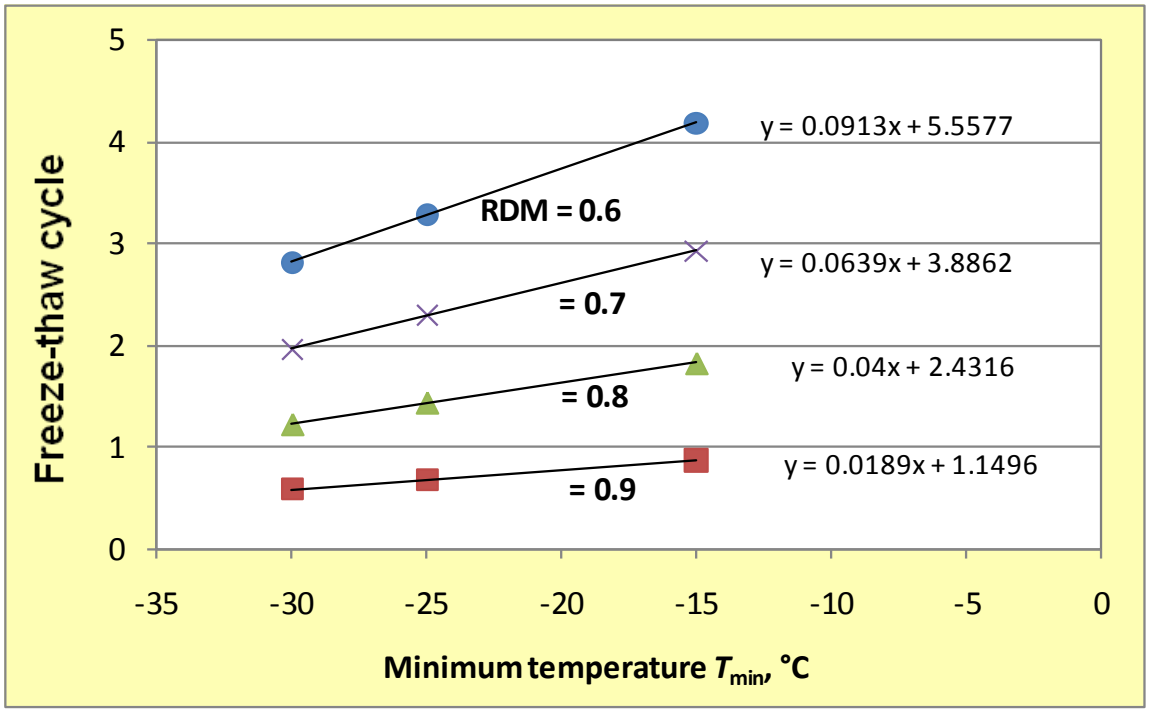

Figure 10 – Results for concrete Mix I after different freeze-thaw cycles at different minimum freezing temperatures.

4.3 Suggestions to test methods

The results from the preliminary study using the thin slice specimens show that it is feasible to measure the S_{cr} value of concrete in a short time with one single freeze-thaw cycle. From the experience of the preliminary study, the following procedures are suggested for the measurement of S_{cr} and S_b to be used in the service life modelling:

Specimens and pre-drying

- Cut 30 pieces of slice specimen of size 100×50×10 or 100×50×15 mm from the central portion (to avoid the skin effect) of three 150 mm concrete cubes (well cured), with the longest size of the slice in the vertical direction of casting.
- Dry the slice specimens at 50 °C for 24 hours and cool down them in a sealed container or plastic box.
- Store 15 of them in a climate chamber/box with 20 °C and 33% RH (with saturated $MgCl_2 \cdot 6H_2O$ and CO_2 adsorbent) for 6 days before testing for water absorption.
- Store the rest 15 pieces in a sealed container or plastic box with CO_2 free atmosphere at the room temperature for the S_{cr} test.

Pre-saturation of the specimens for the S_{cr} test

a) Vacuum-treat 10 pieces of the pre-dried specimens at different residual air pressures or for different duration, depending on the desired range of saturation degree.
b) Fill the container with cool boiled water to immerse the specimens slowly from the bottom up, while the vacuum pump is running.
c) Release the air into the container and keep the specimens in the water for different durations, from hours to days, depending on the desired range of saturation degree.
d) Measure the mass and fundamental frequency of each specimen under the surface dry condition prior to the freeze-thaw test.
e) Put each specimen on two 2-3 mm strips (metallic wires or rubber bands) in a container and fill the container with demineralised water to cover another large surface of the specimen with a layer of 2-3 mm free water.
f) Start the freeze-thaw cycle with the minimum freezing temperature of -20 °C as reference.
g) After one freeze-thaw cycle measure the mass and fundamental frequency of each specimen under the surface dry condition again.
h) Calculate the RDM using equation (10). If none of the RDM is less than 0.9, repeat the procedures from e). If all of the RDM are less than 0.9, use the rest 5 specimens and repeat the procedures from a) with a higher residual air pressure.
i) If the RDM values cover the range of 0.8 and 1, dry the tested specimens at 105 °C to constant mass.
j) Vacuum-treat the dried specimens at a residual air pressure less than 10 mbar for 3 hours.
k) Do the same procedures as in b) and c) but keep the specimens in the water for 18 hours.
l) Measure the mass of each specimen in air (under the surface dry condition), and optionally in water for the volume of the specimen.

The mean value of saturated water content from undamaged (RDM > 0.9) specimens (in the ratio of water content to dry mass or to volume) can now be calculated from the mass data obtained from the above. With this mean value the individual degree of saturation for all the specimens can then be calculated and a plot of RDM vs *S* (degree of saturation) can be drawn.

Taking the RDM = 0.9 as criterion for observable damage, the critical degree of saturation can be obtained through the analysis of the RDM-*S* plot, as shown in Figures 7 and 8.

Test method for natural water absorption and freeze-thaw water uptake

- Measure the mass of each specimen stored at 20 °C and 33% RH.
- Carry out the water absorption test according to the standard procedures, e.g. NT BUILD 368.
- After the clear picture of two absorption lines, keep three specimens in continuation of the absorption test and take 12 specimens to do the procedures d) to g) as in the S_{cr} test, but under different minimum freezing temperatures, e.g. -10 °C, -15 °C, -20 °C and -25 °C (3 specimens per each temperature).
- After each freeze-thaw cycle measure the mass and fundamental frequency of each specimen under the surface dry condition.
- Repeat the freeze-thaw test until the RDM value is less than 0.8.
- Dry all the specimens including the three non-freeze-thaw tested specimens and measure the dry mass of each specimen.
- Follow the procedures k) and l) as in the S_{cr} test to measure the saturated water content of the three non-freeze-thaw tested specimens.

The above procedures for the S_{cr} test will not take very long time, probably in two weeks including pre-drying plus pre-saturation (one week) and freeze-thaw cycle (one or two cycles in most cases) plus drying and re-saturation (one week).

The above procedures for testing natural water absorption and freeze-thaw water uptake may be a little time-consuming, because a number of freeze-thaw cycles are needed. Normally, five cycles should be sufficient to obtain a water uptake curve for regression analysis, like in the natural water absorption test. Therefore, the test period including the pre-drying (one week), the natural water absorption (one week), the freeze-thaw water uptake (one week) and drying and saturation (maximum one week), will be in 4 weeks. This test can be carried out parallel to the S_{cr} test. Therefore, the total period for all of the above tests will be in 4 weeks, shorter than the present slab test which needs at least 8 weeks to obtain the results.

From the above procedures, the critical degree of saturation, the water absorption under the natural contact with water and the water uptake as the pump effect under the freeze-thaw cycles as well as the effect of minimum freezing temperature could be obtained. With these parameters as input data, it is possible to establish practically applicable models (both in deterministic and probabilistic ways) for service life of concrete structures with regard to the frost attack.

5. CONCLUDING REMARKS

As a summary, Fagerlund [11, 13] has established a complete system for calculation of service life of concrete structures with regard to the frost attack. His idea of using thin slice specimens for both the water absorption test and the S_{cr} test [16] has been tried in this study and the preliminary results show that this approach is feasible. Based on the experience from this preliminary study the practical test procedures are suggested. With these test procedures, all test results can be obtained in a reasonably short period (4 weeks), shorter than the current standard test, e.g. the slab test. The obtained results can be used either for estimation of the frost

resistance or possibly as input data in both deterministic and probabilistic modelling of service life of concrete structures with regard to the frost attack.

ACKNOWLEDGEMENTS

The author thanks Prof Göran Fagerlund for his kind help in the literature and constructive discussions. Experimental assistance by Mr Marek Machowski, Chalmers, is appreciated. Financial support from the Swedish Transport Administration (through the research project AL90_B_2007_24882 by previous Swedish Road Administration) is acknowledged.

REFERENCES

1. Jacobsen, S., "Scaling and cracking in unsealed freeze/thaw testing of Portland cement and silica fume concretes", Doctoral thesis 1995:101, NTH, Trondheim, Norway.
2. Palecki, S. & Setzer, M.J., "Investigation of high-performance concrete under frost attack – Interanl damage and water uptake", in "Frost Resistance of Concrete -From Nano-Structure and Pore Solution to Macroscopic Behaviour and Testing", ed. M.J. Setzer, R. Auberg & H.-J. Keck, RILEM Publications PRO 24, April 2002, pp.317-325.
3. Fagerlund, G., "Fatigue effects associated with freeze-thaw of materials", Division of Building Materials, Lund Institute of Technology, TVBM-7156, Lund 2000, 14 pp.
4. Tang, L. & Petersson, P.-E., "Water uptake, dilation and internal deterioration of concrete due to freezing-and-thawing", in "Frost Resistance of Concrete -From Nano-Structure and Pore Solution to Macroscopic Behaviour and Testing", ed. M.J. Setzer, R. Auberg & H.-J. Keck, RILEM Publications PRO 24, April 2002, pp.287-294.
5. ConLife, "Durability data of lab-testing", EU-Project (5th FP GROWTH) G5RD-CT-2000-00346, Deliverable Report 6, 2004.
6. Jacobsen, S., "Liquid uptake mechanisms in wet freeze/thaw: Review and modeling", Proceedings of RILEM Workshop on Frost Damage in Concrete, Minneapolis, USA, 28-30 June 1999, ed by Mark, Bennett & Snyder, pp. 41-51.
7. Taber, S., "Mechanics of frost heaving", *J. Geology*, Vol. 38, 1930, pp. 303-317.
8. Setzer, M.J., "Mechanical stability criterion, triple-phases condition, and pressure differences of matter condensed in a porous matrix", *J. Colloid & Interface Sci.*, Vol. 235, 2001, pp. 170-182.
9. Setzer, M.J., "Micro-ice-lens formation in porous solid", *J. Colloid & Interface Sci.*, Vol. 243, 2001, pp. 193-201.
10. Setzer, M.J., "Development of the micro-ice-lens model", in "Frost Resistance of Concrete -From Nano-Structure and Pore Solution to Macroscopic Behaviour and Testing", ed. M.J. Setzer, R. Auberg & H.-J. Keck, RILEM Publications PRO 24, April 2002, pp.133-145.
11. Fagerlund, G., "A service life model for internal frost damage in concrete", Division of Building Materials, Lund Institute of Technology, TVBM-3119, Lund 2004, 48 pp.
12. Petersson, P.-E., "A service life model for scaling resistance of concrete – reflections" presented at the meeting of the *fib* task group 5.6, Lund, Oct. 2004.
13. Fagerlund, G., "Moisture design with regard to durability – With special reference to frost destruction", Division of Building Materials, Lund Institute of Technology, TVBM-3130, Lund 2006, 128 pp.
14. Petersson, P.-E., "Influence of minimum temperature on the scaling resistance of concrete – Part 1: Portland cement concrete", SP REPORT 1994:22, Swedish National Testing and Research Institute, Borås, Sweden, 1994, 30 pp.

15. RILEM Tentative Recommendation by TC 4 CDC, “The critical degree of saturation method of assessing the freeze/thaw resistance of concrete”, Materials & Structures, Vol. 10, No. 58, 1977.
16. Fagerlund, G., “Modified procedure for determination of internal frost resistance by the critical degree of saturation method”, in “Proceedings of the 3rd Nordic Research Seminar on Frost Resistance of Building Materials”, ed. By K. Fridh, Division of Building Materials, Lund Institute of Technology, TVBM-3087, Lund 1999, pp 29-49.

Frost Resistance of Concrete Containing Secondary Cementitious Materials - Experience from Three Field Exposure Sites

[Reprinted from NCR workshop-proceeding No.3, Nordic Miniseminar – Durability of Exposed Concrete containing Secondary Cementitious Materials, Hirtshals, November 21 – 23, 2001]

Peter Utgenannt
Doctoral candidate
SP Swedish National Testing and Research Institute
Box 857, SE-501 15 Borås, Sweden
e-mail: peter.utgenannt@sp.se

Per-Erik Petersson
Professor, Head of the Department of Building Technology
SP Swedish National Testing and Research Institute
Box 857, SE-501 15 Borås, Sweden
e-mail: pererik.petersson@sp.se

ABSTRACT

Concrete samples made from different cement/binder types, including secondary cementitious materials, have been exposed at three different field test sites for five years. All the sites are situated in Sweden, one in a highway environment, one in a marine environment and one in an environment without salt exposure. The resistance to internal and external frost damage has been regularly evaluated by measurements of change in volume and ultrasonic pulse transmission time. The results after five years' exposure clearly indicate the highway environment as being the most aggressive with regard to external frost damage. The influence of the climate on the internal frost damage is less pronounced. Results show that concretes containing large amounts of slag in the binder have the severest scaling, whether with or without entrained air. For concrete without entrained air, qualities containing OPC + 5 % silica as binder seems to be more susceptible to internal damage than do the other qualities.

Key words: Freeze/thaw, Field test, Laboratory test, Secondary cementitious materials

1. INTRODUCTION

Frost resistance is one of the most important properties determining the durability of concrete in the Scandinavian countries, as well as in other European countries with cold climates. To be able to prove concrete qualities to be frost-resistant a number of test methods have been developed:

for example, Swedish Standard SS 13 72 44 for scaling resistance [1], Finnish Standard SFS 5448 for dilation [2] and the measurement for critical degree of saturation [3].
These test methods have been developed primarily on the basis of experience of traditional concrete. When new types of concrete are introduced - for example, with new types of binders, filler materials, admixtures etc. - we do not know how to evaluate the test results or even if the freeze/thaw test methods used are relevant. More knowledge and experience of the salt/frost resistance of these new concrete qualities in the field is needed. One way to acquire this experience is to expose concrete specimens to representative outdoor environments. Such an investigation was started in Sweden in the mid-nineties. Three field exposure sites were established in the south-west of Sweden: one in a highway environment beside highway 40 (60 km east of Gothenburg), one in a marine environment at Träslövsläge harbour (80 km south of Gothenburg) and one in an environment without salt exposure on SP's premises in Borås (70 km east of Gothenburg). The air temperature and relative humidity ranges are the same at the highway exposure site and at SP's premises, with minimum temperatures between –15 °C and –20 °C, and with a precipitation of about 900 mm per year. The temperatures at the marine exposure site at Träslövsläge harbour are somewhat milder, and the precipitation is about 700 mm per year. The micro-climates surrounding the test specimens, however, vary significantly between the three sites, with the highway microclimate being the most moist and saline, and the climate at SP being the 'mildest', with no salt and only pure precipitation.

A large number of concrete mixtures of varying quality with different binder types/combinations, varying water/binder ratios and air contents were produced and placed at the field exposure sites. The frost damage has been regularly evaluated by measurements of the volume change of the specimens and the change in ultrasonic transmission time through each specimen. This paper presents results after five winter seasons for concrete qualities produced with four different binder combinations: one with Ordinary Portland Cement (OPC), one with a CEM III cement type and two with OPC and secondary cementitious materials.

2. MATERIALS AND SPECIMENS

The binder types/combinations studied in this investigation are shown in Table 1. For chemical composition, see [4].

Table 1 - Binder types/combinations investigated

Binder type/combination	Comments
1 OPC[1)] (CEM I)	Low alkali, sulphur-resistant
2 OPC[1)] + 5 % silica by binder weight	Silica in the form of slurry
3 OPC[1)] + 30 % slag by binder weight	Ground blast furnace slag added in the mixer
4 CEM III/B	Dutch slag cement, ~70 % slag

[1)] OPC = Ordinary Portland Cement (Degerhamn standard [5] is a low-alkali, sulphur-resistant cement)

Ten different concrete qualities were produced for each of the binder types/combinations. Concrete qualities with five different water/binder (w/b) ratios (0.30, 0.35, 0.40, 0.50, 0.75), and with and without entrained air, were produced for all binder combinations. 0-8 mm natural and 8-16 mm crushed aggregate was used for all mixes. A naphthalene-based plasticizer, Melcrete, was used for mixtures with w/b-ratio of 0.40 and lower. The air-entraining agent used, L16, is a

tall-oil derivative. A summary of concrete constituents and properties is presented in Table 2 below, for a complete presentation see [4].

Table 2 - Concrete qualities used in this investigation.

Binder type	w/b-ratio	Eqv. w/c-ratio[1]	Cement (kg/m^3)	SCM[2] (kg/m^3)	AEA[3]	Air content fresh (%)	Slump (mm)	Compressive strength (MPa) SS[4]	Recalc[5]	Scaling (kg/m^2)[6] 28	56
OPC	0.30	0.30	500	-	Yes	4.8	240	95	87	0.024	0.035
	0.35	0.35	450	-	Yes	4.8	190	95	87	0.054	0.085
	0.40	0.40	420	-	Yes	4.6	125	67	60	0.014	0.023
	0.50	0.50	370	-	Yes	4.6	90	49	44	0.017	0.022
	0.75	0.75	260	-	Yes	4.7	100	21	18	0.127	0.141
	0.30	0.30	500	-	No	1.1	120	102	93	0.156	0.256
	0.35	0.35	450	-	No	1.2	140	91	83	1.94	4.39
	0.40	0.40	420	-	No	0.8	130	87	79	3.11	7.92
	0.50	0.50	385	-	No	0.8	70	56	50	5.09	14.5
	0.75	0.75	265	-	No	0.9	60	31	27	4.34	>15
OPC+5% silica	0.30	0.29	475	25	Yes	4.6	100	103	94	0.041	0.119
	0.35	0.33	427.5	22.5	Yes	4.5	90	91	83	0.022	0.041
	0.40	0.38	399	21	Yes	4.8	105	72	65	0.023	0.035
	0.50	0.48	361	19	Yes	4.6	70	57	51	0.020	0.026
	0.75	0.71	237.5	12.5	Yes	4.3	70	25	22	0.19	0.20
	0.30	0.29	475	25	No	1.1	125	121	111	0.12	0.20
	0.35	0.33	427.5	22.5	No	1.1	90	105	96	0.36	0.89
	0.40	0.38	399	21	No	0.5	100	84	76	1.67	3.25
	0.50	0.48	370.5	19.5	No	1.2	60	67	60	1.86	4.61
	0.75	0.71	256.5	13.5	No	0.3	75	35	31	3.45	6.58
OPC+30% slag	0.30	0.34	350	150	Yes	4.8	230	90	82	0.031	0.045
	0.35	0.40	315	135	Yes	4.8	130	86	78	0.086	0.139
	0.40	0.45	294	126	Yes	4.4	110	65	58	0.041	0.067
	0.50	0.57	259	111	Yes	4.8	80	49	44	0.021	0.033
	0.75	0.85	175	75	Yes	4.4	100	20	17	0.490	0.538
	0.30	0.34	350	150	No	0.7	220	101	92	0.097	0.128
	0.35	0.40	315	135	No	1.1	140	91	83	1.78	3.61
	0.40	0.45	294	126	No	0.9	120	78	71	1.78	3.83
	0.50	0.57	273	117	No	1.3	80	52	46	0.864	1.94
	0.75	0.85	185.5	79.5	No	0.5	80	25	22	1.58	4.37
CEM III (~70% slag)	0.30	0.30	520	-	Yes	4.8	200	78	71	0.245	0.356
	0.35	0.35	460	-	Yes	4.7	200	74	67	0.434	0.615
	0.40	0.40	420	-	Yes	4.3	120	61	55	0.568	0.845
	0.50	0.50	380	-	Yes	4.5	70	46	41	0.993	1.66
	0.75	0.75	255	-	Yes	4.4	90	26	23	2.05	3.16
	0.30	0.30	520	-	No	0.8	200	99	90	0.221	0.281
	0.35	0.35	470	-	No	0.7	200	80	72	0.490	0.653
	0.40	0.40	420	-	No	0.9	125	68	61	0.837	1.14
	0.50	0.50	400	-	No	1.0	65	54	48	1.21	1.61
	0.75	0.75	265	-	No	0.1	100	31	27	3.94	6.89

[1] Eqv. w/c-ratio= water/(cement + 2∗silica + 0.6∗slag). Not applicable for CEM III cement.
[2] SCM – Secondary Cementitious Materials
[3] AEA – Air Entraining Agent
[4] Dry stored cubes tested according to SS 13 72 10 at the age of 28 days
[5] Recalculated to wet stored cubes according to $f_{wet,cube}=0.76*(f_{dry,cube})^{1.04}$
[6] According to the 'Slab test', SS 13 72 44, freeze/thaw started at the age of 31 days

All concrete batches were produced in the autumn of 1996, and a number of 150 mm cubes were cast from each batch. The cubes were demoulded 24 hours after casting, and stored in lime-saturated water for six days. They were then stored in a climate chamber (50 % RH / 20 °C)

for a period of between one and a half and three months. Between eight and twelve days before the specimens were placed at the field test sites, the cubes were cut, resulting in two specimens with the shape of a half 150 mm cube with one cut surface and the rest mould surfaces. After cutting, the specimens were stored in a climate chamber (50 % RH / 20 °C) until placed at the test site. During this second conditioning period, the volume of, and transmission time through, each specimen were measured. Two specimens of each mixture were then placed at each test site.

At the highway environment test site, the specimens were placed in steel frames close to the road, so that they were splashed by the passing traffic. At the marine test site, the specimens were mounted on top of a pontoon, thus exposing them to the saline marine environment but with no direct contact with the sea water, except when splashed over them by storms. The specimens at the test site without salt exposure were placed on top of loading pallets: here, they were exposed only to water from precipitation. At all sites, the specimens were exposed with the cut surface turned upwards.

3. TEST PROCEDURES

In order to be able to detect both internal and external frost damage, the change in volume and ultrasonic pulse transmission time was measured regularly. The first measurement was carried out before placing the specimens at the test sites. The specimens at the highway site have subsequently been measured once a year, and the specimens at the other two sites after two, four and five years.

The volumes of the specimens are calculated from results obtained from measuring the weight of the specimens in water and in air respectively. The ultrasonic pulse transmission time through the specimen is measured as a mean of three measurement positions, where possible, on each specimen.

The following laboratory tests were carried out on each concrete mix in order to determine the concrete characteristics:

Testing the fresh concrete:

- Air content
- Density
- Slump
- Remoulding test

Testing the hardened concrete:

- Compressive strength in accordance with Swedish standard (SS) 13 72 10.
- Salt/frost resistance in accordance with SS 13 72 44 ('the slab test').
- Microscopical determination of the air void system, in principal in accordance with ASTM C 457.

Results from these tests are given partly in Table 2 above, and fully in Reference 4.

4. RESULTS

Figures 1-4 present results from measurements of the volume change after five years of exposure at the three field exposure sites. The reference value is the initial volume before exposure.

Figures 1-3 show the results for concrete produced without entrained air, exposed at the three exposure sites, while Figure 4 shows the results for concrete with entrained air (4-5 %) exposed at the test site in a highway environment. Each point is a mean value of measurements on two specimens.

Figures 5-7 show the relative transmission time after five years' of exposure at the three field exposure sites. The reference value is that of measurements before exposure. Each point is a mean value of up to three measurements on each two test specimens, i.e. a mean value of up to six measurements. For some qualities with w/b-ratio 0.75, no value is presented. This is because damage to the concrete surfaces was so severe that measurements were not possible.

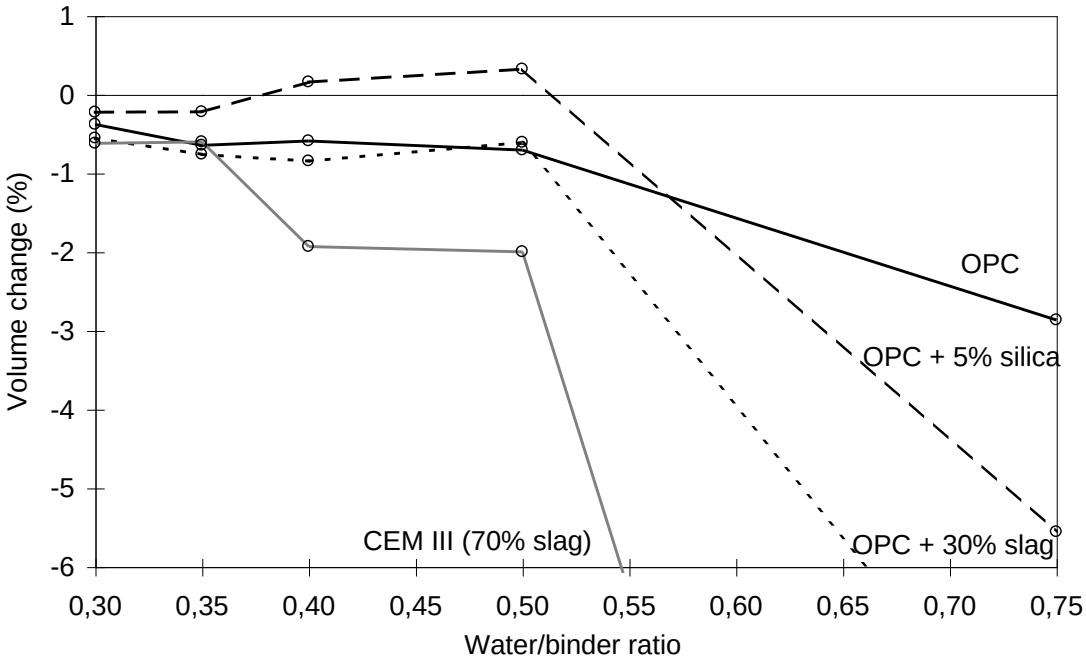

Figure 1 - Volume change after five winter seasons at the highway exposure site (Highway 40). Concrete with different binder combinations and water/binder ratios. No entrained air.

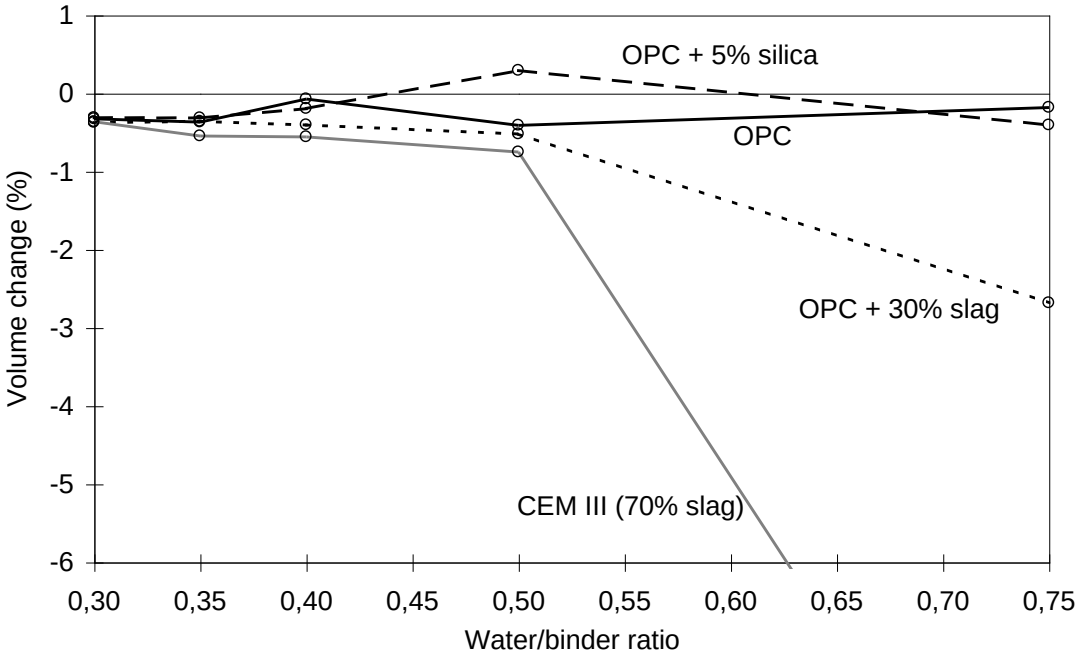

Figure 2 - Volume change after five winter seasons at the marine exposure site (Träslövsläge harbour). Concrete with different binder combinations and water/binder ratios. No entrained air.

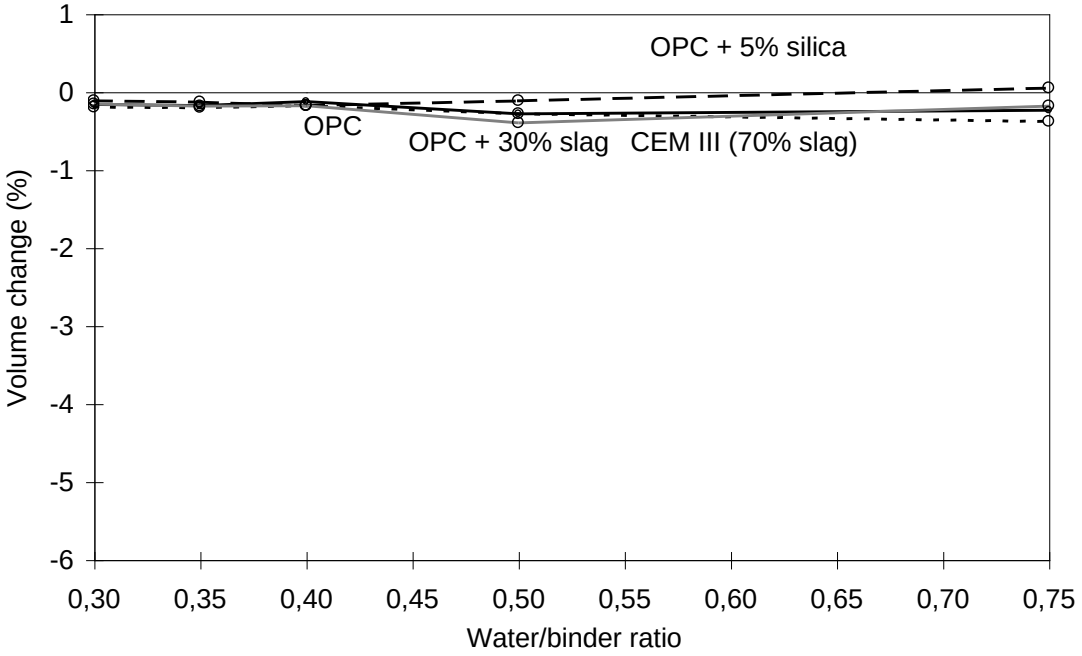

Figure 3 - Volume change after five winter seasons at the no-salt exposure site (SP in Borås). Concrete with different binder combinations and water/binder ratios. No entrained air.

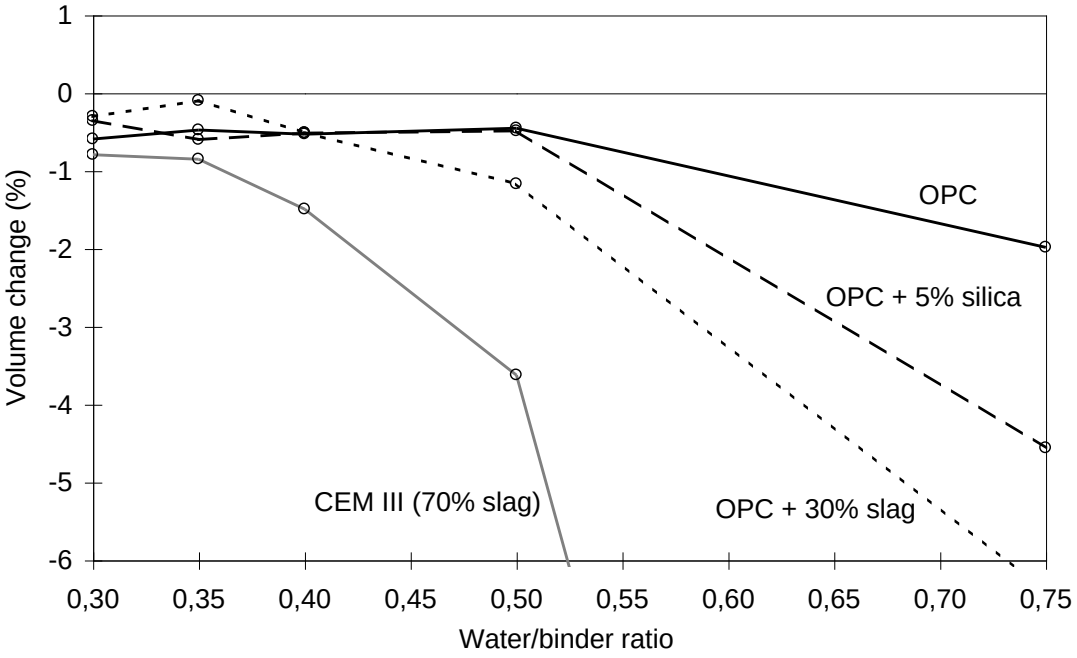

Figure 4 - Volume change after five winter seasons at the highway exposure site (Highway 40). Concrete with different binder combinations and water/binder ratios. With entrained air (4-5 %).

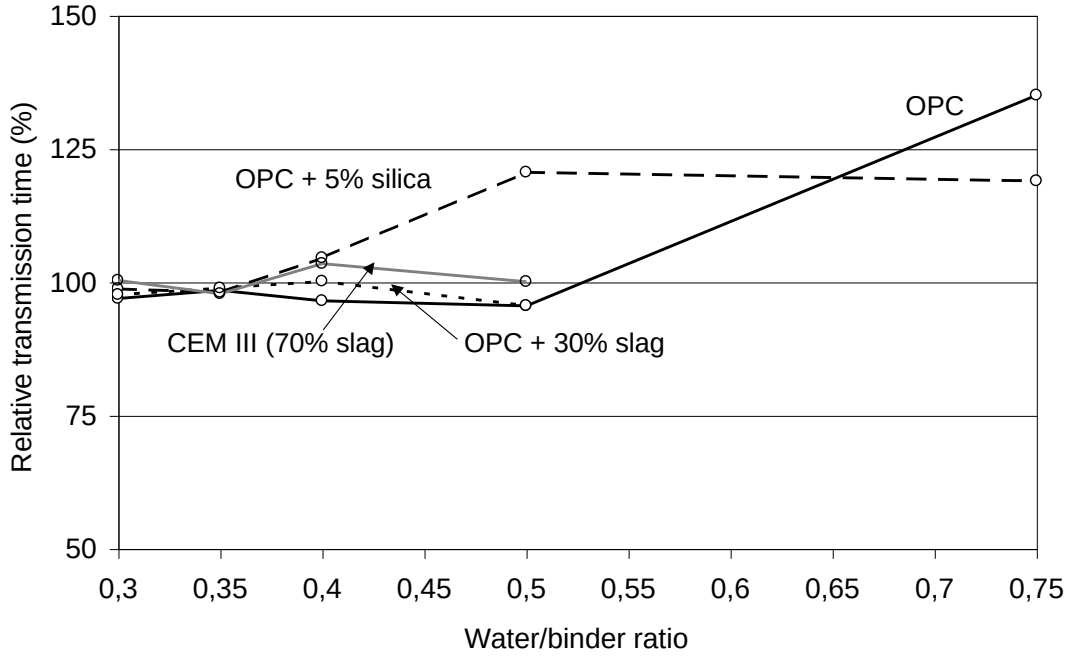

Figure 5 - Relative transmission time after five winter seasons at the highway exposure site (Highway 40). Concrete with different binder combinations and water/binder ratios. No entrained air.

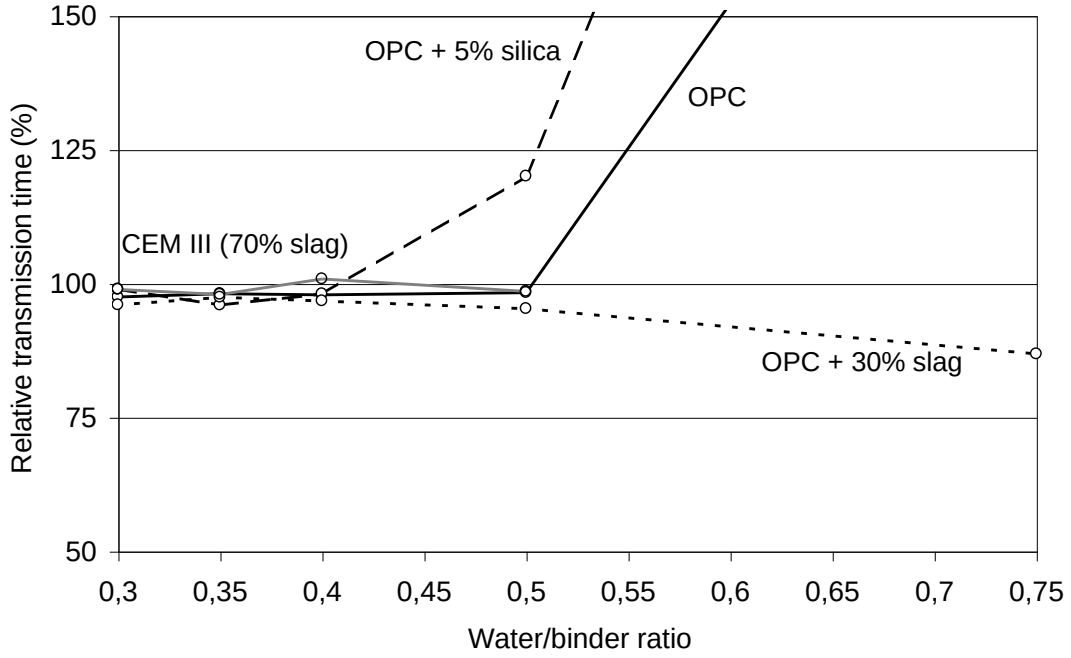

Figure 6 - Relative transmission time after five winter seasons at the marine exposure site (Träslövsläge harbour). Concrete with different binder combinations and water/binder ratios. No entrained air.

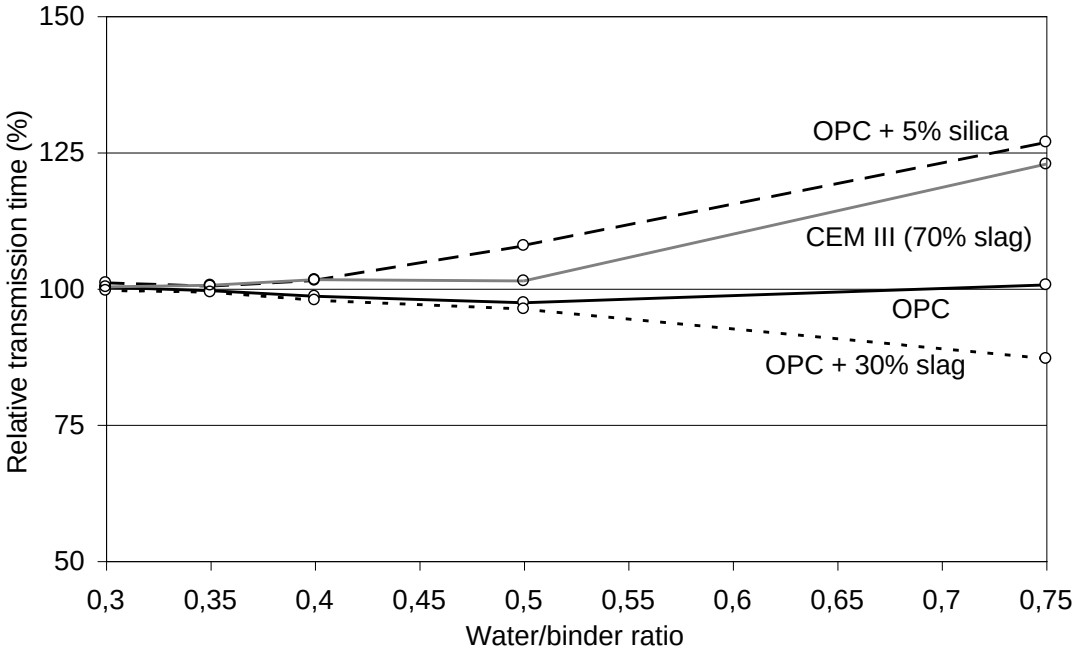

Figure 7 - Relative transmission time after five winter seasons at the no-salt exposure site (SP in Borås). Concrete with different binder combinations and water/binder ratios. No entrained air.

5. DISCUSSION

5.1 External frost damage

Figures 1, 2 and 3 show the external damage in the form of volume change after five winter seasons for different concrete qualities, all without entrained air, exposed in three different climates. Without comparing results from the different concrete qualities, it is clear that the climate has a large influence on the amount of external frost damage, i.e. surface scaling. Concrete exposed in a saline highway environment, Figure 1, shows much more extensive surface scaling than does concrete exposed in a salt-free environment. Concrete exposed in the marine environment shows external damage, but not as severe as concrete exposed in the highway environment, at least for qualities with w/b-ratios of 0.40 and over. These considerable differences in resistance to surface scaling can probably be explained by differences in:

- **Temperature**. The temperature in the marine environment is milder and fluctuates less than the temperature at the highway environment or the salt-free exposure site. However, the air temperature at these two latter sites is about the same.
- **Moisture conditions**. The moisture conditions at the different exposure sites vary significantly. During the winter months, the specimens at the highway site are subjected to a very moist environment, being constantly splashed by passing traffic. The specimens at the SP test site, however, are exposed only to natural precipitation.
- **Salt concentration**. The salt concentration in the water splashed over the samples at the highway site is, at least occasionally, much higher than the salt concentration in the marine environment. At the SP test site there is no exposure to salt.

Some significant differences with regard to surface scaling can be seen when comparing the different concrete qualities. For example, qualities with slag as part of the binder (CEM III and OPC + 30 % slag) show more severe external damage than mixtures with OPC and OPC + 5 % silica concrete, at least for qualities with w/b-ratio of 0.75. This is seen both at the highway and the marine exposure site. Concrete exposed at the salt-free test site, however, shows only small volume changes, irrespective of binder combination. Another significant difference is the increase in volume for some concrete qualities with OPC + 5 % silica as binder and with a w/b-ratio over 0.35. This increase is seen primarily at the highway and marine test sites. An increase in volume is probably caused by internal damage, i.e. micro-cracks: see further discussion below. A limitation of the volume measurements is that the measured volume is a net volume of both a negative and a positive element, in the respective forms of a volume loss due to surface scaling and a possible increase in volume due to internal cracking. Concrete qualities with an apparent volume loss might, therefore, also have a small increase in volume caused by internal cracking without this being observed. It is therefore important to complement volume measurements with other techniques in order to detect possible internal damage, e.g. ultrasonic pulse transmission time measurements.

Figure 4 shows the volume change after five winter seasons for concrete mixtures with entrained air exposed to the saline highway environment. In general, the volume changes for concrete with high water/binder ratios and entrained air are less than for concrete without entrained air (Figure 1). However, this is not valid for concrete qualities with CEM III as the binder. The volume change for qualities with CEM III as the binder and with entrained air is of the same order as (and sometimes even greater than) that for concrete without entrained air (w/b-ratios 0.50 and 0.75). For these qualities, entrained air does not seem to improve the scaling resistance. This

behaviour is confirmed by freeze/thaw testing in the laboratory, see Table 2. For concrete with CEM III as the binder, the air entrained qualities show damage of the same order as for concrete without air. For concrete with other binder types in this investigation, as expected, a significant improvement in scaling resistance is seen for qualities with entrained air compared to qualities without entrained air.

Comparing the results for concrete with and without entrained air after five years of exposure show in general only small differences in volume change for concrete with w/b-ratio 0.5 and below. However, the increases in volume for concrete qualities with OPC + 5 % silica that were observed in samples without entrained air are, as expected, not observed when entrained air is used.

5.2 Internal frost damage

Figures 5, 6 and 7 show the relative transmission time after five years of exposure for different concrete qualities, all without entrained air, exposed in three different climates. A relative transmission time over 100 indicates possible internal damage. Values over about 110 are more certain indications of internal damage. The results presented in Figures 5-7 show that a number of concrete qualities probably have internal damage and that there does not seem to be any significant difference between the different exposure climates. Table 3 shows the concrete qualities with possible internal damage at each test site.

Table 3 - Concrete qualities with potential internal damage at the three test sites. Detected by ultrasonic pulse transmission time.

Concrete quality	Highway	Marine	No salt exposure
OPC no air w/b 0.75	Damaged	Damaged	No D. indication
OPC+5 % silica no air w/b 0.75	Damaged	Damaged	Damaged
OPC+5 % silica no air w/b 0.50	Damaged	Damaged	Damaged
OPC+5 % silica no air w/b 0.40	Damaged	No D. indication	No D. indication
CEM III (70 % slag) no air w/b 0.75	Not measured	Not measured	Damaged

Combining the results from volume measurements with the transmission time measurements gives clear indications of internal damage for the concrete qualities with OPC + 5 % silica as binder shown in Table 3. Both an increase in volume and an increase in transmission time clearly indicate internal damage, probably micro-cracking. The surfaces of the qualities that show increased transmission time but no detectable increase in volume are too severely damaged to permit the detection of an increase in volume due to internal cracking. Microscopic techniques, such as analysis of polished sections or thin sections, could be used for finding further evidence of internal damage.

Polished sections were cut from each concrete quality listed in Table 3 to confirm and show possible internal cracking. The sections confirmed that the qualities judged as having internal damage when tested with ultrasonic pulse transmission time all showed internal cracking. Figure 8 show pictures of polished samples impregnated with epoxy resin and fluorescent dye for the three qualities with OPC + 5 % silica as binder listed in Table 3, exposed at the highway test site. The pictures show internal cracking in all three qualities, which increases in severity with increasing w/b-ratio.

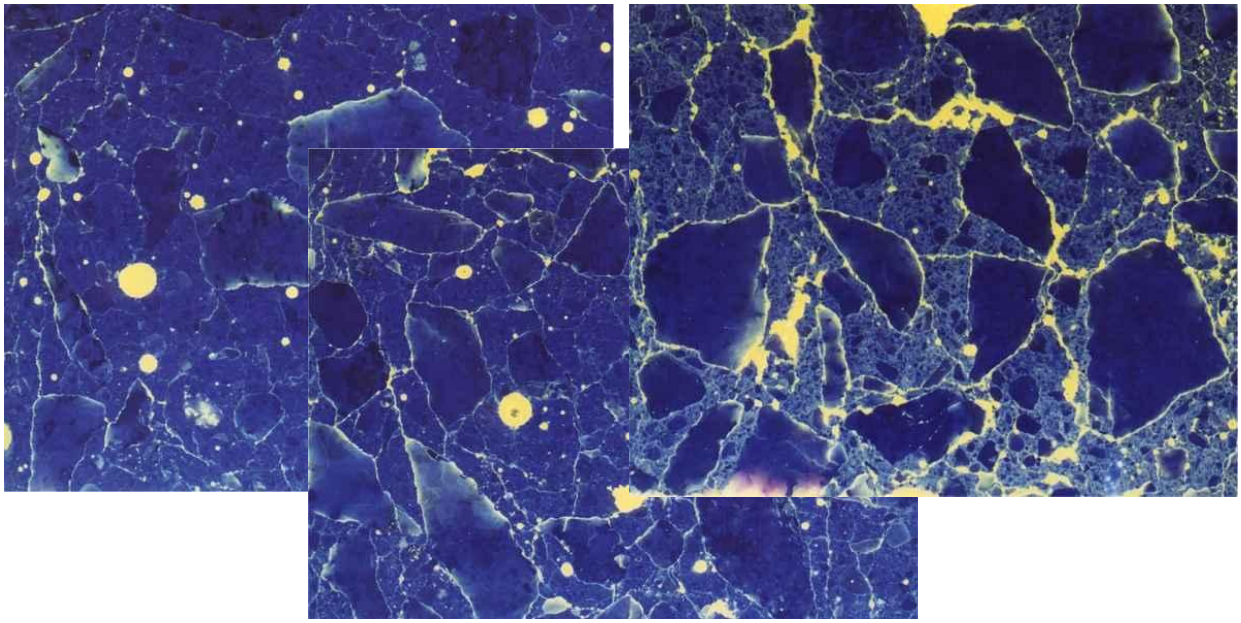

Figure 8 - Pictures of polished samples impregnated with epoxy resin and fluorescent dye of three concrete qualities exposed for five years at the highway exposure site. All with OPC + 5 % silica as binder and no air. From left: w/b 0.40; w/b 0.50; w/b 0.75.

The results from this investigation indicate that the concrete qualities with OPC + 5 % silica as binder and without entrained air seem more susceptible to internal frost damage than the other concrete qualities.

For the concrete quality with CEM III as binder in Table 3 it was not possible to measure the transmission time because of excessive surface damage. Microscopic analyses, however, show that the amount of internal damage, if any, is limited, see Figure 9. From the results discussed above, it seems as if the concrete qualities containing slag as part of the binder and without entrained air in this investigation are somewhat more resistant to internal damage than at least the concrete qualities with OPC + 5 % silica as binder. On the other hand, the concrete qualities with large amounts of slag as part of the binder seem to be more susceptible to scaling.

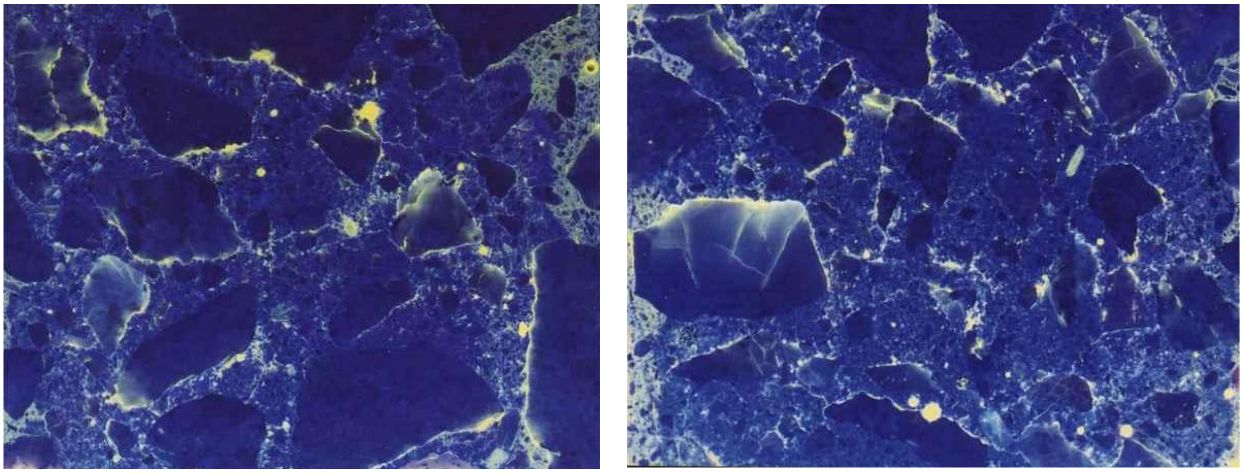

Figure 9 - Pictures of polished samples, impregnated with epoxy glue and fluorescent dye, of two concrete qualities exposed for five years at the highway and the marine exposure sites. From left: CEM III, no air and w/b 0.75, highway climate; CEM III, no air and w/b 0.75, marine climate.

A certain degree of 'healing' of specimens exposed at the highway site has been noted during the yearly measurements. Figure 10 shows results from yearly measurements of ultrasonic pulse transmission time on the three damaged concrete qualities with OPC + 5 % silica as binder.

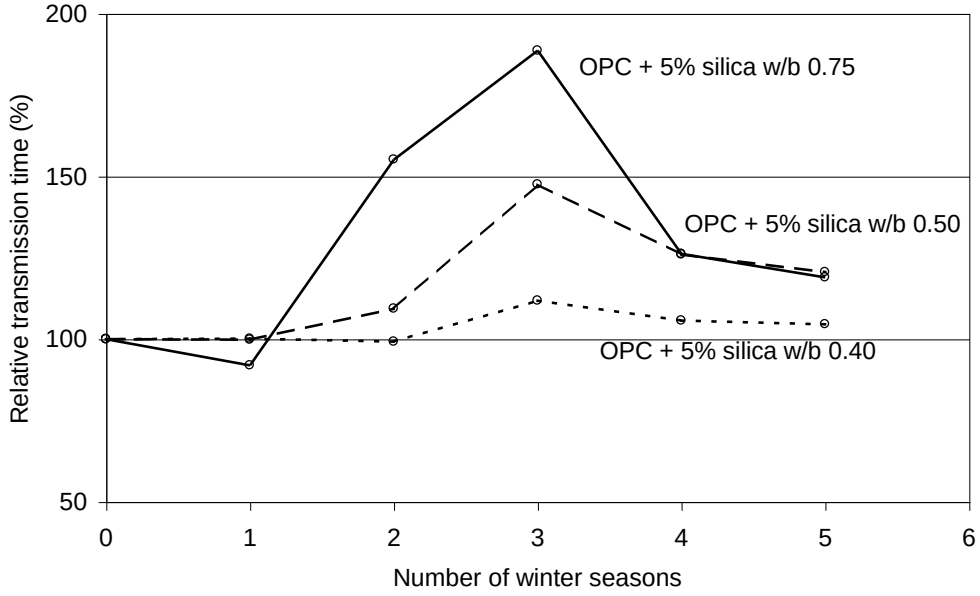

Figure 10 - Relative transmission time during five years of exposure at the highway exposure site.

The results in Figure 10 indicate a 'healing' effect after the third year, leading to reduced relative transmission time. Even though the reduction in relative transmission time or 'healing' seem substantial, the reduction can be caused by relatively limited healing. Only a few healing points are needed for an ultrasonic pulse to find a faster, shorter way through damaged material: see Figure 11. The healing can be explained by reaction between unhydrated cement and moisture transported in to the cracks, forming barriers of hydration products in the cracks and enabling the ultrasonic pulse to find a shorter way through the material.

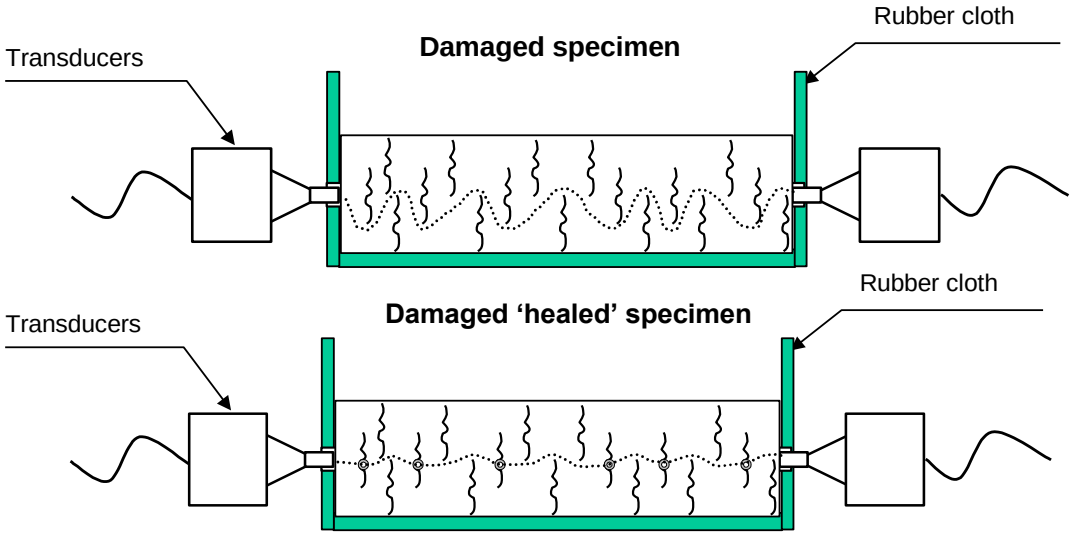

Figure 11 - Sketches of an ultrasonic pulse during transmission time measurements in a damaged specimen (top) and a specimen that has 'healed' (bottom).

This type of healing, where the hydration products form local barriers between cracks, gives no substantial healing in form of increased strength, durability or resistance to moisture or chlorides. Most of the network of micro cracks will probably still be open to an infiltration of moisture and chlorides, even though local healing creates a short cut for the ultrasonic pulse, resulting in a significantly shorter transmission time. This healing effect makes it hazardous to draw conclusions from single or even regular (if at long intervals) measurements of transmission time. A single measurement, after five year, on the concrete qualities shown in Figure 10 would lead to the conclusion that there might be some internal damage but not particularly severe. Evaluating results from yearly measurements and microscopic analysis (Figure 8) gives an indication of more severely damaged concrete. This is important knowledge when evaluating results not only from measurements in the laboratory but especially also when evaluating results from measurements in the field. From practical and economic points of view, it might be difficult to make measurements on building structures in the field on a more regular basis.

From the results described above, it can be noted that concrete with OPC or OPC + 5 % silica, with entrained air and a water/binder ratio of 0.50 or lower, seems to be salt/frost resistant in an aggressive highway environment, at least after five years' of exposure. Concrete qualities containing large amounts of slag as binder, however, seem to be less resistant to external salt/frost damage than concrete with OPC or OPC with some silica, at least when exposed to aggressive climates such as the highway or marine climate. These results are in agreement with results from an extensive field exposure investigation presented in [6]. In that investigation, a large number of concrete qualities with different amounts of slag and fly ash in the binder were exposed to the marine climate at the Treat Island exposure site, Canada. Results from that investigation clearly show that salt/frost resistance decreases with increasing amounts of slag as part of the binder; a result that is confirmed by the present investigation. As in the present investigation, the investigation at Treat Island also showed the positive effect of low water/binder ratio on the salt/frost resistance of concrete. The negative effects of high slag contents in the binder on the salt/frost resistance of concrete have been reported by several researchers, see [7, 8, 9, 10]. One probable explanation for this negative effect is the coarsening of the pore structure found in the carbonated skin of concrete containing slag [7, 9, 11]. Another probable explanation, presented in [9], is the existence of metastable carbonates in the carbonated zone of concrete rich in slag.

5.3 Correlation between laboratory and field tests

When testing the durability in the laboratory, e.g. salt/frost resistance, results are wanted that are relevant to durability in the actual field conditions. In the present investigation, each concrete quality was tested in the laboratory at the prescribed age of 28 days in accordance with the Swedish Standard for salt/frost resistance, SS 13 72 44 (the 'slab test'). Comparing the laboratory results with results from the field exposure site at SP's site (no salt exposure) is not relevant, since salt/frost resistant concrete are not prescribed in this climate. Concrete exposed at the marine and highway test sites is, however well suited for 'calibration' of the laboratory test method. Since the climate at the highway has proven to be most aggressive with regard to salt/frost resistance, the laboratory results are compared with results from this test site.

Figure 12 shows results from the laboratory tests and the volume change after five years of highway exposure. The diagram shows the scaling (kg/m²) after 56 freeze/thaw cycles as a function of the volume loss (%) after five years' highway exposure. The acceptance criterion in the laboratory test is 1 kg/m^2 (illustrated by a horizontal line). An acceptance criterion of 1.5 vol-

ume % (shown by the vertical line) after five years' exposure has been chosen for the field exposure specimens, corresponding to scaling of approximately 0.6 kg/m^2. Filled symbols represent concrete without entrained air. Symbols with a white centre represent concrete with entrained air. Enlarged symbols represent qualities with internal damage.

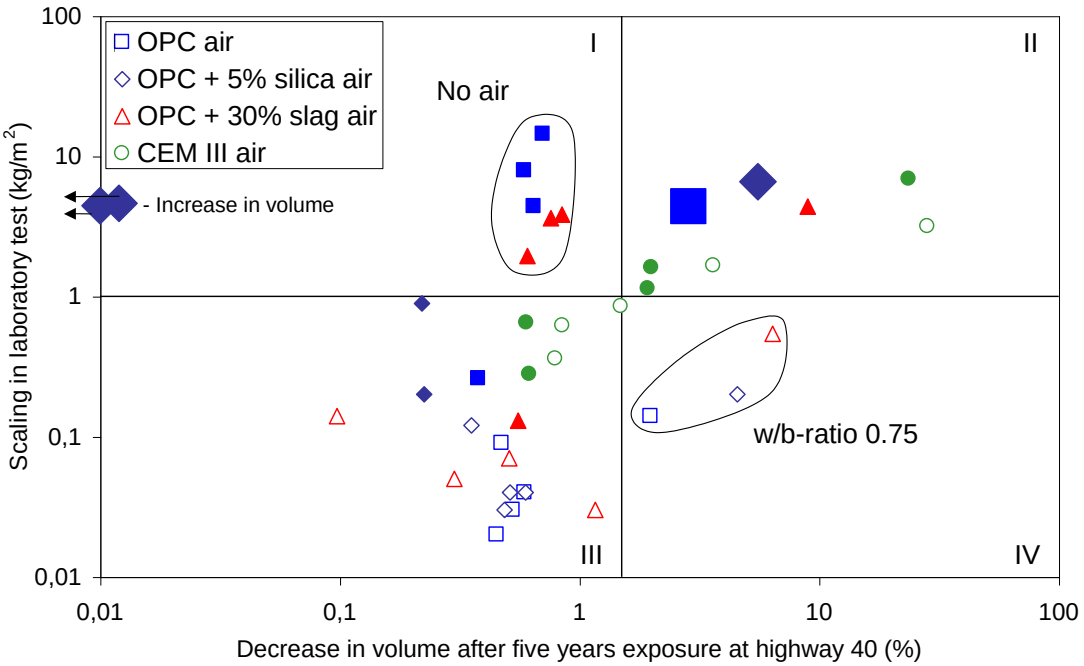

Figure 12 - Scaling resistance (tested in the laboratory) as a function of the decrease in volume for specimens exposed in the highway environment for five winter seasons. Filled symbols represent concrete without entrained air. Symbols with a white centre represent concrete with entrained air. Large symbols represent internal damage.

From the results presented in Figure 12, it can be seen that only three qualities fall into the IV quadrant, which is the worst case, and means that they are accepted by the test method, but fail in field exposure. These are air entrained qualities, however, with high water/binder ratios (0.75). The standard test method is primarily intended to be used for bridge concrete, with entrained air and with a w/b-ratio below 0.5.

Most qualities falls into quadrants II or III, which means that the test method and 'reality' correspond. Some concrete qualities fall into quadrant I, which means that the test method rejects them. However, as the concrete in quadrant I show only limited damage in the field, the test method results are on the safe side. None of these qualities has any entrained air, which makes them especially susceptible to frost damage. During the first five years, the climate has not been aggressive enough significantly to damage these qualities. However, one winter season with a more aggressive climate might cause internal damage as well as scaling on these qualities without entrained air, moving them into quadrant II. Two concrete qualities show an increase in volume and an increased transmission time, indicating internal frost damage. These qualities also fail the acceptance criterion when tested in the laboratory.

One explanation for the limited scaling in the field for the concrete qualities in quadrant I might be a positive effect of ageing. In a field investigation reported in [12], it was found that concrete aged and exposed in a marine climate showed better scaling resistance when tested in the labo-

ratory after aging than did virgin concrete. This increase in scaling resistance was especially apparent for concrete without entrained air, as was also found in this investigation. One effect of ageing that markedly improves the scaling resistance for OPC concrete is carbonation see [10].

On the whole, the results for concrete with w/b-ratio equal to or below 0.5 and with entrained air, shown in Figure 12, indicate that the slab test classifies these concrete qualities as could be expected. This is true for all binder combinations tested.

The results presented here are valid only for the materials, e.g. cement and binder types, used in this investigation. Other materials may lead to different results.

6. CONCLUSIONS

The following conclusions can be drawn after five years' exposure at the field exposure sites in a highway environment, a marine environment and a salt-free environment:

- There are substantial differences in external frost damage, depending on the environment. The most extensive external frost damage is observed on concrete specimens exposed in the highway environment. Concrete exposed in the salt-free environment shows only small changes in volume after five winter seasons.

- For all concrete qualities, scaling takes place only when exposed to salt. Internal damage, however, is observed on concrete qualities exposed at all three test sites, even when no salt is present.

- Concrete with OPC or OPC + 5 % silica as binder, with entrained air and a water/binder ratio of 0.5 or below, has good resistance to internal and external damage. Concrete with CEM III, however, suffers from severe scaling even with w/b-ratio below 0.5 and with entrained air.

- Internal damage is observed only for concrete qualities without entrained air and, furthermore, in most cases for concrete qualities with high water/binder ratios. However, for concrete qualities with OPC + 5 % silica as binder, internal damage is found at lower w/b-ratios, down to w/b 0.4.

- A 'healing' effect is observed on specimens with internal damage (cracking), making results from ultrasonic transmission time measurements hazardous to interpret. Interpreting results from single measurements can therefore lead to incorrect conclusions.

- Comparing results from laboratory testing in accordance with SS 13 72 44 (the 'slab test'), with results after five years of exposure at the field exposure sites, shows that the laboratory standard classifies most concrete qualities correctly.

7. ACKNOWLEDGEMENTS

This project is financially supported by FORMAS, the Development Fund of the Swedish Construction Industry and the cement producer Cementa AB.

REFERENCES

1. SS 13 72 44, 'Concrete testing- Hardened concrete- Frost resistance', Swedish Standards Institution (SIS, Stockholm), 3rd edition, 1995.
2. SFS 5448, 'Concrete, Durability, Freezing dilation', Finnish Standardisation Association (SFS), Helsinki, 1988.
3. Fagerlund, G., 'The critical degree of saturation method of assessing the freeze/thaw resistance of concrete', *Materials and Structures*, Vol.10, No.51, pp.217-229, 1977.
4. Utgenannt, P., 'The effect of binder on the frost resistance of concrete - Test specimens produced in 1996 - Material and production data and results from life testing in the laboratory', Swedish National Testing and Research Institute, BTB report no 1, 1997, (in Swedish).
5. Malmström, K., 'Cementsortens inverkan på betongs frostbeständighet' [The effect of cement type on the frost resistance of concrete], Swedish National Testing and Research Institute, Rapport 1990:07, 1990, (in Swedish).
6. Bremner, T.W. et.al., 'Role of supplementary cementing materials in concrete for the marine environment', in 'Durability of concrete – Aspects of admixtures and industrial by-products', Proceedings from the 2nd International seminar on - Some aspects of admixtures and industrial by-products, (Swedish council for building research, Gothenburg), 1989, pp. 23-32.
7. Gunter, M. et.al., 'Effect of curing and type of cement on the resistance of concrete to freezing in deicing salt solutions', ACI, SP 100, vol. 1, 1987, pp. 877-899.
8. Vesikari, E., 'The effect of ageing on the durability of concrete including by-products', in 'Durable concrete with industrial by-products', Proceedings from VTT Nordic research symposium 89, (Technical research center of Finland, Espoo), 1988, pp. 104-112.
9. Stark, J. et.al., 'Freeze-thaw and freeze-deicing salt resistance of concretes containing cement rich in granulated blast furnace slag', *ACI Materials Journal*, Vol. 94, No.1, 1997, pp. 47-55.
10. Utgenannt, P., 'Influence of carbonation on the scaling resistance of OPC concrete', Proceedings from the RILEM Workshop on Frost Damage in Concrete, Minneapolis, USA, 1999.
11. Matala, S., 'Effects of carbonation on the pore structure of granulated blast furnace slag concrete', Helsinki University of Technology, Faculty of Civil Engineering and Surveying, Concrete Technology, Report 6, Espoo, 1995.
12. Petersson, P.-E., 'Scaling resistance of concrete – Field exposure tests', Swedish National Testing and Research Institute, SP-report 1995:73, Borås, Sweden, 1995, (in Swedish).

Results of the Laboratory Freeze-Thaw Tests and their Transferability to Practical Conditions

Christoph Müller
Dr.-Ing.
Verein Deutscher Zementwerke
Forschungsinstitut der Deutschen Zementindustrie
Tannenstrasse 2, DE-40476 Düsseldorf, Germany
E-Mail: mc@vdz-online.de

ABSTRACT

When freeze-thaw tests and freeze-thaw tests with de-icing salt were carried out on concrete, the situation in the specialist bodies of the German Committee for Structural Concrete (DAfStb) regarding publication of the state-of-the-art report "Transferability of laboratory freeze-thaw tests to practical conditions" was as follows (quotation from the preliminary remarks to the state-of-the-art report): "It is known that concrete that is reliable under real-life conditions can fail in laboratory tests. The reverse case is practically unknown. This would suggest that the laboratory tests are more stringent than the Central European climate. But how much more stringent – or are there environmental conditions that justify such stringent tests?" The facts presented in the report showed that the information that had been available was not sufficient to make a final judgment on the transferability of laboratory freeze-thaw tests to practical conditions. More research appeared necessary. Because of this, the DAfStb initiated a research priority in 2001. About nine years and eight research projects later it would be presumptuous to say that all the questions posed at the beginning can be answered in full. However, the results of the projects and their central evaluation have produced a wealth of data and have provided a lot of additional knowledge that allows an increasingly better interpretation of the laboratory results. The article provides a summary of the main results of the collaborative research project. The text and pictures were taken from [1, 2, 3]. The article is rounded off with experiences from laboratory freeze-thaw tests in the Research Institute of the Cement Industry in Düsseldorf, Germany (FIZ) from [4, 5].

Key words: blended cements, degree of saturation, freeze-thaw tests with and without de-icing salts, measurements on structures, moisture, temperature

1 INTRODUCTION

According to DIN EN 206-1, Section 5.3 "Requirements in relation to exposure classes" [6], concrete's resistance to environmental effects is deemed to be proven if defined concrete properties and limit values for the composition are complied with (prescriptive concept). Alternatively, the requirements for concrete may be derived on the basis of performance-related procedures. This method is, for example, especially important if the performance of concrete is to be determined with the use of new concrete constituents (such as new cements). If performance is to be assessed, methods should be used that reflect the actual conditions based on acknowledged and tested examinations and which include accepted performance criteria. Basically, uncertainties exist in all test methods as regards the extent to which the test results achieved in the laboratory actually reflect the behaviour of the concrete under real-life conditions. One of the reasons for this is that there can be considerable differences between stress in nature and in the freeze-thaw test methods. Apart from the amount of moisture in the concrete, the cooling and thawing rates, the maximum and minimum temperatures and the time the stress is applied (test age or maturity) all play a part too. To close these knowledge gaps, the German Committee for Structural Concrete (DAfStb) formed the working group on "Transferability of laboratory freeze-thaw tests to practical conditions". The research projects handled within the scope of this working group included studies at Aachen University (Prof. Brameshuber), Leipzig University (Prof. König/Dehn), Hannover University (Prof. Lohaus), Stuttgart University (Prof. Reinhardt), Technical University of Munich (Prof. Schießl), Duisburg-Essen University (Prof. Setzer), Bauhaus University Weimar (Prof. Stark) and Karlsruhe University (Prof. Müller).

Table 1 shows how the collaborative research project was split into four sub-projects. In sub-projects 1 and 2 test pieces were produced in the laboratory and their behaviour under freeze-thaw and freeze-thaw with de-icing salt conditions was investigated. The CDF and CIF test methods [7, 8, 9] were used. Parallel to this, test pieces were stored outdoors for several years and checked periodically. Forty five different concrete compositions were used; the compositions complied with the requirements of the exposure classes of DIN EN 206-1/DIN 1045-2 [6, 10] and were also outside the limit values required for the exposure classes. The storage locations were distributed throughout Germany (Farchant, Meschede, Weimar, Stuttgart, Hilpoltstein) and concrete samples were also stored in Sweden (Boras). The object of sub-project 3 was to develop a test method to simulate stress according to exposure class XF2. This involved modifying the CDF method.

Table 1 - Overview and contents of sub-projects of the DAfStb-Working Group on "Transferability of laboratory freeze-thaw tests to practical conditions" [3]

Sub-project 1 Frost resistance	Sub-project 2 Frost de-icer resistance	Sub-project 3 Development of test methods	Sub-project 4 Structural investigations
- Production of test pieces - Testing freeze-thaw resistance in the laboratory (CIF) - Outdoor storage of the test pieces - Measuring the ultrasonic transit time, moisture content and temperature during storage - Testing, documenting and assessing the condition of the stored test pieces	- Production of test pieces - Testing frost de-icer resistance in the laboratory (CDF) - Outdoor storage of the test pieces - Measuring the ultrasonic transit time, the chloride concentration, moisture content and temperature during storage - Testing, documenting and assessing the condition of the stored test pieces	- Modification of the existing test method (CDF) in consideration of: - Time-dependent moisture content, test age - Temperature profile, concentration of the test solution	- Visual assessment of the structural condition - Measuring the chloride concentration, the moisture content and the temperature of the structure - Drill core extraction to determine the depth of carbonation, bulk density, compressive strength, water absorption, pore structure, air void parameters - Freeze-thaw tests and/or freeze-thaw tests with de-icing salt on the drill cores (CDF, CIF)

In sub-project 4 various structures (sewage treatment plant, bridges, sluices, tunnels, quay walls, motorway) were investigated and monitored over several years with technical measuring equipment. If the structures were new, the production conditions were documented during the construction period and test pieces were also manufactured from the concrete during this period to determine the concrete-technological parameters in the laboratory. Drill cores were extracted during the subsequent monitoring period and from existing structures. The focuses of the investigations were to track the conditions of the structures and to determine the properties and structural parameters of the concretes. Another aim was to acquire data that would provide information about the actual stress that the structures are subjected to during the frost period.

2 THERMAL STRESS

The aim was to discover the extent to which the thermal stress in the laboratory test corresponds to real-life conditions. Investigations in sub-project 4 of the collaborative research project regarding real-life thermal stress showed that on frosty days (T_{min}< 0 °C, T_{max}> 0 °C) the maximum temperature range can be 20 K (from -10 °C to +10 °C). The frequency of such events is given as <5 % in [11]. Hence, compared to extreme real-life conditions on frosty days, the temperature range in the test method, which is -20 °C to +20 °C (ΔT 40 K), is about twice as high. The cooling and thawing rate of the test method is 10 K/h. This value can be exceeded in real life, especially on hydraulic engineering structures; although it must be said that such extreme

values are rare. The most frequent cooling and thawing rates are about an order of magnitude lower (1 to 3 K/h). Another parameter is the minimum temperature. On icy days (T_{max}< 0 °C) the temperature can fall to below -20 °C. Consequently, the temperatures in the test method cover real-life conditions and also have an accelerating effect, as there is a very low frequency of extreme temperature ranges and icy days with -20 °C and high rates of temperature change in winter. Hence, several winters are compressed (time lapse).

3 MOISTURE IN STRUCTURES

As opposed to the temperature profile in structural components, which is relatively easy to measure, determining the depth-related moisture content of concrete components remains a challenge for measuring technology. Accordingly, it should be stressed that within the scope of the collaborative research project, it was possible to provide extensive data material for many different structures with the studies by Brameshuber et al. [12–17]. Moisture measurements with the multi-ring electrodes (MRE) use to start at a depth of 7 mm below the surface. Consequently, there is currently no data available as regards the moisture content in the edge section from 0 to 6 mm. To assess the moisture condition of the concrete edge section in case of freeze-thaw attack, it would be desirable if future investigations of the edge section were possible in which more results could be obtained for the moisture content, for example, by continuous measurement at depths of 1 mm, 3 mm and 5 mm.

From a large number of measurements Guse and Müller [3] developed a schematic presentation of the seasonal changes in the degree of saturation in the edge section at a depth of 7 mm below the surface for components under the conditions of the four exposure classes (Figure 1). It can be seen in this figure that the seasonal fluctuations in exposure classes XF1 and XF2 are much more pronounced than in exposure classes XF3 and XF4. High saturation degrees occur in exposure classes XF1 and XF2 as rare peaks, which are generally followed by a drying phase. In the deeper edge section of 8 to 30 mm the effect of seasonal weather on the moisture level weakens considerably (see Figure 2) and is hardly detectable at all at a depth of approx. 30 mm below the surface. Generally, in exposure classes XF1 and XF2 from a depth of about 30 mm a largely even moisture level was measured, which is a lot lower than under the conditions of exposure classes XF3 or XF4.

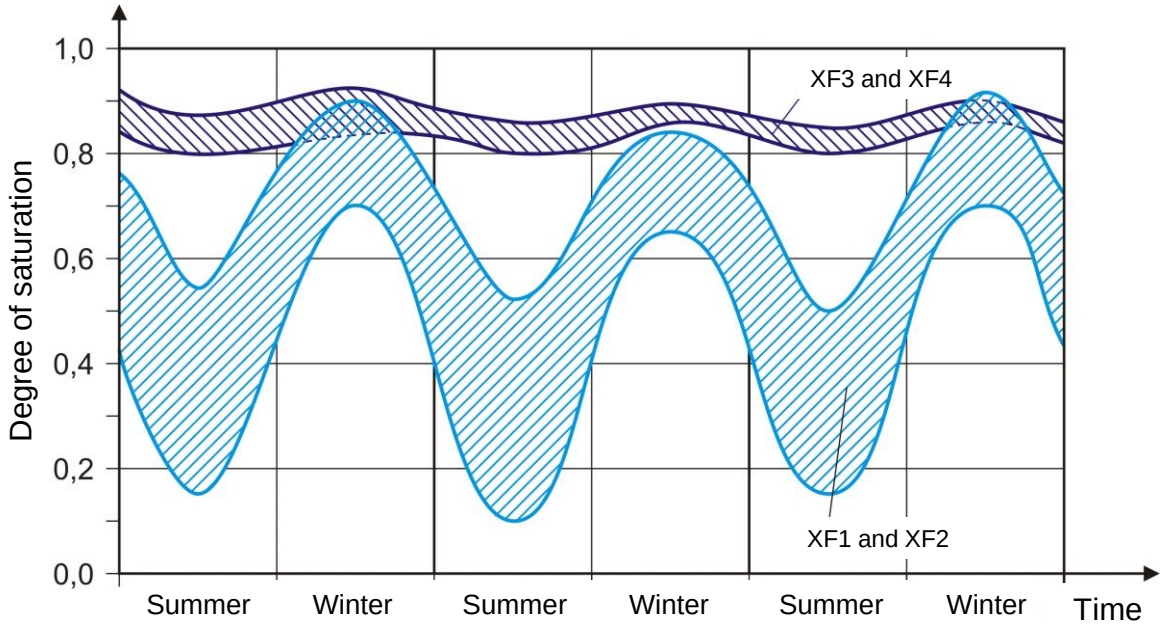

Figure 1 - Schematic representation of the seasonal fluctuations of the degree of saturation (moisture content) of investigated concrete elements without air entraining at a depth of 7 mm below the surface. Degree of saturation: proportion of the water-filled pore volume of concrete in relation to water-filled pore volume of concrete under a pressure of 15 MPa [3]

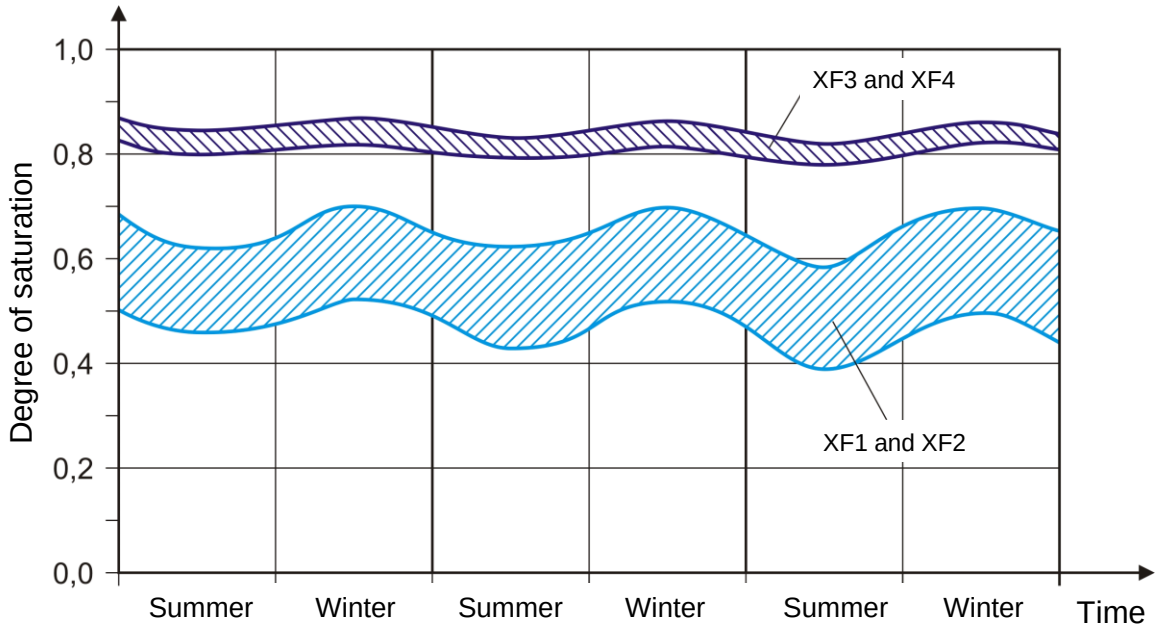

Figure 2 - Schematic representation of the seasonal fluctuations of the degree of saturation (moisture content) of investigated concrete elements without air entraining at a depth of 8 mm to 30 mm below the surface [3]

In the case of building elements in constant or periodical contact with water in exposure classes XF3 and XF4, such as sluices and sedimentation tanks, the degree of saturation in the edge section (depth of 7 mm) in the area between high and low water was largely constant and usually

corresponded to the value that was determined in the water absorption test on the respective concrete in the laboratory at atmospheric pressure, as is shown, for example, in Figure 4. In the edge section of this building element there is little change in moisture content from 8 to 30 mm and there is also practically no fluctuation (see Figure 1 and Figure 2).

As a comparison with the schematic presentations in Figures 1 and 2, Figures 3 and 4 show the results of moisture measurements in a wall of Hohenwarthe Sluice, in Germany. Figure 3 shows the fluctuations in saturation degrees due to weathering in the wall above the high water level – exposure class XF1 (no operationally-related water contact with the concrete surface). At measured depths of 17 mm and 22 mm there were pronounced fluctuations, similar to those shown for XF1 in Figure 1. In the deeper areas (42 mm and 87 mm) the degree of saturation is largely constant, as shown for XF1 in Figure 2.

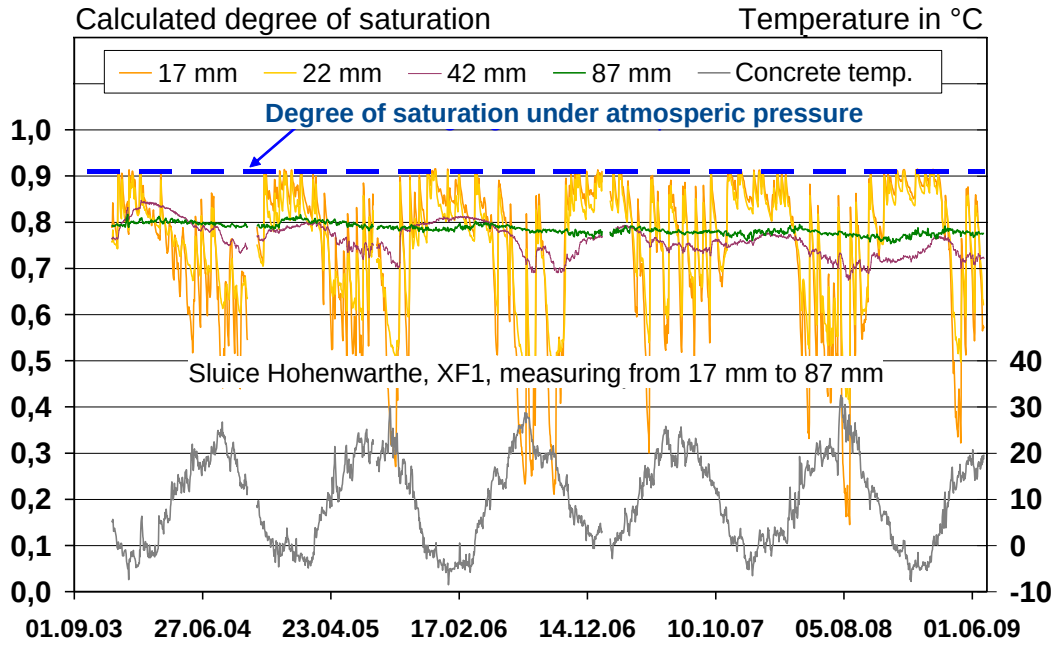

Figure 3 - Schematic representation of the seasonal fluctuations of the degree of saturation (moisture content) from measurements approximately 0.25 m above the upper level in Hohenwarthe sluice, exposure class XF1, measuring from 17 mm to 87 mm [1]

The wall area of the sluice between the low and high water levels is classified in exposure class XF3. For the measuring point roughly 0.25 m below the high water level, Figure 4 shows almost constant water saturation of the concrete for all measurement depths during the measurement period, as shown schematically for XF3 in Figures 1 and 2. The degree of saturation did not exceed the value that the concrete reached in the laboratory test to determine water absorption. The sharp drop in the degree of saturation in September and October 2005 can be attributed to the sluice being shut down. Based on the results of the measurements, it can be seen that the maximum moisture level or degree of saturation in the edge section of the structures that were investigated did not exceed the value determined in capillary suction during the preliminary storage for the CDF and CIF tests. A continuous increase in saturation above this level, such as occurs with freeze-thaw attack during the CDF and CIF laboratory experiments was not observed on the structures during a winter.

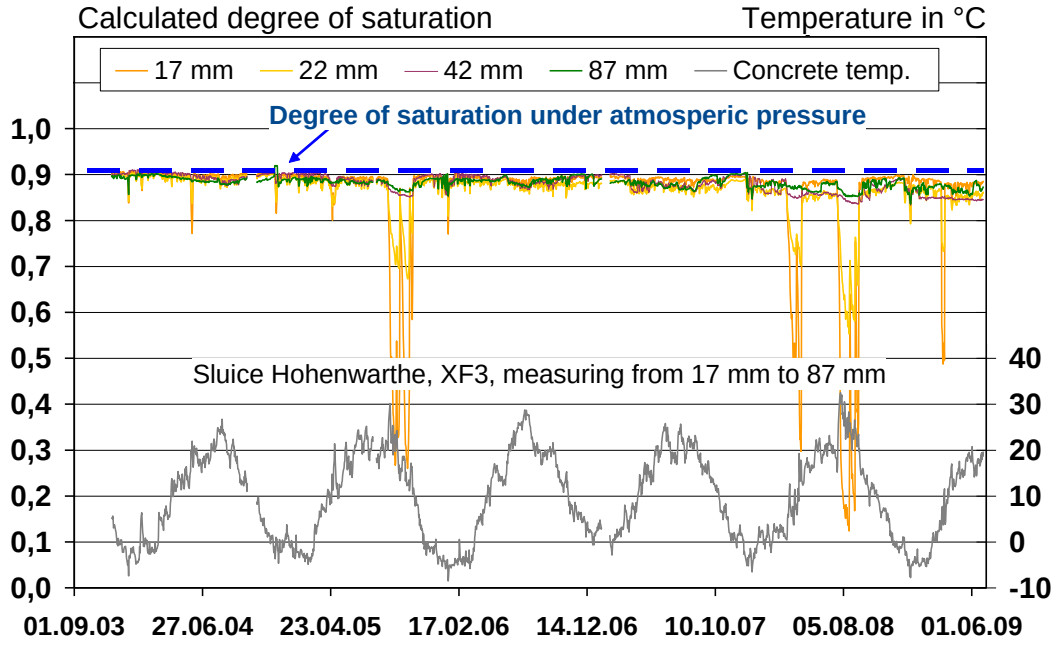

Figure 4 - Schematic representation of the seasonal fluctuations of the degree of saturation (moisture content) from measurements approximately 0.25 m below the upper level in Hohenwarthe sluice, exposure class XF3, measuring from 17 mm to 87 mm [1]

In view of the definition of the moisture levels for the exposure classes in DIN EN 206-1/DIN 1045-2, according to which in exposure classes XF1 and XF2 you could expect "moderate water saturation" and in exposure classes XF3 and XF4 "high water saturation", it can be derived from the investigations that, on the whole, this characterises only the lower moisture level of a structure in exposure classes XF1 and XF2 compared to structures in exposure classes XF3 and XF4. As opposed to XF3 and XF4, in exposure classes XF1 and XF2 the moisture level of the concrete edge section is subject to pronounced fluctuation and in all exposure classes can reach the value that is determined with capillary water absorption at atmospheric pressure in the laboratory.

Consequently, when freeze-thaw attack on structures is being assessed, it should be assumed that a high degree of saturation may occur in the edge section generally regardless of the exposure class. However, the frequency depends on the weather and use and occurs extremely rarely, if at all, in exposure classes XF1 and XF2, and, as opposed to XF3 and XF4, only in the direct edge area. Consequently, the service life of a specific concrete composition will be considerably longer under the conditions of exposure classes XF1 or XF2 than under the conditions of exposure classes XF3 or XF4.

4 RESISTANCE OF CONCRETE UNDER FREEZE-THAW AND FREEZE-THAW WITH DE-ICING SALT CONDITIONS USING DIFFERENT CEMENTS

4.1 German regulations

The current concrete standards DIN EN 206-1 and DIN 1045-2 contain the application regulations for standardized common cements in relation to exposure classes. When these standards

were introduced, application restrictions applied to some cements – based mainly on the lack of practical experience with these cements in Germany. In these cases the proof of suitability for use in specific exposure classes was provided by a national technical approval from the German Institute for Building Technology (DIBt).

Currently, the following cement types may be used in all exposure classes according to the concrete standard in Germany:

- Portland cement CEM I
- Portland-slag cements CEM II/A-S and CEM II/B-S
- Portland-burnt shale cements CEM II/A-T and CEM II/B-T
- Portland-limestone cements CEM II/A-LL
- Portland-fly ash cements CEM II/A-V and CEM II/B-V
- Portland-composite cements CEM II/A-M with other main constituents S, LL, T, D and V
- Portland-composite cements CEM II/B-M with national technical approval for its application
- Blastfurnace cements CEM III/A [1]

Therefore, the listed cement types with the named exception can be used without restriction to produce concrete with a high resistance to freeze-thaw and freeze-thaw with de-icing salt; in other words, they may be used in concrete for exposure classes XF1, XF2, XF3 and XF4.

4.2 Experiences with freeze-thaw tests using different cements

With the correct composition, processing and curing according to German standard DIN 1045, concretes with CEM II and CEM III/A cements are highly resistant to freeze-thaw and freeze-thaw with de-icing salt. Consequently, they are suitable for engineering structures and concrete roads. Only CEM III/A in strength class 32.5 N and CEM III/A 32.5 R with more than 50 mass % blastfurnace slag are excluded for exposure class XF4. Figure 5 shows some results from freeze-thaw tests with de-icing salt on concretes containing different cement types using the CDF method.

[1] Exposure class XF4: CEM III/A of strength class ≥ 42.5 N or of strength class 32.5 R with up to 50 mass % blastfurnace slag

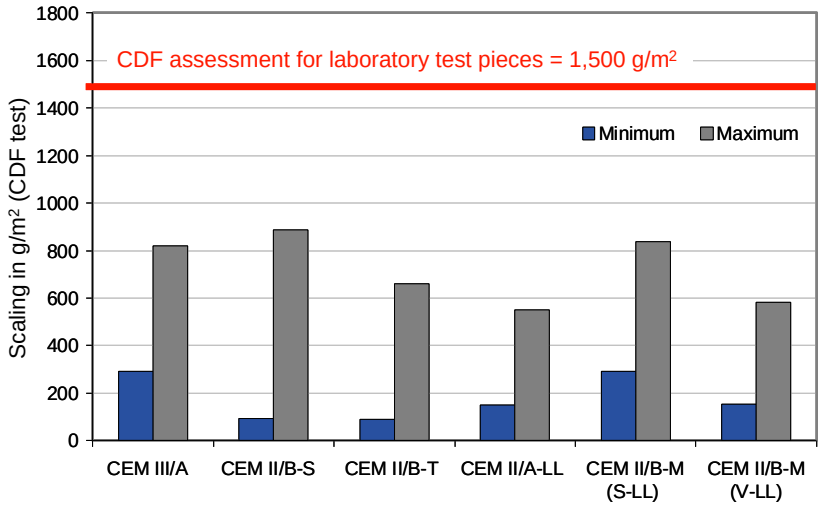

Figure 5 - Resistance of air-entrained concrete to freeze-thaw with de-icing salt using the CDF method, cement content 320 to 365 kg/m³; w/c ratio 0.41 to 0.50; strength classes of the cements: 32.5 R and 42.5 N [18; Data: 19]

If freeze-thaw with de-icing salt resistance has to be tested, as a general rule the following criterion is applied to evaluate the results: after 28 freeze-thaw cycles scaling must not exceed 1,500 g/m² for a concrete that is meant to have adequate resistance to freeze-thaw with de-icing salt. This corresponds to a scaling depth of around just 0.6 mm. This criterion may not be applied to samples taken from structures.

As an industry that uses a high volume of energy and raw materials, the cement industry is very much affected by demands to conserve resources and reduce the use of energy and also by the global issue of climate control. Cement manufacturers are facing these challenges by continuously improving their production processes in terms of energy and raw materials consumption. Based on the aim of continuing along this path, there is also growing demand for new types of cement not included in the European cement standard EN 197-1 because their special composition has not yet been deemed "traditional" or "well tried and proven", even if their compositions are not necessarily very different from the cements covered by EN 197-1. The cement standard EN 197-1 defines the composition of cements with several main constituents whose durability and performance has been proved in practice. These do not include, for example, cements with 10 – 25 mass % limestone (LL) in combination with 10 to 40 mass % fly ash (V) or blastfurnace slag (S) ("CEM X"). Investigations in the Research Institute of the Cement Industry (FIZ) have shown that concretes with cements such as this – which have been optimised in terms of chemical mineralogy or granulometry according to their intended use – could satisfy durability-relevant requirements. The same also applies, for instance, to CEM II/B-LL cements with up to 30 mass % limestone.

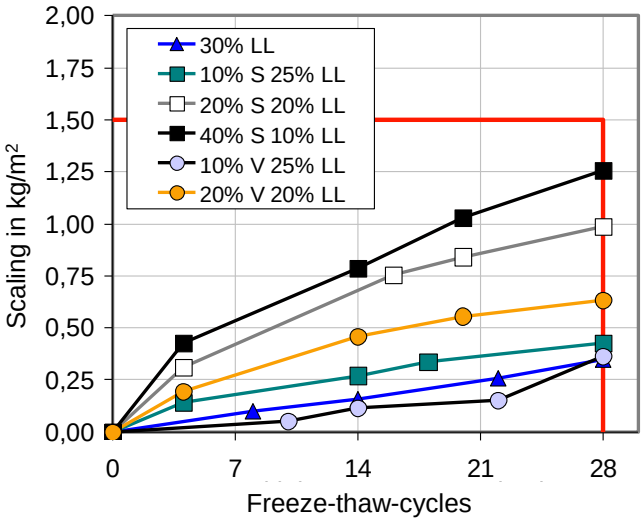

Description of the cements: see Table 4

Figure 6 - Scaling of air-entrained concretes with c = 320 kg/m³ and w/c = 0.50 in the CDF test depending on the number of freeze-thaw cycles, cements in strength class 32.5 R according to EN 197-1 [5]

In the test to establish resistance to freeze-thaw with de-icing salt, air-entrained concretes achieved results well below the assessment criteria used in Germany (Figure 6). These results cannot be generalised at present. They can, however, be used for further development work.

4.3 Comparison of the results of different test methods

The assessment of freeze-thaw resistance depends to some extent on the test method that is used. Over the past years, within the scope of various research projects, the Research Institute of the Cement Industry in Düsseldorf carried out freeze-thaw and freeze-thaw tests with de-icing salt on concretes with different cement types that have not or only seldom been used under real-life conditions in Germany. In some cases the tests were compared with various other testing methods. The cube test and the CF test according to CEN/TS 12390-9:2006 were used to determine scaling. Internal damage was determined by means of the relative dynamic modulus of elasticity (RDM) using the beam test and the CIF test according to the CEN report CEN/TR 15177:2006.

In the beam test, none of the investigated concretes showed a reduction in relative dynamic modulus of elasticity of more than 3%. Concretes partly showed a significant decrease in RDM in the CIF test. With the beam test, no significant change in the RDM was detected (Table 2).

Table 2 - Assessment of freeze-thaw resistance [4]

Cement [4]	Cube test				CF/CIF		Beam test
	c = 300 kg/m³; w/c = 0,60				c = 320 kg/m³; w/c = 0,50		
	Scaling after					Rel E_{dyn} after	
	56 FTC		100 FTC		28 FTC		56 FTC
	≤ 5 [1]	≤ 3 [1]	≤ 10 [1]	≤ 5 [1]	≤ 1,00 [2]	≥ 75 [2]	≥ 95 [3]
	mass %				kg/m²	%	
RefC	yes	yes	yes	yes	yes	yes	n. d.
1-2	yes	yes	yes	yes	yes	yes	yes
12-1	yes	yes	yes	yes	yes	no	yes
13-1	yes	no	yes	no	yes	74,4	yes
15	yes	yes	yes	yes	yes	no	yes
18	yes	yes	yes	yes	yes	no	yes
19	yes	no	yes	no	yes	no	yes
2-2	yes	yes	yes	yes	n. d.		
3-2	yes	yes	yes	yes			
14	yes	yes	yes	yes			
16	yes	yes	yes	yes			
17	yes	yes	yes	no			

1) Concrete tested with the cube test has sufficient freeze thaw resistance (~ XF1), if the scaling is lower than 5 mass % after 56 FTC and 10 mass % after 100 FTC. These values can be lower for concrete for exposure class XF3 (3 mass % after 56 FTC and 5 mass % after 100 FTC) [20]. To achieve a national technical approval for cements with which there is no experience in Germany, the limit value is 10 mass % after 100 FTC for applications in exposure class XF3.

2) Concrete for exposure class XF3 must not have a relative dynamic modulus of elasticity after 28 FTC of less than 75% and scaling > 1.00 kg/m² [7].

3) The acceptance criterion according to ÖNORM B 3303 [21] is a decrease in the relative dynamic modulus of elasticity of 5% after 56 FTC in comparison to a concrete which is classified in exposure class XF3 according to ÖNORM B 4710-1 [22]. In this study, no reference concrete was tested. Taking into account that none of the tested concretes had a relative dynamic modulus of elasticity of less than 97% after 56 FTC, this criterion was met by all the concretes that were investigated.

4) Information about the cements:

RefC	CEM I
1-2	65% clinker + sulphate; 35% limestone 1 (BET 11,880 cm²/g)
12-1	50% clinker + sulphate; 30% granulated blastfurnace slag (gbfs); 20% limestone 1
13-1	30% clinker + sulphate; 50% granulated blastfurnace slag (gbfs); 20% limestone 1
15	65% clinker + sulphate; 35% limestone 5 (BET 42,410 cm²/g)
18	50% clinker + sulphate; 30% granulated blastfurnace slag (gbfs); 20% limestone 5
19	30% clinker + sulphate; 50% granulated blastfurnace slag (gbfs); 20% limestone 5
2-2	65% clinker + sulphate; 35% limestone 2 (BET 50,590 cm²/g)
3-2	65% clinker + sulphate; 35% limestone 3 (BET 24,360 cm²/g)
14	65% clinker + sulphate; 35% limestone 4 (BET 65,780 cm²/g)
16	65% clinker + sulphate; 35% limestone 6 (BET 47,510 cm²/g)
17	65% clinker + sulphate; 35% limestone 7 (BET 73,810 cm²/g)

The slab test and the CDF test according to CEN/TS 12390-9:2006 were used to assess resistance to freeze-thaw with de-icing salt.

Figure 7 shows a comparison of the results of freeze-thaw with de-icing salt tests on four concretes, using the CDF and slab tests.

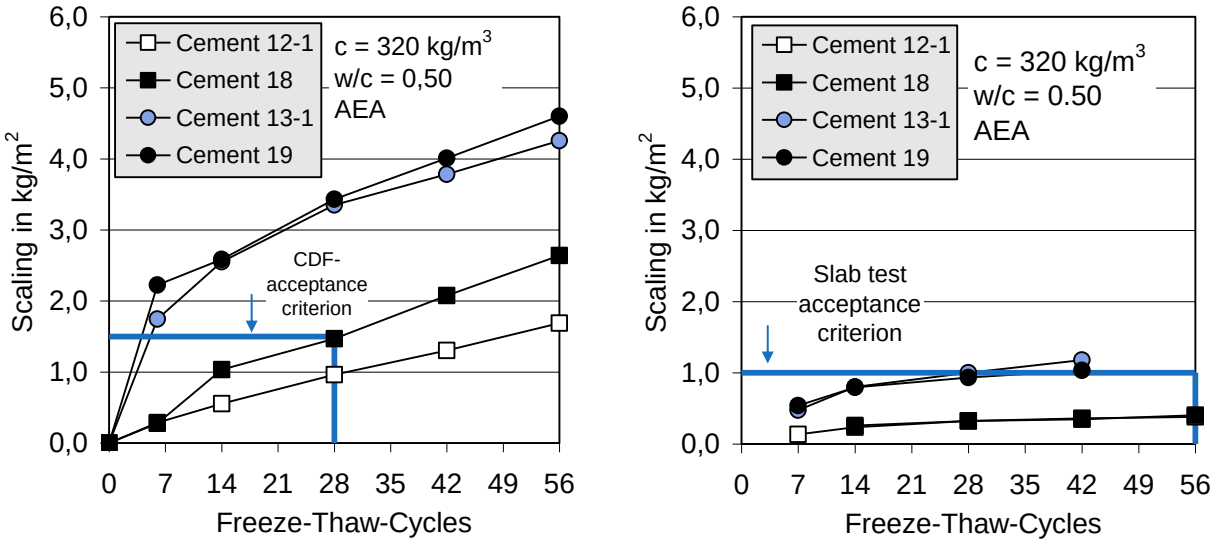

Figure 7 - Comparison of the results of freeze-thaw with de-icing salt tests on four concretes, using the CDF and slab tests [4] – information about the cements: see Table 2

In these and in other cases a comparison of the results shows some considerable differences in the degree of scaling in concretes with the same composition. One of the reasons is that within the pre-storage of the specimens carbonation of the test surface can occur to a much higher extent in the CDF test compared to the slab test.

In all cases the two test methods led to the same assessment of the concretes (Table 3).

Table 3 - Assessment of freeze-thaw resistance with de-icing salt [4]

Cement	Concrete	Scaling	
		CDF test	Slab test
		28 FTC ≤ 1.50 [7] kg/m²	56 FTC ≤ 1.00 [8]
RefC	c = 320 kg/m³ w/c = 0.50, AEA	yes	n. d.
1-2		yes	yes
12-1		yes	yes
13-1		no	no
15		yes	n. d.
18		1,468	yes
19		no	no
2-2		yes	n. d.
3-2		yes	n. d.
14		yes	n. d.
16		yes	n. d.

n. d.: not determined
Information about the cements: see Table 2

Within the scope of the investigations carried out in [5], apart from resistance to freeze-thaw with de-icing salt, freeze-thaw resistance was also tested. Tests were carried out using the cube and CF methods. In the CF method the relative dynamic modulus of elasticity was also deter-

mined (CIF). In some cases, the tests using the different methods did not produce the same assessment when the acceptance criteria generally used in Germany were applied (Table 4).

Table 4 - Summary of the investigation results for freeze-thaw and freeze-thaw with de-icing salt resistance [5]

Cement	**Cube test**	**CDF test**	**CF test**	**CIF test**
	c = 300 kg/m³ w/c = 0.60	**c = 320 kg/m³ w/c = 0.50 AEA**	**c = 320 kg/m³ w/c = 0.50**	
		Scaling after		**Rel Edyn after**
	100 FTC	**28 FTC**		**28 FTC**
	< 10 mass %	**< 1.5 kg/m²**	**< 1.0 kg/m²**	**> 75 %**
30LL1-70	yes	yes	yes	yes
30LL1-70 plant	yes	yes	yes	yes
35LL2-80	no	yes	yes	no
30W1-B	no	yes	yes	no
10V4 25LL1-70	yes	yes	yes	no
10S4 25LL1-70	yes	yes	yes	yes
10S4 25LL1-70 plant	yes	yes	yes	yes
10S3 25LL2-80	no	yes	yes	no
20V4 20LL1-70	no	yes	yes	no
20V4 20LL1-70 plant	yes	yes	yes	yes
30V7 20LL1-70	no	yes	yes	yes
20S3 20LL2-80	yes	yes	yes	no
30S3 20LL2-80	yes	no	yes	no
40S3 10LL2-80	yes	no	yes	no
20S4 20LL2-80	yes	yes	yes	no
20S4 20LL2-80 plant	yes	yes	yes	no
40S4 10LL2-80	yes	yes	yes	no
40S4 10LL2-80 plant	yes	no	yes	no

(Description of the cements: data based on cement containing sulphate agents. Example: 10S3 25LL1-70: 10 mass % blastfurnace slag, fineness 3000 g/m² according to Blaine, 25 mass % limestone from plant 1 with 70 mass % $CaCO_3$, 65 mass % clinker + sulphate agents. V = siliceous fly ash; W = calcareous fly ash. Plant = large-scale production – all other cements: produced in the laboratory)

We can see that in 12 cases the investigation with the CIF test where the assessment was carried out by determining the relative dynamic modulus of elasticity in concrete with w/c = 0.50 and no artificial air pores would lead to a negative assessment of the concrete's resistance to freeze-thaw. On the other hand, where the cube test was used only in 5 cases would this have produced a negative assessment of the concrete with w/c = 0.60 without artificial air pores if concrete scaling is used as a criterion. Scaling of all concretes with w/c = 0.50 without artificial air pores was below the value of 1.0 kg/m² after 28 FTC.

5 SUMMARY

Where the standardised performance of concrete is to be assessed on the basis of tests, methods should be used that reflect the actual conditions based on acknowledged and well-tried tests and which contain the accepted performance criteria.

Investigations into the thermal stress on structures showed that on individual frosty days during the monitoring period from 1999 to 2006 the maximum temperature range of 20 K occurred, i.e. from -10 °C to +10 °C. On some icy days the temperature fell to below -20°C. The temperature range of the test methods considered (CDF and CIF) is -20 °C to +20 °C ($\Delta T = 40$ K). The cooling and thawing rate of the test methods is 10 K/h. This value may be exceeded under real-life conditions, especially on hydraulic engineering structures. In these cases cooling rates of up to 12 K/h and thawing rates of up to 15 K/h were observed. It should be remembered that these extreme values are very rare (< 1 %) and that the most common values were about an order of magnitude lower (1 to 3 K/h). This covers extreme real-life conditions on frosty and icy days and also creates an accelerating effect, since the frequency of extreme temperature ranges, icy days with -20 °C and higher rates of temperature change in winter is very low.

Apart from the thermal stress, the moisture level that the test pieces reach during the laboratory tests must also be considered. The main question is whether this moisture level or degree of saturation in the edge section of the test piece corresponds to the conditions of the structural surface to be assessed in winter. The mass determinations during the laboratory test consistently show that water absorption of the test pieces is not complete after the 7-day preliminary storage period (capillary suction at 20 °C) and that it continues during the freeze-thaw attack. After 28 cycles in the CIF/CDF test, moisture absorption during freeze-thaw attack can reach values that correspond to or exceed the level during preliminary storage.

In most cases concrete surfaces of bridges, tunnels, road surfaces, walls of hydraulic engineering structures above the high water mark are subject to fluctuations in the moisture level which is characterised by the fact that a high degree of water saturation is always followed by a drying period. Measurements of the moisture level in structures showed that generally the level in the edge section of the structure does not exceed the value that is obtained during capillary water absorption of concrete samples in the laboratory at 20 °C; in other words, during the 7-day storage period (capillary suction) before the start of the freeze-thaw attack in the CIF and CDF tests.

To summarise, in [3] it is determined that with the CDF test used to simulate freeze-thaw attack with de-icing salt it is possible to accelerate the decisive damaging process in an experiment (time lapse effect of scaling). The stress on concrete in actual structures is mapped by the single-axis heat, moisture and thawing agent only via one surface of the test piece. Therefore, based on scaling it is possible to assess concretes for exposure class XF4 in terms of the minimum required or adequate performance and also to validate equivalent performance. The acceptance criterion of 1,500 g/m² after 28 freeze-thaw cycles was confirmed in the investigations. In Germany, concretes for exposure class XF3 that are investigated for use in waterways engineering using the CIF method are to be assessed on the basis of the acceptance criteria defined by the German Federal Waterways Engineering and Research Institute (BAW). Currently, outside the area covered by these regulations there are no definitions regarding the minimum number of freeze-thaw cycles that have to be achieved in the laboratory test without any damage occurring to the concrete (relative dynamic modulus of elasticity RDM ≥ 80 % [23]). It remains unclear to which extent the reduction in the relative dynamic modulus of elasticity measured in the laboratory in the CIF test can be used as a measure for the damage to be expected under real-life conditions in exposure class XF3.

In comparative tests of resistance to freeze-thaw with de-icing salt using the slab and CDF tests, there were very different levels of scaling on concretes with the same composition in some cases. Classification using the criteria currently applied was identical in the cases that were investigated. In the freeze-thaw resistance test on concretes with w/c = 0.60 using the cube

method (assessment of scaling) and using the CIF test on concretes with w/c = 0.50 (assessment of the relative dynamic modulus of elasticity) the CIF test produces a negative assessment more often than the cube test within the investigations reported in this paper. The freeze-thaw resistance test on concrete with w/c = 0.60 using the cube method corresponds to the measures that have been previously defined for cement approval by the German Institute for Building Technology (DIBt). Cements in concrete that passed this test have also stood the test under real-life conditions.

When assessing test methods the degree of saturation that the edge section of the concrete can reach under real-life conditions and the stage of the laboratory test that this state corresponds to must be especially considered. A moisture level that leads to a degree of saturation that will never be reached in real-life conditions produces an unrealistic damage profile. To limit unavoidable differences between the damage profile in the laboratory test and in real life, the acceptance criteria must be defined in a way that considers practical building experiences.

REFERENCES

1. Brameshuber, W.; Rahimi, A.: Ergebnisse des DAfStb-Verbundforschungsvorhabens „Übertragbarkeit von Frost- Laborprüfungen auf Praxisverhältnisse“: Bauwerksuntersuchungen zum Frost- und Frost-Tausalzwiderstand von Beton. [Results of the DAfStb collaborative research project "Transferability of laboratory freeze-thaw tests to practical conditions": Structural investigations into freeze-thaw and freeze-thaw resistance with de-icing salt]. beton 59 (2009) No. 12, pp 574-577.
2. Guse, U.; Müller, H. S.: Ergebnisse des DAfStb-Verbundforschungsvorhabens "Übertragbarkeit von Frost-Laborprüfungen auf Praxisverhältnisse": Frost- und Frost-Tausalzwiderstand von Beton (Laborprüfung und Auslagerung). [Results of the DAfStb collaborative research project "Transferability of laboratory freeze-thaw tests to practical conditions": Freeze-thaw resistance with and without de-icing salt of concrete (laboratory test and outdoor storage)]. beton 59 (2009) No. 12, pp 570-572.
3. Müller, H. S.; Guse, U.: Übertragbarkeit von Frost- Laborprüfungen auf Praxisverhältnisse – Zusammenfassung des DAfStb-Verbundforschungsvorhabens [Transferability of laboratory freeze-thaw tests to practical conditions – Summary of the DAfStb collaborative reseach project]. beton 59 (2009) N0. 12, pp 564-569.
4. ECOserve NETWORK. CLUSTER 2: Production and Application of Blended Cements: Research Activities - CONTRACT N°: G1RD-CT-2002-00782 – Final report; Date of issue of this report: 30.11.2005
5. Müller, C.; Severins, K.; Hauer, B.: Neue Erkenntnisse zur Leistungsfähigkeit von Zementen mit den Hauptbestandteilen Kalkstein, Hüttensand und Flugasche [New findings regarding the performance of cements with the main constituents limestone, blastfurnace slag and fly ash]. beton 59 (2009) No. 10, pp 69-478; No. 11, pp 531-537.
6. DIN EN 206-1:2001-07 Beton - Teil 1: Festlegungen, Eigenschaften, Herstellung und Konformität; Deutsche Fassung EN 206-1:2000 mit DIN EN 206-1/A1:2004-10 und DIN EN 206-1/A2:2005-09 [DIN EN 206-1:2001-07 Concrete - Part 1: Definitions, properties, manufacture and conformity; German version of EN 206-1:2000 with DIN EN 206-1/A1:2004-10 and DIN EN 206-1/A2:2005-09]
7. Bundesanstalt für Wasserbau (BAW): Merkblatt "Frostprüfung von Beton" – Ausgabe Dezember 2004 [German Federal Waterways Engineering and Research Institute (BAW): Fact sheet "Frost test of concrete" – December 2004 issue]

8. CEN/TS 12390-9:2006, "Testing hardened concrete - Part 9: Freeze-thaw resistance – Scaling"
9. CEN/TR 15177:2006, "Testing the freeze-thaw resistance of concrete - Internal structural damage"
10. DIN 1045-2:2008-08 Tragwerke aus Beton, Stahlbeton und Spannbeton - Teil 2: Beton - Festlegungen, Eigenschaften, Herstellung und Konformität, Anwendungsregeln zu DIN EN 206- [DIN 1045-2:2008-08 Load-bearing structural elements made from concrete, reinforced concrete and pre-stressed concrete - Part 2: Concrete - Definitions, properties, manufacture and conformity, application regulations for DIN EN 206-]
11. Guse, U.; Müller, H.S.: Übertragbarkeit von Frost-Laborprüfungen auf Praxisverhältnisse - Bauwerksuntersuchungen. [Transferability of laboratory freeze-thaw tests to practical conditions – structural investigations]. Research report No. 02 30 79 0671 for the project DAfStb V 419, Institute for Solid Construction and Building Materials Technology at Karlsruhe University, 2006
12. Brameshuber, W.; Spörel, F.; Warkus, J.: Messung des tiefenabhängigen Feuchtegehalts an Betonbauwerken der Expositionsklassen XS (Meerwasser) und XF (Kläranlage) [Measuring depth-related moisture level of concrete structures in exposure classes XS (seawater) and XF (sewage treatment plant)]. Research Report F 844 for the project of DAfStb V 420, Institute of Building Materials Research (ibac) at Aachen University, 2007
13. Brameshuber, W.; Spörel, F.: Messung der Feuchte und Temperatur in Bauwerken zur Feststellung ihrer Beanspruchung im Hinblick auf die Umweltklassen nach EN 206 + Anwendungsregeln (DIN 1045-2) [Measurements of moisture and temperature in structures to determine their stress in terms of environmental classes according to EN 206 and application regulations (DIN 1045-2)]. Interim Report F 788/2 for the project of BAW 1300-483/00, Institute of Building Materials Research (ibac) at Aachen University, 2007
14. Brameshuber, W.; Spörel, F.: Frostwiderstand (XF1 und XF3) von CEM III-Betonen - langjährige Auslagerung im Vergleich zum Laborprüfverfahren [Freeze-thaw resistance (XF1 and XF3) of CEM III concretes – long-term outdoor storage compared with laboratory test methods]. Research project F 878, Institute of Building Materials Research (ibac) at Aachen University, article for CEMEX HOZ seminar in Duisburg on 26 April 2007
15. Brameshuber, W.; Spörel, F.; Warkus, J.: Europäische Bemessungsvorschriften für den Brückenbau - Beanspruchung von Betonbauwerken [European measurement regulations for bridge construction – stress on concrete structures]. Research Report F 790 for the project of BMVBS 15.324/2000/FR, Institute of Building Materials Research (ibac) at Aachen University, 2007
16. Brameshuber, W.; Cvetković, V; Spörel, F.: Einfluss der Meerwasserzusammensetzung auf die Intensität eines Frostangriffes - Vergleichende Untersuchungen bei Betonzusammensetzungen nach DIN 1045-2 bzw. DAfStb-Richtlinie "Massige Bauteile aus Beton mit dem CIF/CDF-Test" [Influence of seawater composition on the intensity of a frost attack – comparative investigations with concrete compositions according to DIN 1045-2 and DAfStb guideline "Massive concrete construction components with the CIF/CDF test"]. Research Report F 950 for the project of DAfStb V 451, Institute of Building Materials Research (ibac) at Aachen University, 2008
17. Brameshuber, W.; Spörel, F.; Warkus, J.: Messung des tiefenabhängigen Feuchtegehalts an Betonbauwerken der Expositionsklassen XS (Meerwasser) und XF (Kläranlage) [Measuring depth-related moisture level of concrete structures in exposure classes XS (seawater) and XF (sewage treatment plant)]. Research Report F 966 for the project of DAfStb V 454, Institute of Building Materials Research (ibac) at Aachen University, 2008

18. CEM II- und CEM III/A-Zemente im Betonbau – Nachhaltige Lösungen für das Bauen mit Beton (2008) [CEM II and CEM III/A cements in concrete construction – sustainable solutions for building with concrete (2008)] – can be obtained via www.beton.org
19. Verein Deutscher Zementwerke: Ergebnisse aus den Prüfdatenbanken des Forschungsinstituts der Zementindustrie und der VDZ-Mitgliedsunternehmen (unveröffentlicht) [Results from the test databases of the German Cement Works Association and member companies (unpublished)].
20. Siebel, E.: Frost- und Frost-Tausalz-Widerstand von Beton [Freeze-thaw resistance with and without de-icing salt of concrete] In: Beton 42 (1992), No. 9, pp 496-501
21. ÖNORM B 3303: Betonprüfung; Österreichisches Normungsinstitut [Concrete testing; Austrian Standards Institute]
22. ÖNORM B 4710-1 : 2002-01. Concrete – Part 1: Specification, production, use and verification of conformity (Rules for the implementation of ÖNORM EN 206-1)
23. Setzer, M.J. et al (2004): Test methods of frost resistance of concrete: CIF-Test: Capillary suction, internal damage and freeze thaw test – Reference method and alternative methods A and B. Materials and Structures, Vol. 37 – No. 274, pp. 743-753

Moisture flow into Concrete Exposed to Frost and Ice

Stefan Jacobsen
Professor, dr.ing Concrete Technology
Department of Structural Engineering, NTNU
N-7491 Trondheim
stefan.jacobsen@ntnu.no

ABSTRACT
Exposure of concrete to freeze/thaw, ice and moisture causes transport in the material and the mechanisms responsible are reviewed. Hydraulic pressure may cause transport during both freezing and thawing whereas suction under the curved meniscus between ice and water in the pores is increasingly active as freezing progresses from surface inwards. Diffusion towards cold side requires a "trapping", here suggested in the air voids. Internal frost damage with cracking causes increased concrete volume and suction of water from the surface. Ice pressure towards a rough concrete surface can cause very high local Hertzian indentation contact pressure for a wide range of concrete surface roughness. Even though plasticity of ice can reduce the contact pressure it can be high enough during short time to cause melted water and water from the liquid like layer on ice to be pressed into the concrete. Damage by abrasion of moving ice sheets on concrete structures is likely caused by this indenting pressure of concrete in ice.

Key words: concrete, moisture flow, experiments, freezing and thawing, ice, contact pressure

1. INTRODUCTION

Frost damage on concrete can occur when exposed to frost and moisture. Examples of vulnerable structures in the Nordic countries are hydroelectric and marine structures, sidewalks, bridges, facades, air fields etc. Concrete with poor material quality (not properly air entrained, with too high w/b, made with improper workmanship and curing conditions) may suffer frost damage (surface scaling and/or internal cracking) when frozen wet with or without de-icers. A clear relation between internal frost damage and water saturation has been found [1]. Furthermore, wet frost exposure has been found to increase the transport [2]. This paper discusses various driving forces for transport during freezing with water or ice at the concrete surface. Some ways to quantify the transport in the different cases are proposed. Hopefully this can lead to improved frost durability by reduced transport into the concrete.

2. OBSERVED MOISTURE FLOW IN WET FROST EXPOSURE

When concrete is submerged in water or de-icer salt solution while frozen and thawed the uptake of moisture/salt solution is accelerated compared to absorption at constant temperature, see figure 1.

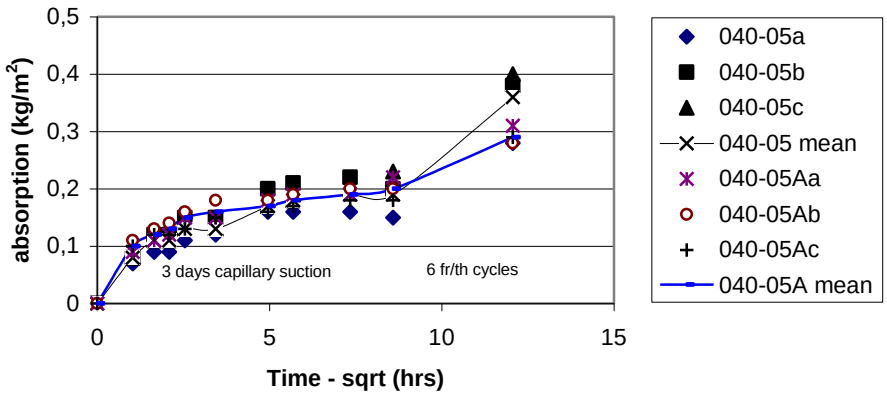

Figure 1 - Accelerated liquid (3 % NaCl solution) uptake due to the pumping effect of w/b = 0.40 in CDF-test set up with 2.8 °C/h cooling rate [2]

The transport into the concrete varies depending on the exposure, the concrete material composition and the preparation of the concrete sample [3]. A conceptual model was proposed for the development of frost damage in various types of exposure [4]. The rate of flow measured during the wet freeze/thaw pumping effect can be seen in the right part of the plot in figure 1. In [5, 6] a review was made of experimental studies measuring the absorption during freeze/thaw in widely differing test set-ups, rate of cooling, minimum temperature, time at minimum temperature and type of liquid (water, deicer salt). For experiments with a temperature gradient dT/dx the "pumping flow" varied within a wide range; 10^{-5} – 10^{-7} kg/(m^{2}s) [5].

The two most well-known cases of transport of moisture in porous materials due to temperature variations have large practical relevance for civil engineering in the Nordic countries and the northern hemisphere. The first is from building physics; flow of moisture from warm to cold side of a building wall due to high humidity indoors combined with a thermal gradient. The other case is from soil mechanics; the flow of water upwards from the warmer ground water table towards the frozen ground penetrating downwards.

Powers explained inwards flow in a concrete specimen frozen and thawed in water by hydraulic pressure [7, 8]. His discussion was based on observations of cracking and scaling during freeze/thaw. The observation of inflowing moisture during freezing being captured in the concrete after thawing was termed irreversible flow in [9], see figure 2. The latter experiments were made with de-icing salt solution, keeping the concrete surface wet at all times during freeze/thaw with highly concentrated solutions. The test set-up [9] was a further development of the experiments by Lindmark [10]. There, thin mortar discs were submerged in various salt solutions at constant low temperatures and weighed regularly to measure flow. One important difference in [9] was to apply a temperature gradient over the relatively thick slab as opposed to the constant temperature in the thin discs [10].

(copy from Tange Hasholdt, 2002)

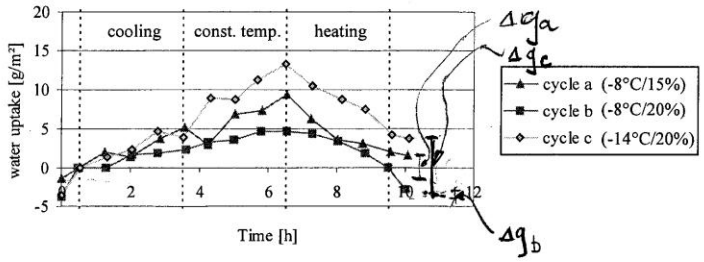

Figure 2.2: Typical water uptake registered during test condition a, b, and c respectively (the actual values are measured for mortar 47.5A01). Each curve represents the average of three specimens. w/c = 0.47, 7% air, $\bar{L}$ = 0.29mm.

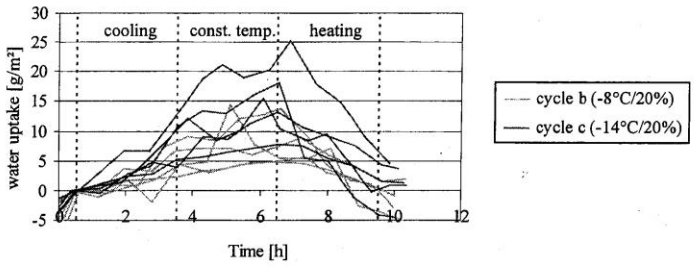

Figure 2.4 Water uptake during b-cycles (minimum temperature –8°C) and c-cycles (minimum temperature –14°C). The concentration is 20% in both cycles.
All mixes (w/c = 0.40 ~ 0.55)

Figure 2 - Irreversible flow during one freeze/thaw cycle, from PhD of Tange Hasholdt 2002 [9]

3. MOISTURE FLOW MECHANISMS AT EXPOSURE TO FROST AND ICE

Significant progress was made in the above cited studies to understand transport during frost action. In the following the transport mechanisms are discussed based on a "standard" exposure case with water or ice at the surface. A negative inwards temperature gradient is applied from a wet surface, and then reversed as thawing starts.

3.1 Hydraulic pressure and -suction

The Hydraulic Pressure Hypothesis (HPH) was presented by Powers [7, 8] and also discussed with the contemporary soil scientist Terzhagi [7]. HPH is based on the flow caused by the ≈ 9 % increase of volume as water freezes and is pressing unfrozen water as freezing progresses from surface inwards. If the cement paste is saturated one may assume that the flow obeys D'arcys law:

$$g = -K\frac{dP}{dx} \qquad (1)$$

where g is steady-state flow (kg/m^{2}·s) and K is coefficient of permeability (kg/Pa·m·s) assumed constant with K = k/η where k = intrinsic permeability (kg/m) and η = viscosity (Pa·s).

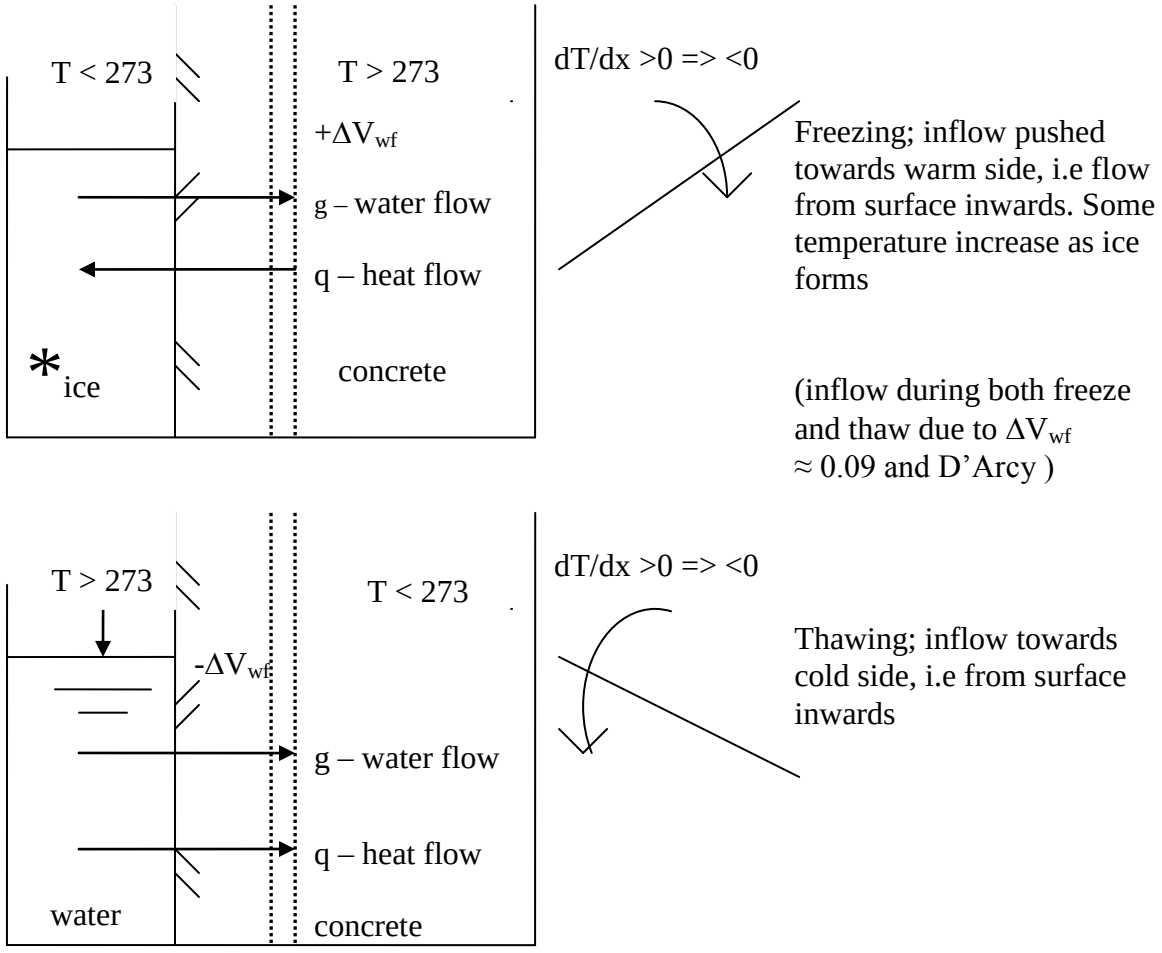

Figure 3 - Hydraulic pressure and –suction during freezing and thawing of concrete in water

The concrete in figure 3 is shown without air voids. With voids the hydraulic pressure falls towards these, and the closer their spacing the lower the pressure between the voids, reducing water flow g. From this idea leading to flow into air voids Powers developed the air void spacing concept. (Note that if the pressure is due to suction in the concrete [11-13] as discussed below, the air voids will be equally effective in releasing the pressure.) A main point about HPH is that, depending on the heat flow and availability of water, it is probably equally effective on both freezing and thawing. Thus water is pumped in at almost all times during wet freeze/thaw exposure. It can even be argued that increased frost damage due to salt on the surface is related to prolonged period of absorption, assuming pure water ice inside.

3.2 Suction in capillary pore water due to surface tension water-ice

There are observations that HPH cannot explain, such as for example shrinkage instead of expansion during freezing of highly saturated concrete. Suction created by the capillary tension between pore water and ice can be assumed to obey La Place:

$$dp = -\frac{2\sigma_{ls}}{r} \qquad (2)$$

Here dp (N/m^2) is pressure difference between water and ice in a saturated pore, σ_{ls} = surface tension between water and ice (0.031 N/m) and r is pore radius (m) at the meniscus excluding adsorbed layers. The curved interface causes suction in the pore water as ice formation starts in the pore system. This increases the free energy of unfrozen water compared to ice as temperature is reduced below zero. To reduce the free energy difference between water and ice water flows towards ice and can then also be sucked in when available at the surface, see figure 4 [11-13]. If the concrete is properly air entrained the ice forms in the air voids without damage.

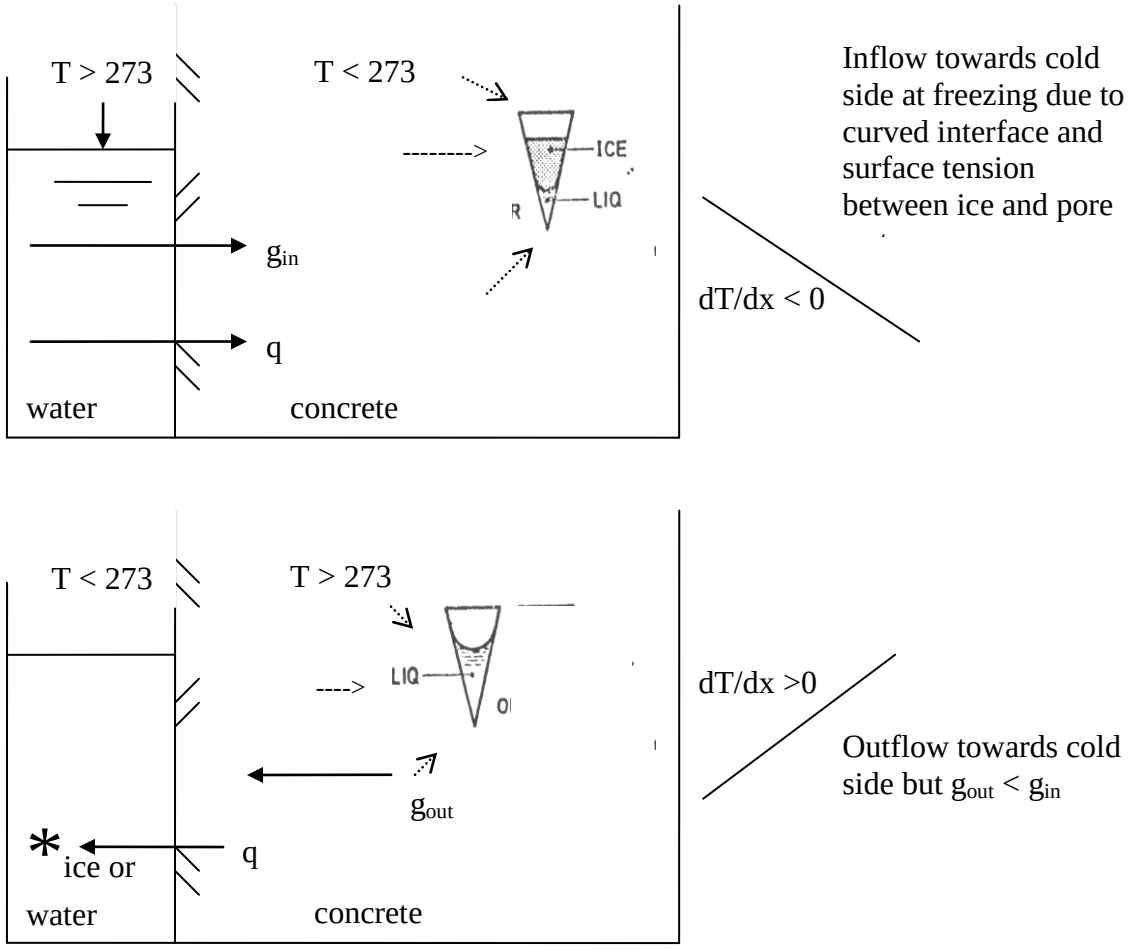

Figure 4 - Suction from surface tension over curved interface between ice and pore water

Lindmark [10] measured flow into his mortar slices frozen with various combinations of water and salt solution in the pores while submerged in liquid salt solutions at constant sub-zero temperatures, i.e. no gradient. He argued that the relatively high flow he observed into the specimens was caused by the suction under the meniscus expressed as increased gradient of chemical potential between pore water and ice. His explanation is in fact bridging between the frost transport with pure water and with salt solution.

From Clausius-Clapeyron derived for the system ice-water in a pore, the energy consumed as enthalpy at freezing can be approximated to balance the work of mechanical suction created by

the surface tension in the curved interface between ice and pore water. This can be used for transport calculations where the flow will depend on freezing point depression, temperature gradient, freeze able water content, enthalpy and actual interface in the pore system. For a water-ice interface the following transport expression was deduced [6]:

$$g_{in} = \frac{K\Delta H_f}{(V_w - V_i)} \cdot \frac{1}{T} \cdot \frac{dT}{dx} \qquad (3)$$

where g is steady-state flow in through a section with freezing temperature T, V_w and V_i are volumes of water and ice respectively, ΔH_f = enthalpy on freezing (J) for the particular pore water and freezing temperature, and T = freezing temperature of water (K). Figure 5 below shows calculated (eq.3) and measured transport. The experimental values are from the reviews of flow in varying wet freeze/thaw experiments [5, 6] measured by a number of researchers. However, only tests with a temperature gradient in the sample during freeze/thaw are included. The test parameters include varying materials, preparation, conditioning, test set-up, rate of cooling, minimum temperature and time at minimum temperature and type of liquid (water, deicer salt). The permeability was taken from [14]

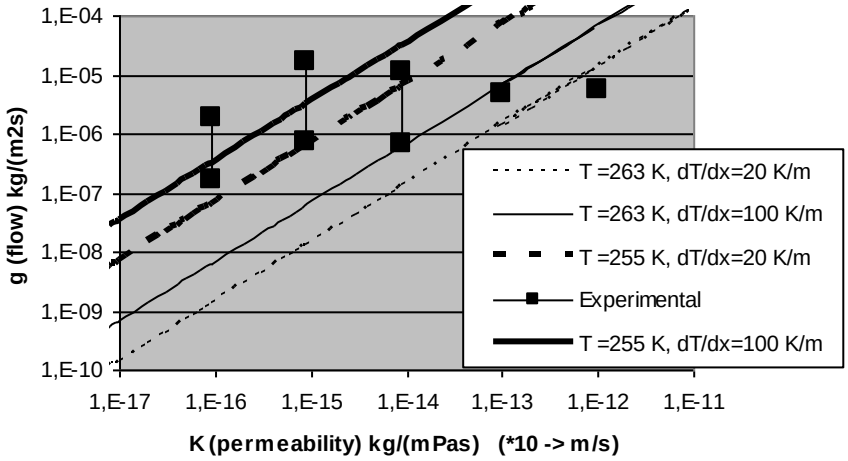

Figure 5 - Flow through a section at temperature T along falling temperature gradient dT/dx with wet surface (eq.(3)).

The results in figure 5 include a number of assumptions and simplifications (contact between ice and water in the pore system, availability of liquid at the surface, constant permeability coefficient, simplified calculation of freeze able water for typical concrete pore system etc). The resulting calculated flow can probably vary a decade due to uncertainties about each of the assumed quantities. Still, the estimated flow is in the right order of magnitude for a wide range of experimental data which is an indication that the effect of the suction between ice and water is important.

As the freeze/thaw cycle and the temperature gradient reverse the ice in the concrete specimen will melt first at the surface and due to the hysteresis between freezing and thawing [15] there can still be some transport into the specimen due to this mechanism.

3.3 Vapour diffusion from warm to cold side

In this case the macroscopic transport has the same origin as in the building wall mentioned above. The flow is directed towards the cold side according to Ficks law due to the reduced vapour concentration there:

$$-\frac{dv}{dx}=\frac{g}{\delta_v} \tag{4}$$

Here, dv (kg/m^3) is vapour concentration difference in the pore air, dx (m) length, δ_v (m^2/s) vapour diffusivity and g (kg/(m^{2}s)) is transport rate. Values of δ_v for a range of concretes and potentials are given in [16]. Figure 6 shows the flow of heat and moisture.

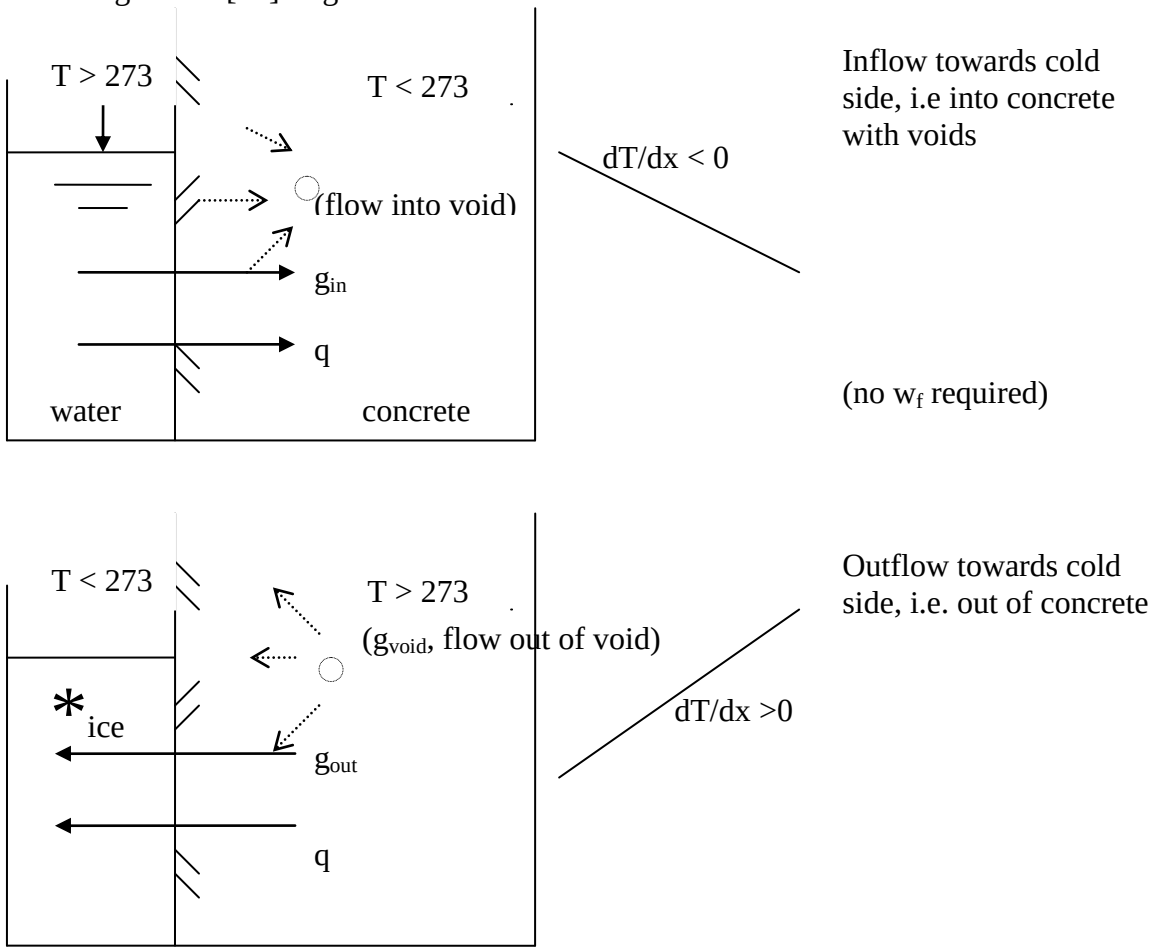

Figure 6 - Diffusion of vapour towards cold side

The trapping of moisture in the concrete after a freeze/thaw cycle, the irreversible flow [9], is however not explained. As the temperature gradient reverses completely on thawing, so does the flow and an additional "trapping" mechanism is needed. This could be trapping of moisture in voids. Diffusion may cause flow into voids when the vapour content in the voids is low, i.e. when cold. Furthermore, if the vapour gradient (dv/dx) is too low at some stage during thawing, the diffusion out of the voids (g_{void}) can be lower than into the voids. Then, less moisture flows out of the cement paste on thawing (g_{out}) compared to the flow into the concrete (g_{in}), since g_{out}

will be partly fed by g_{void}. The difference in inflow and outflow surfaces could affect this. If we assume that the total flow into the concrete is driven by the vapour pressure difference between the external surface and the air voids we can write:

$$g_{voids} = g_{in} \cdot \frac{A_{concrete}}{A_{voids}} \tag{5}$$

where exposed concrete surface ($A_{concrete}$) is much smaller than the surface of the voids (A_{voids}). A simplified case of diffusion into voids in saturated high performance cement paste is given in [17].

3.4 Suction due to cracking and permanent volume increase

If there is frost damage to the concrete in the form of internal cracking this will inevitably create void space as the cracks open and these new openings suck in available water, see figure 7.

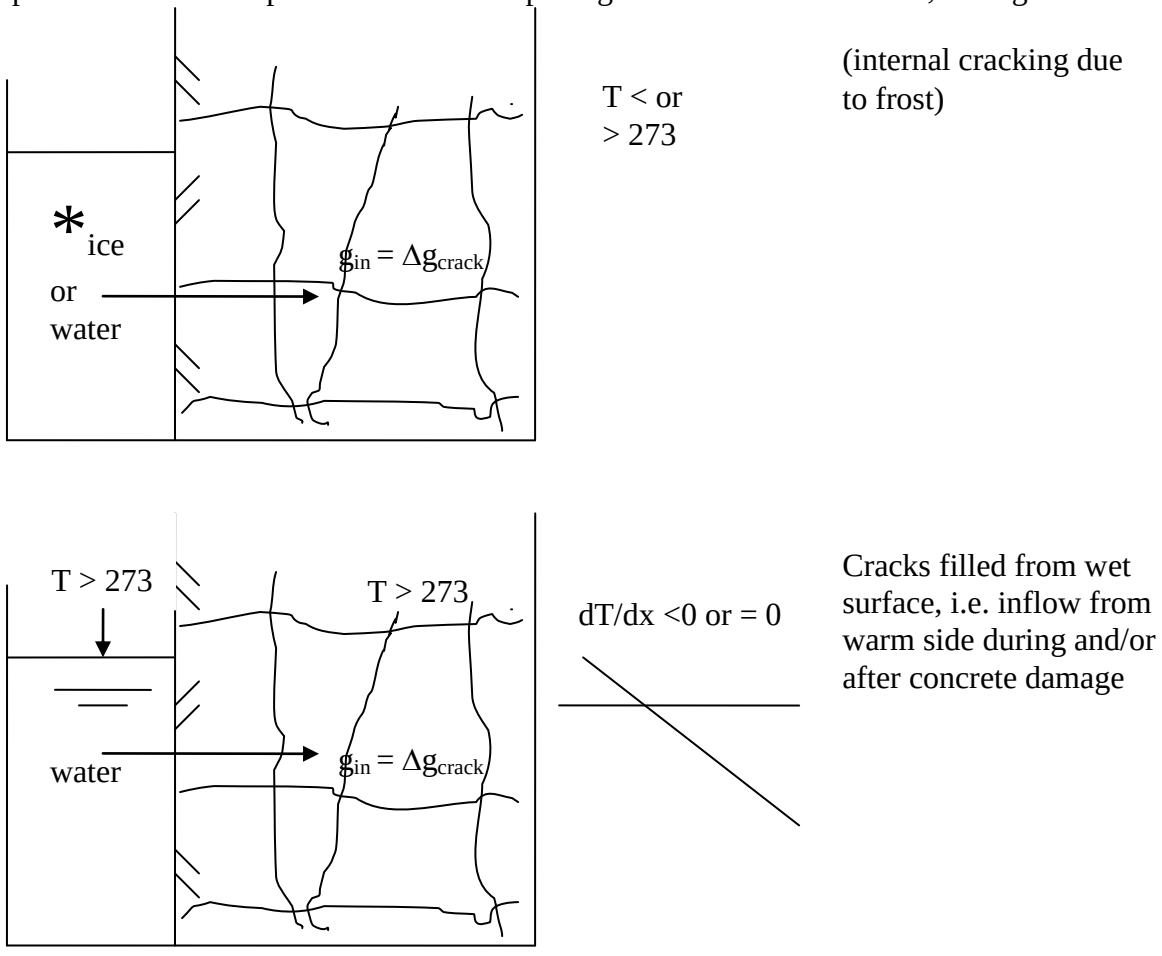

Figure 7 - Suction due to filling of cracks that open during frost damage

The flow g_{in} is proportional to the crack volume created, which is a function of crack density:

$$g_{in} = \Delta g_{crack} \approx \frac{\Delta V_{cracks}}{V_{spec}} = \frac{d^3}{(d-1)^3} - 1 \quad (6)$$

where ΔV_{cracks} = volume increase due to cracks, V_{spec} = volume of uncracked specimen and d = crack spacing (crack distance/crack width) [mm/mm] in a square grid crack pattern. Equation (6) has been found to fit well with observations of frost damage and subsequent absorption [18-21]. In addition to the suction of bulk water from the surface into the crack volume it has been found using low temperature calorimetry that on internal frost damage some water is displaced into gel space where it cannot freeze, even at -55 ºC [22, 23]. Apparently some of the absorbed water is held very tightly.

3.5 Ice pressure indenting rough concrete surface into ice with liquid like layer

Ice can be forced into direct mechanical contact with a concrete surface for different reasons. It can be due to a propagating ice front, different thermal expansion coefficients concrete-ice, sea ice forced towards marine structures or ice in the reservoir on the upside face of a concrete dam. On marine structures exposed to sea ice an average ice pressure P_{ice} in the order of 1 MPa is realistic [24]. Such ice pressure towards a rough concrete surface may cause an indentation pressure forcing water in the ice-concrete interface into the concrete pores.

Ice pressure due to a propagating ice front or stress caused by thermal incompatibility between ice and concrete can occur in a freeze/thaw test of concrete in water, for example in ASTM C666 procedure A [2]. In this test the concrete specimen is fully submerged in water during repeated freezing and thawing. At minimum temperature of around -18 º the concrete specimen is confined in a "box" of ice. Restrained stress can arise between concrete and ice due to the larger thermal contraction of ice ($\alpha_i \approx 10^{-4}$ ºC^{-1}) compared to concrete ($\alpha_c \approx 10^{-5}$ ºC^{-1}). The elastic modulii have smaller relative differences: $E_i \approx 10$ GPa for short time elastic modulus of ice at -15 ºC [25, 26] and $E_c \approx 20 - 30$ GPa for ordinary concrete, respectively. When restrained by the concrete the ice will develop tensile stress whereas there will be compressive stress in the concrete as temperature is reduced some ΔT below zero. The order of magnitude of the stress caused by thermal incompatibility can be estimated in a simplified manner by assuming linear elastic behaviour and bond between concrete and ice. The magnitude of the stress will be of the type:

$$\sigma = \alpha \cdot \Delta T \cdot E \quad (7)$$

At full restrain and elastic behaviour without relaxation a stress increase from ice towards concrete in the order of 1 MPa per degree temperature drop in the solid laminar ice-concrete specimen is predicted. The geometry, temperature-time history, stress relaxation, tensile strength of ice, bond ice-concrete etc means there are numerous load situations. Particularly the tensile strength, time and relaxation will lead to lower stress. Still the estimate illustrates that ice can be forced towards a concrete surface merely due to thermal incompatibility.

The ice pressure towards the rough concrete surface can cause very high local contact pressure according to contact mechanics [27, 28]. Water is available from the liquid like layer (LLL) on ice [25] with thickness h given by:

$$h = \frac{\Delta G_v}{\Delta S_v (273 - T)} \quad (8)$$

With ΔG_v = bulk free energy per unit area of LLL (J/m^2), ΔS_v = entropy of melting at (273-T) degree supercooling (J/Km^3)). According to the phase equilibrium along the ice-water line from the triple point towards increasing pressure, there can be much more water in the contact zone at very high pressure.

An estimate of the indentation pressure as ice is forced towards a rough concrete surface can be made based on assumptions about geometry and elastic properties of ice and concrete. Figure 8 shows the contact between a plane ice surface with a mean ice pressure P_{ice} = 1 MPa and a rough concrete surface simplified as a combination of half-spheres and plane vertical surfaces. The equally distributed reaction forces, F, from each half-sphere and the radii, a, of the contact zones are also drawn.

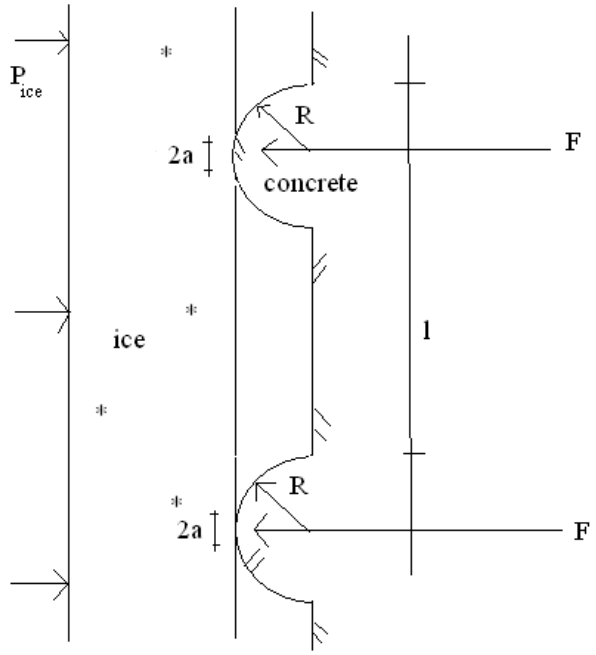

Figure 8 - Plane ice surface with average pressure P_{ice} towards rough concrete surface with half-spheres regularly spaced, reaction forces, F, and contact radii a.

The mean contact pressure P_m under the assumed elastic contact zone of radius a in figure 8 is 2/3 of the maximum contact pressure P_o and given according to Hertz:

$$P_m = \frac{2}{3}P_o = \frac{F}{\pi a^2} \tag{9}$$

Where the contact radius is:

$$a^3 = \frac{3FR}{4E^*} \tag{10}$$

And the reduced E-modulus E* depends on Poissons ratio ν and the modulii of ice and concrete:

$$\frac{1}{E^*} = \frac{1-\nu_i^2}{E_i} + \frac{1-\nu_c^2}{E_c} \tag{11}$$

Table 1 shows parameter variations used to calculate mean contact pressure P_m between concrete spheres and ice as ice is forced towards concrete with a mean pressure P_{ice} = 1 MPa.

Table 1 - Sphere radius (R), distance (l), force on sphere (F) and radius of contact zone (a)

R (mm)	l (mm)	F (N)	a (mm)
5	10 - 40	100 - 1600	0.37 – 0.94
0.5	1 - 10	1 - 100	0.04 – 0.17
0.05	0.1 - 1	0.01 - 1	0.004 – 0.02

Figure 9 shows P_m as function of sphere radius and distance expressed as a simplified surface roughness (R/l^2). The elastic modulii of ice and concrete were 9 and 25 GPa, whereas the Poisson ratios were 0.3 and 0.25 respectively.

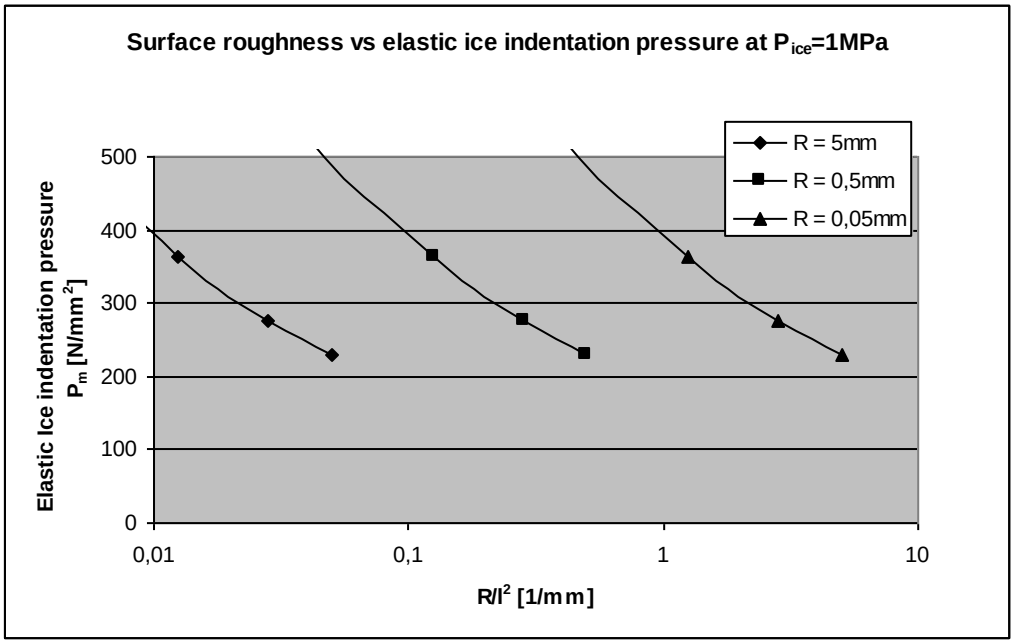

Figure 9 - Surface roughness vs elastic ice indentation pressure for concrete into ice

Figure 9 shows that the indentation pressure can be very high for a wide range of variations of surface shapes for the actual mean P_{ice}. The lower pressure is limited by the proximity of the individual spheres that are assumed arranged in a grid. The maximum roughness calculated in this simplified manner is limited to $(R/l^2) = 1/(4R)$ with $l_{min} \geq 2R$.

The ice load is distributed evenly over the actual number of spheres resulting in point loads F on the individual spheres varying from 0.01 to 1600 N for the variations in table 1. The contact radii are largest for the larger spheres (a ≈ 0.5 – 1 mm) with large distances (10 – 40 mm), whereas many small spheres will reach equal local stress levels in very small contact areas in the order of 4 – 10 microns with 0.1 – 1 mm distances.

The very high local contact pressure will melt more ice than in the LLL (eq(8)), increasing from the triple point along the ice-water line towards increasing pressure. Thus, even more water will be available due to indentation. The very high local contact pressure can cause a hydraulic

pressure that can rupture the concrete which has maximum tensile strength ≈ 5 - 10 MPa. The water may also cause frost damage after penetration into the pore system where it may freeze. The length of the flow will be reduced as the pore water pressure reduces by sideways or inwards flow. Still there should be local areas near the contact zone with very high pressure that can be responsible for rupture of thin layers of concrete near the surface with a locally highly saturated pore system.

The above calculation based on elastic contact pressure will be most valid for impact and ice contact during very short time. Due to time dependant deformations the plasticity and time dependency of ice deformation will generally lower the ice pressure towards the indenting sphere. Finite element modelling [28] has shown that P_m can be reduced to about 50 % of the elastic case, and to spread outside the radius of the elastic contact zone (a). The shape and size of the plastic zone depends on material properties, notably yield stress and elastic modulus [28].

Three of the main assumptions of elastic (Hertzian) contact mechanics apply to the ice-concrete sphere contact. These are: large radii of curvature of the contacting bodies compared to the circle of contact, the dimensions of each body are large compared with the circle of contact and frictionless contact so that only normal pressure is transmitted. However, a fourth main assumption: no pressure outside the zone of contact, will rapidly be violated as ice is deformed and the area of contact between ice and concrete is extended from only spheres to the vertical parts between the half-spheres in figure 8. As the ice load is sustained the concrete surface will eventually be exposed to a mean pressure equal to P_{ice}. Still, at initial contact an elastic type pressure should be expected for short periods. These are expected to be at least partly responsible for the damage due to ice abrasion [29-32]. The damaging effect by abrasion of the weaker and softer ice on concrete can thus at least partly be explained.

4. CONCLUSIONS

Five different mechanisms that cause flow during freeze/thaw and frost conditions are reviewed. Hydraulic pressure may occur during both freezing and thawing, whereas capillary suction under the curved meniscus between ice and water also is active during freezing and thawing, but mostly with temperature gradient falling from surface inwards and liquid at the surface. Diffusion due to lower vapour pressure at the cold side requires a suggested “trapping” effect in the air voids since the transport towards the cold side is reversed from freeze to thaw. Crack opening due to internal frost damage increases the concrete volume, thereby sucking in water from the surface. Ice pressure towards a rough concrete surface can cause very high liquid pressure in local ice-concrete contact zones. Local Hertzian contact pressure can become very high for a wide range of concrete surface roughness. Even though plasticity of ice will reduce the contact pressure it may be high enough during short time to cause both flow into the concrete and damage. An example of such damage is abrasion by moving ice sheets towards marine concrete structures.

REFERENCES

1. Fagerlund G. PhD Lund Inst of Technology, Byggnadsteknik Report 34 (1972) 411 p.
2. Jacoben S. dr.ing thesis 1995:101, Norw. Inst. of Techn, Norway (1995) 286 p.

3. Jacobsen S., Bager D., Kukko H., Tang L. and Nordstrøm K., 'Measurement of internal cracking as dilation in the SS 137244 frost test', Nordtest project 1389-98, Norw. Build. Res. Project report 250 ISBN 82-536-0645-1 (1999) 26 p./5 app.
4. Bager D.H and Jacobsen S., 'A model for the destructive mechanism in concrete caused by freeze/thaw action', in 'Frost damage in Concrete', RILEM PRO 25, ISBN 2-912143-31-4, D.Janssen, M.Setzer, M.Snyder (eds.) (2002) pp.17-40
5. Jacobsen S., 'Liquid uptake mechanisms in wet freeze/thaw: review and modelling', ref as [4] pp.41-51
6. Jacobsen S., Melandsø F., Nguyen H.T. Flow calculation and thermodynamics in wet frost exposure of cement based materials, Advances in concrete through science and engineering, Int Symp. During Rilem spring meeting, North Western Univ (2004) 14 p.
7. Powers TC A working hypothesis for further studies of frost resistance of concrete PCA Bulletin 5 (1945) 245-271, with discussions by R.Terzhaghi et al 5A (1946) 272-1 – 272-20
8. Powers T.C.: The air requirement of frost resistant concrete, Proc HRB 29 (1949)184-211
9. Tange Hasholdt M. 'Experimental investigation of water uptake during cyclic freeze/thaw action', Dr.thesis part 3, DTI-Aalborg Un., ISBN 87-7756-701-3 (2002) 39 p.
10. Lindmark S., 'Mechanisms of salt frost scaling of portland cement bound materials' Dr.th. Lund Sweden TVBM1017 (1998) 266 p
11. Powers T.C. and Helmuth R.A.: Theory of volume changes in HPP during freezing, Proc HRB V.32 (1953) 285-297
12. Radjy F.F.: 'Freezing and frost damage', Lecture notes Sellevold E.J et al Building Materials, Techn Univ of Denmark, Building Materials Laboratory (august 1971) 45 p.
13. Setzer M.: Basic phenomena of frost action, RILEM TC 117 FDC Research seminar, Lund, Ed.: G.Fagerlund, M.Setzer, LTH report TVBM 3048, Sweden (1991) pp.7-17
14. Herholdt A et al. 'Beton Bogen', Aalborg Portland 2nd ed Denmark (1985) 731 p.
15. Bager D, Sellevold E. Cem con res V.16 (1986) pp.709-720, 835-844, V.17 (1987) pp.1-11
16. Hedenblad G. PhD Lund Inst of Tech., Div of Building Materials, Report TVBM 1014 (1993) 250 p.
17. Jacobsen S. Cem Con Res 35 (2005) 213-219
18. Jacobsen S., Gran H., Bakke J. and Sellevold E. Cem Con res V.25 No.8 (1995) 1775-1780
19. Jacobsen S., Marchand J., Boisvert L. Cem Con Res 26 6 (1996) 869-881
20. Gerard B.: Contribution des couplages mechanique-chimie-transfert dans la tenue a long term des ouvrages de stockage de déchets radioactifs Thèse PhD LMT Cachan-EdF-U.Laval (1996) 290+79 p.
21. Gerard B, Jacobsen S., Marchand J.: Concrete cracks II: Observation and permeability – a review, Proc. Consec 98 E&FN Spon ISBN 0-419-23860-3 (1998) 183-197
22. Sellevold EJ, Bakke J.A and Jacobsen S.: High strength concrete without air entrainment.: effect of rapid temperature cycling above and below 0 ° C, Int. worksh. Fr/th and deicer salt scaling of concrete, Université Laval Qué. Canada (1993) 153-164
23. Jacobsen S., Sellevold E.J. and Matala S. Cement and conc research 26, 6 (1996) 919-931
24. Sodhi D.S. Local ice pressure measured during ductile and brittle crushing of ice, proc Works Ice Abrasion on Concrete Structures, Nordic Concrete Federation, ISSN 0800-6377 (2008) 35-44
25. Hobbs P.V. Ice Physics, Clarendon Press, Oxford (1974) p.394
26. Schulson E.M, Duval P. Creep and Fracture of Ice, Cambridge University Press (2009) p.57
27. Hertz H. Journal of Pure and Applied Math. 92 (1881) 156-171 (in German)
28. Fischer-Cripps A.C. Introduction to Contact Mechanics, Springer (2007) p.101
29. Møen E et al Ice abrasion data on concrete structures – an overview ref as [24] (2008) pp.59-103

30. Jacobsen S., Sistonen E., Huovinen S., Marchand J., Tremblay M-H. Ice abrasion, frost, deicer salt scaling and reinforcement corrosion on concrete structures: interaction and service Life, CONSEC'07, France, LCPC, Ed. F.Toutlemonde et.al (2007) pp.1137-1152
31. Jacobsen S., Sistonen E., Huovinen S., Marchand J., Tremblay M-H. Abrasion and scaling of concrete by ice, studded tires and frost salt: interaction and service life modelling, 2nd Int Symposium on Advances in Concrete through science and Engineering, Quebec RILEM Proc 51 (2006) 23 p.
32. Huovinen, S., (1990) "Abrasion of concrete by ice in aretic sea structures", VTT Publications 62, (Doctoral thesis), Espoo, 110 p, app. 31 p.

NCF Workshops 1975 – 2010

Wednesday, 12 May 2010

No.	Date	Place and convenor	Theme	Documentation
1	11.09 1975	Dansk Betongforening København (P. Nepper-Christensen, A. Nielsen)	Termiske problemer ved udførelse av massive betongkonstruksjoner	Kompendium utgitt av Dansk Betonforening, november 1975.
2	26.02 1976	Avd. Betongbyggnad, Chalmers Tekniska Högskola, Gøteborg (A. Losberg)	Lettballastbetong som konstruksjons-materiale	Rapport 77:3 fra Institusjonen for konstruksjons-teknikk CTH, 1977. (Ikke anmäldt i Nordisk Betong).
3	19.06 1976	Cement- og Betonginstituttet, Stockholm (U. Bellander, G. Fagerlund)	Accelerade provningsmetoder	Majoriteten av rapporter publisert i Nordisk Betong, 5:1976. Øvrige rapporter (forfattere og titler) listet i samme nr. av Nordisk Betong).
4	23.03 1977	Avd. for Konstruksjonsteknikk, Høgskolan i Luleå. (L. Elfgren, K Gylltoft)	Utmattning av betongkonstruksjoner	Teknisk rapport 1977:57 T fra Tekniska Høgskolan i Luleå.
5	09.06 1977	Avd. för Byggnadsmateriallära Lunds Tekniska Høgskola. (L.O. Nilsson).	Fukt i betong	Anmält i Nordisk Betong 6:1977 av L.O. Nilsson
6	18.04 1977	Forskningsinstiuttet for Cement og Betong (FCB)	Skjær (Skjuvning)	Nordisk Betongforskningssem inar "Skjær i Betongkonstruksjoner " FCB Rapport STF 65 A77033.
7	29.09 1977	Aalborg Portland, Aalborg (P. Nepper-Christensen)	Bruddmekanikk	Rapport No 6:1977. Dansk Betonforening.

8	26.01 1978	Statens Tekniska Forskningscentral, Betongtekniska laboratoriet. Otnäs. (H. Poijärvi)	Uppvärmning och värmebehandling av färsk betong under arbetsplatsförhållanden	Seminarium för Uppvärmning och värmebehandling av färsk betong under arbetsplatsförhållanden. Rapport från VTT Esbo 1978.
9	24.04 1979	Statens Tekniska Forskningscentral, Betongtekniska laboratoriet. Otnäs. (A. Sarja)	Reparation av betongkonstruktioner	VTT Symposium 7, Esbo 1980.
10	Oktober 1979	Det Norske Veritas (N. Ellingsvåg).	Utmattning av betongkonstruktioner	FCB-rapport. STF65 A80025, datert 80-06-10.
11	16-17.10 1979	Cement och Betonginstitutet, Stockholm (J. Byfors)	Betong och betongkonstruktioner i tidlig ålder	CBI-rapport finns. Kopia kan rekvireras från CBI.
12	26.11 1979	CBI, Stockholm (C. Molin)	Håltagning och rivning av betong	CBI-rapport finns ej och kommer ej heller att publiceras.
13	21.03 1980	DTH, København (K. Madsen)	Metoder och data för praktisk beräkning av svinn och krypning	Dialog Nordic Seminar on Deformations in Concrete Structures. Copenhagen March 1980, Nr 1-80
14	16.04 1980	Finska Betongforeningen och VTT, Tammerfors	Arbetsmiljø vid betongarbeten	Arbetsmiljøn – riskförebyggande åtgärder vid betongarbeten. VTT-symposium 14/1981
15	21.04 1980	SINTEF FCB, Trondheim	Dynamisk påkjente konstruksjoner	Dynamisk påkjente konstruksjoner. FCB rapport 5TF65 A80032, 1980
16	19.05 1980	Aalborg Portland, Aalborg (Lars Hjorth)	Cementsubstitutions-materialer	Aalborg Portland, CBL særtryk nr. 7
17	12.11 1980	CBI, Stockholm	Armering och armeringsarbetetn ergonomi	CBI-rapport

18	15.05 1981	NTH, Trondheim	Ikke-lineær analyse av armerte betongkonstruksjoner	Ikke lineær analyse av armerte betongkonstruksjoner . Institutt for statistikk, NTH Trondheim Rapport nr. 81-2. Okt. 1981
19	10.12 1981	FCB, Trondheim (O.E. Gjørv / K.E. Løland)	Silika i betong	Condensed silica fume in concrete. Inst. for bygningsmateriallære Rapport BML, 82610 februar 1982
20	23.10 1982	CBI, Stockholm (G. Fagerlund)	Betongs frostbeständighet	CBI rapport 2:83
21	25.05 1983	CBI, Stockholm	Handtering av betong på byggarbetsplatser	
22	05.04 1984	SBI, Stockholm	Samverkanskonstruktioner stål-betong	Stålbyggnadsinstitutet. Publikasjon nr. 92, april 1984
23	23.05 1984	CBI, Stockholm	Organiske fibre i betong	Organiska fiber i betong. Sammenfattningar. Kompendium. CBI, Stockholm.
24	29-30.10 1984	Køge (Dirch H. Bager)	Beton & frost	Dansk Betonforening. Publikation 22:85
25	12.03 1985	VTT Helsingfors	Anslutningar mellan betongelement	"Connections between precast concrete elements". VTT-symposium 62 (1985)
26	15.05 1985	VTT Helsingfors	Reparation, tilstandsvurdering	"Reparasjon av betongkonstruksjoner" VTT-symposium 66 (1986)
27	23.10 1985	CTH Göteborg	Vidheftning	Bond and anchorage of reinforcement in concrete. CTH, Div. of Cement Structures Publication 86:1, Göteborg

28	05-05.02 1986	Fortifikasjonförvaltningen, Stockholm	Dynamisk belastede betongkonstruktioner	Dynamisk belastede betongkonstruksjoner. Fortifikasjonsforvaltningen Forskningsbyraan. Rapport A4:86 Eskilstuna 1984
29	23.05 1986	FCB/NTH, Trondheim	Utmatting av betongkonstruksjoner	Fatigue of Concrete. Papers presented at a Nordic mini-seminar Trondheim, 1985.SINTEF-rapport 5TF65 A86082
30	21.10 1986	VTT Esbo	Betongkonstruksjoner under tvangsbelastning	Betongkonstruksjoner under tvangsbelastning. VTT-symposium 76
31	06.11 1986	LTH Lund	Bruddmekanik	Fracture Mechanics of Concrete. Division of Building Materials, LTH, Lund November 6/86
32	20.11 1987	Dansk Ingeniørforening, København	Hydrasjon av cement	Seminar om Hydration of Cement, Aalborg Portland, Februar 1988
33	18.02 1988	VTT, Helsingfors	Bestandighet, livslengde	Durable concrete with industrial by-products. VTT Symposium 89. Esbo 1988
34	15.03 1988	FCB, Trondheim	Fliskledt betong i våtrom – skader og utredning	Fliskledt betong i våtrom – skader og utbedring. SINTEF-rapport 5TF65 A88041, juni 1988
35	05.04 1988	DTH, København	Kraftoverførsel til armering i revnet betong	Notits i Nordisk Betong 2:1988
36	15.11 1988	FCB, Trondheim	Karbonatisering av betong	Karbonatisering av betong. SINTEF-rapport 5TF65 A88065
37	09.05 1989	Dansk Ingeniørforening, korrosionscentralen	Kloridinitert korrosjon	Ingen publisering på dette miniseminaret.

38	02.06 1989	FCB Trondheim	Betongkonstruksjoners brannmotstand	Fire Restance of Concrete. Papers presented at a mini-seminar Trondheim 1989
39	23-24.11 1989	CTH Göteborg	Utmatting av betongkonstruksjoner	Fatigue of Concrete Structures. CTH publikasjon P-90:8, Göteborg mai 1990
40	febr. 1990	Vegdirektoratet, Oslo	Høyfast betong i veier	-
41	14.08 1990	BML Trondheim	Fersk betongs reologi	-
42	20.11 1990	KTH Stockholm	Oforstorande provning av betongkonstruksjoner	-
43	17.04 1991	NTH/SINTEF, Trondheim (Ø. Vennesland)	Elektrokjemiske metoder for rehabilitering av armerte betongkonstruksjoner	
44	05.12 1991	HTH, Oslo (E. Sellevold)	Bindemidler i høyfast betong – reaktivitet, struktur og egenskaper	
45	24.01 1992	VTT, Esbo (Juha Saarima)	Mikroskopi och Mildanalys	Microscopy and image analysis of building materials. Espoo, Finland, 1992. VTT Symposium 136, Technical Research Center of Finland, Espoo 1993, 54 pp ISBN 951-38 4087-5
46	19.11 1992	Aalborg Universitetscenter (L. Pilegaard Hansen)	Utmatting av betong	Fatigue of Concrete Structures. Dept. of Building Technology and Structural Engineering, Aalborg Universtetscenter, AUC, Aalbort 1992, 126 pp, ISSN 0902-7513-R9307

47	13-14.01 1993	CTH, Göteborg (L.O. Nilsson)	Kloridtransport i betong	Cloride penetration into concrete structures. Institutionen för byggnadsmaterial, Chalmers Tekniska Högskola, Publication 93:1, Göteborg, Januari 1993
48	22-23.04 1993	Lund University (Göran Fagerlund, Erik J. Sellevold)	Nordisk Miniseminar NBS-MK Frost	Mødereferat
49	Juni 1995	Aalborg	Modern Design of Concrete Structures	
50	16-17.04 1996	Lund University (Sture Lindmark, Göran Fagerlund)	Frost Resistance of Building Materials	Report TVBM-3072
51	08.11 1996	Tekniska Högskolan i Luleå (Hans Hedlund, Patrick Groth)	Licentiatseminarier	
52	28.11 1996	NTNU/SINTEF, Trondheim (E. Sellevold, T.E. Hammer)	Early volume change and reactions in paste – mortar – concrete	
53	10.12 1996	CBI Stockholm	Livslängdbedömning inkluderande korrosionens propageringsskede	
54	10.07 1997	Lund University (Göran Fagerlund, Bertil Persson)	Self Desiccation of Concrete	Report TVBM-3075
55	22.08 1997	VTT, Esbo	Fuktmätning och fukttransport i betongkontstruktioner utsatta för temperatur- och fuktvariationer	VTT Symposium No 174 ”Moisture Measurements”
56	18.06 1999	Lund University (Göran Fagerlund, Bertil Persson)	Self Desiccation of Concrete	Report TVBM-3085
57	31/08+1/0 91999	Lund University (Katja Fridh, Göran Fagerlund)	Frost Resistance of Building Materials	Report TVBM-3087
58	07-08.10 1999	Skagen (Dirch H. Bager)	Water in Cement Paste & Concrete – Hydration and Pore Structure	Workshop Proceeding No.1, Nordic Concrete Federation 1999

59	01.09 2000	DTU / Lyngby (Mette Geiker, Henrik Stang)	Steel Fibre Reinforced Self-Compacting Concrete	
60	26-27/4 2001	Trondheim (Kåre Johansen)	Self Compacting Concrete	SINTEF Report STF22 A01614
61	22-23/05 2001	Chalmers (L.O. Nilsson)	Armeringskorrosion och chlorider i betong	
62	12-13/06 2001	KTH / Stockholm (Johan Silfwerbrand)	Fibre-reinforced Concrete Structures	Workshop Proceeding No.2, Nordic Concrete Federation 2001
63	21-23/11 2001	Hirtshals (Dirch H. Bager)	Durability of exposed Concrete containing Secondary Cementitious Materials	Workshop Proceeding No.3, Nordic Concrete Federation 2001
64	14-15/6 2002	Lund University (Göran Fagerlund, Bertil Persson)	Self Desiccation of Concrete	Report TVBM-3104
65	29/8 2002	CBI (Johan Silfwerbrand)	Diagnos av bärande konstruktioner	CBI rapport
66	22-23/5 2003	Teknologisk Institut (Claus V. Nielsen)	Concrete and Fire	Summary paper in NCR 2:03
67	6/10 2003	Veidekke ASA/Oslo (Terje Kanstad)	Design Rules for Steel Fibre Reinforced Concrete Structures	Workshop Proceeding No.4, Nordic Concrete Federation 2003
68	3-4/11 2003	Teknologisk Institut (Lars Nyholm Thrane)	Form Filling Ability of Self-compacting Concrete	Summary paper in NCR 2:04
69	31/3+1/4 2005	NTNU / Trondheim (T. Kanstad, Ø. Bjøntegaard, E.J. Sellevold)	Crack Risk Assessment of Hardening Concrete Structures	Workshop Proceeding No.5, Nordic Concrete Federation 2005
70	25-26/10 2007	Helsinki (Stefan Jacobsen/NTNU & AkerArktic)	Ice Abrasion on Concrete Structures	Workshop Proceeding No.6, Nordic Concrete Federation 2008
71	15/11 2007	NTNU / Trondheim (Terje Kanstad)	Fibre Reinforced Concrete	Workshop Proceeding No.7, Nordic Concrete Federation 2008
72	12-14/11 2008	Hirtshals (Eigil V. Sørensen)	Nordic Exposure Sites - Input to revision of EN 206-1	Workshop Proceeding No.8, Nordic Concrete Federation 2008
73	2-5/3 2010	Vedbæk (Dirch H. Bager)	Freeze-thaw Testing of Concrete - Input to revision of CEN test methods	Workshop Proceeding No.9, Nordic Concrete Federation 2010

.